NASA/TM–20240012725
NESC-RP-21-01718

Space-Shielding Radiation Dosage Code Evaluation

Phase 2: SHIELDOSE-2 Radiation-Assessment Code

Insoo Jun
Jet Propulsion Laboratory, Pasadena, California

Rubén García Alía
European Organization for Nuclear Research, Genève, Switzerland

Remi Benacquista
TRAD, Labège, France

Alexandre Cappe
TRAD, Labège, France

Bryan Fodness
Experimental & Mathematical Physics Consultants, Gaithersburg, Maryland

Alexander Henderson
Marshal Space Flight Center, Huntsville, Alabama

Thomas M. Jordan
Experimental & Mathematical Physics Consultants, Gaithersburg, Maryland

Stefano Marin
European Organization for Nuclear Research, Genève, Switzerland

Larisa Milic
Experimental & Mathematical Physics Consultants, Gaithersburg, Maryland

Francesc Salvat Pujol
European Organization for Nuclear Research, Genève, Switzerland

Giovanni Santin
European Space Agency, Paris, France

André Donadon Servelle
European Organization for Nuclear Research, Genève, Switzerland

Robert C. Singleterry
Langley Research Center. Hampton, Virginia

Athina Varotsou
TRAD, Labège, France

Vasilis Vlachoudis
European Organization for Nuclear Research, Genève, Switzerland

Brian X. Zhu
Jet Propulsion Laboratory, Pasadena, California

Steven J. Gentz/NESC
NASA Langley Research Center, Hampton, Virginia

October 2024

NASA STI Program Report Series

Since its founding, NASA has been dedicated to the advancement of aeronautics and space science. The NASA scientific and technical information (STI) program plays a key part in helping NASA maintain this important role.

The NASA STI program operates under the auspices of the Agency Chief Information Officer. It collects, organizes, provides for archiving, and disseminates NASA's STI. The NASA STI program provides access to the NTRS Registered and its public interface, the NASA Technical Reports Server, thus providing one of the largest collections of aeronautical and space science STI in the world. Results are published in both non-NASA channels and by NASA in the NASA STI Report Series, which includes the following report types:

- TECHNICAL PUBLICATION. Reports of completed research or a major significant phase of research that present the results of NASA Programs and include extensive data or theoretical analysis. Includes compilations of significant scientific and technical data and information deemed to be of continuing reference value. NASA counterpart of peer-reviewed formal professional papers but has less stringent limitations on manuscript length and extent of graphic presentations.

- TECHNICAL MEMORANDUM. Scientific and technical findings that are preliminary or of specialized interest, e.g., quick release reports, working papers, and bibliographies that contain minimal annotation. Does not contain extensive analysis.

- CONTRACTOR REPORT. Scientific and technical findings by NASA-sponsored contractors and grantees.

- CONFERENCE PUBLICATION. Collected papers from scientific and technical conferences, symposia, seminars, or other meetings sponsored or co-sponsored by NASA.

- SPECIAL PUBLICATION. Scientific, technical, or historical information from NASA programs, projects, and missions, often concerned with subjects having substantial public interest.

- TECHNICAL TRANSLATION. English-language translations of foreign scientific and technical material pertinent to NASA's mission.

Specialized services also include organizing and publishing research results, distributing specialized research announcements and feeds, providing information desk and personal search support, and enabling data exchange services.

For more information about the NASA STI program, see the following:

- Access the NASA STI program home page at http://www.sti.nasa.gov

- Help desk contact information:

https://www.sti.nasa.gov/sti-contact-form/ and select the "General" help request type.

NASA/TM–20240012725
NESC-RP-21-01718

Space-Shielding Radiation Dosage Code Evaluation

Phase 2: SHIELDOSE-2 Radiation-Assessment Code

Insoo Jun
Jet Propulsion Laboratory, Pasadena, California

Rubén García Alía
European Organization for Nuclear Research, Genève, Switzerland

Remi Benacquista
TRAD, Labège, France

Alexandre Cappe
TRAD, Labège, France

Bryan Fodness
Experimental & Mathematical Physics Consultants, Gaithersburg, Maryland

Alexander Henderson
Marshal Space Flight Center, Huntsville, Alabama

Thomas M. Jordan
Experimental & Mathematical Physics Consultants, Gaithersburg, Maryland

Stefano Marin
European Organization for Nuclear Research, Genève, Switzerland

Larisa Milic
Experimental & Mathematical Physics Consultants, Gaithersburg, Maryland

Francesc Salvat Pujol
European Organization for Nuclear Research, Genève, Switzerland

Giovanni Santin
European Space Agency, Paris, France

André Donadon Servelle
European Organization for Nuclear Research, Genève, Switzerland

Robert C. Singleterry
Langley Research Center. Hampton, Virginia

Athina Varotsou
TRAD, Labège, France

Vasilis Vlachoudis
European Organization for Nuclear Research, Genève, Switzerland

Brian X. Zhu
Jet Propulsion Laboratory, Pasadena, California

Steven J. Gentz/NESC
NASA Langley Research Center, Hampton, Virginia

National Aeronautics and
Space Administration

Langley Research Center
Hampton, Virginia 23681-2199

October 2024

Acknowledgments

The assessment team is grateful to the space-radiation technical community for their assistance and contributions, and particularly to peer reviewers Kerry Lee (The Aerospace Corporation) and Neal Nickles (BAE System Inc.), and NESC reviewers Sara Wilson (LaRC) and Joe Minow (MSFC).

Available from:

NASA STI Program / Mail Stop 050
NASA Langley Research Center
Hampton, VA 23681-2199

NASA Engineering and Safety Center Technical Assessment Report

Space-Shielding Radiation Dosage Code Evaluation Phase 2: SHIELDOSE-2 Radiation-Assessment Code

TI-21-01718

NESC Lead: Steven J. Gentz/NESC

Technical Lead: Insoo Jun/JPL

September 26, 2024

Report Approval and Revision History

NOTE: This document was approved at the September 26, 2024, NRB.

Approved: Timmy Wilson Digitally signed by Timmy Wilson Date: 2024.10.01 19:14:53 -04'00'	
NESC Director	

Version	Description of Revision	Office of Primary Responsibility	Effective Date
1.0	Initial Release	Steven Gentz, NESC Chief Engineer's Office, MSFC	09/26/2024

Table of Contents

List of Figures

List of Tables

Technical Assessment Report

1.0 Notification and Authorization

Emily Willis of the Marshall Space Flight Center (MSFC) Natural Environments Branch requested the NASA Engineering and Safety Center (NESC) provide an independent assessment of the National Institute of Standards and Technology (NIST) computer code SHIELDOSE-2 (1994) used to determine space-shielding radiation dose predictions to materials. This request was based on concerns on the accuracy and range of applicability of SHIELDOSE-2, which may not sufficiently be addressed in existing literature. Additionally, NASA programs and their prime contractors are requesting suggested alternate tools when SHIELDOSE-2 is identified as not applicable.

The independent assessment received authority to proceed on January 13, 2022, and its plan was approved on February 3, 2022.

Key stakeholders for this effort include:

- MSFC Natural Environments Branch
- Space Environments – Radiation Dose Analysis/Transport Communities
- NASA programs including Space Launch System, Multi-Purpose Crew Vehicle, Gateway, Human Landing System, spacecraft projects, and technology-development initiatives

2.0 Signatures

Submitted by:

Steven Gentz Digitally signed by Steven Gentz
Date: 2024.09.30
16:41:43 -05'00'

Mr. Steven J. Gentz

Significant Contributors:

Jun, Insoo Digitally signed by Jun, Insoo
Date: 2024.09.30
13:32:19 -07'00'

Dr. Insoo Jun

Signatories declare the findings, observations, and NESC recommendations compiled in the report are factually based from data extracted from program/project documents, contractor reports, open literature, and/or generated from independently conducted tests, analyses, and inspections.

3.0 Team Members for Phase 2

Name	Discipline	Organization
Core Team		
Steve Gentz	NESC Lead	LaRC
Insoo Jun	Technical Lead	JPL
Alexander Henderson	Geant4	MSFC
Brian Zhu	ITS (TIGER), Data compilation	JPL
Tom Jordan	NOVICE code developer	Experimental & Mathematical Physics Consultants (EMPC)
Brian Fodness	NOVICE expert	EMPC
Larisa Milic	NOVICE expert	EMPC
Robert Singleterry	MCNP (Monte Carlo N-Particle Transport)	LaRC
Makoto Asai	Geometry and Tracking 4 (Geant4) Radiation for Space (GRAS)	Jefferson National Accelerator Facility
Giovanni Santin	GRAS/MULASSIS (Multi-Layered Shielding Simulation Software)	ESA
Rubén García Alía	FLUKA (Fluktuierende Kaskade) expert	European Organization for Nuclear Research (CERN)
Francesc Salvat Pujol	FLUKA development team	CERN
Stefano Marin	FLUKA development team	CERN
André Donadon Servelle	FLUKA development team	CERN
Vasilis Vlachoudis	FLUKA development team	CERN
Remi Benacquista	FASTRAD	TRAD
Athina Varotsou	FASTRAD	TRAD
Alexandre Cappe	FASTRAD	TRAD
Consultants		
Joe Minow	Space Environments NASA Tech Fellow	MSFC
Emily Willis	Natural Environments	MSFC
Anthony Destefano	Natural Environments	MSFC
Erin Hayward	Radiation Materials Testing	MSFC
Jarvis Caffrey	Radiation Dose Analysis Expert	MSFC
Tim Barth	Model and Simulation Evaluation	KSC
Tom Carstens	Radiation Dose Analysis Expert	GSFC
Hugh Evans	Radiation Dose Analysis Expert	ESA
Mark Millinger	Radiation Dose Analysis Expert	JSC/ESA
Business Management		
John LaNeave	Program Analyst	LaRC/MTSO
Assessment Support		
Lynne Hartman	Project Coordinator	LaRC/AMA
Linda Burgess	Planning and Control Analyst	LaRC/AMA
Dee Bullock	Technical Editor	LaRC/AMA

3.1 Acknowledgements

The assessment team is grateful to the space-radiation technical community for their assistance and contributions, and particularly to peer reviewers Kerry Lee (The Aerospace Corporation) and Neal Nickles (BAE System Inc.), and NESC reviewers Sara Wilson (LaRC) and Joe Minow (MSFC).

4.0 Executive Summary

Per a request by the Artemis Program, the NASA Engineering and Safety Center (NESC) initiated a two-phased study: (1) to better understand and document the SHIELDOSE-2 code capabilities and limitations, and (2) to recommend alternative tools to use for cases where SHIELDOSE-2 is not applicable. SHIELDOSE-2 is commonly used in the early spacecraft design phases (e.g., concept development and preliminary design) because it has been established that it provides reasonably reliable results with relatively rapid computation time. The Phase 1 study was completed, for which the main focus was to compile and provide the best knowledge on the current understanding of SHIELDOSE-2's application ranges and limitations. The results of Phase 1 are presented in a separate report (NASA/TM-20230010640, July 2023).

The original requests from the Artemis Program were:

1. What is the thinnest thickness where SHIELDOSE-2 can be used?
2. In this thin material, how does the density scaling hold for different materials other than aluminum?

To adequately answer these questions required 'true' values against which the SHIELDOSE-2 results could be directly compared (e.g., experimental data or reference simulation results). However, no literature or previous studies for such values were found. Therefore, it was concluded that the direct answers to these questions were not readily available, and to obtain those true values was beyond the scope of this study.

Alternatively, in Phase 2, the NESC assessment team performed a comprehensive comparison between SHIELDOSE-2 and other widely used radiation transport codes. The codes included in this study are (alphabetically) FASTRAD, FLUktuierende KAskade (FLUKA), Geometry and Tracking version 4 (Geant4), Geant4 Radiation Analysis in Space (GRAS), Integrated Tiger Series (ITS), Monte Carlo N-Particle (MCNP), and NOVICE. The results from each code were compared to the SHIELDOSE-2 lookup tables. The intent of the inter-comparison study was to provide indirect clues on addressing the original request from the Artemis Program by presenting a reference database for future users of SHIELDOSE-2 and other codes for thin shielding applications in space.

Key findings of the study responding to the original requests by the Artemis Program are:

1. Because the thickness applicability is closely related to the lowest energy of electrons and protons used in building the SHIELDOSE-2 table (5 keV for electrons and 10 keV for protons), SHIELDOSE-2 could be used for materials as thin as the ranges corresponding to those energies. The continuous slowing down approximation (CSDA) range of 5 keV electrons is 1.092E-4 g/cm^2 or ~0.40 µm in aluminum, and the CSDA range of 10 keV protons is 5.943E-5 g/cm^2 or 0.22 µm in aluminum.
    a. This means that SHIELDOSE-2 could be used for aluminum slabs as thin as a fraction of µm of material.
    b. However, the accuracy of the results needs more validation as the dose profiles in aluminum obtained with other widely-used radiation transport tools are not generally in good agreement (Figures 7.2-1 through 7.2-10).
2. Application of density scaling to the SHIELDOSE-2 table are not generally reproduced by other codes, especially for low-energy electrons and protons. This implies that the density scaling should not be used to the SHIELDOSE-2 results in applications where

≤0.1 MeV electrons or ≤10 MeV protons are important (material thickness ~0.5 mm). Thicker material results were not the focus of this study.

5.0 Assessment Plan

The Phase 1 assessment (i.e., NASA/TM−20230010640) reviewed the capability and limitation of the SHIELDOSE-2 radiation-analysis tool, especially in light of the lack of documented knowledge on its validity range of thin materials (for this report, "thin" is defined to be less than or equal to 0.0254 cm (or '10 mil') aluminum). The Phase 1 assessment included:
(1) a comprehensive review of SHIELDOSE-2 documents and related references,
(2) investigating the validity of zero detector thickness assumed in SHIELDOSE-2 when estimating doses in various detector materials, and (3) a series of first-order simulations to understand the effect of typical density scaling for materials other than aluminum.

In Phase 2 of this assessment, extensive simulations were performed to benchmark more complex non-Monte Carlo and Monte Carlo radiation-analysis codes appropriate to detailed spacecraft design and operational phases in the current and planned space environments. The results were used to provide the database for various codes' predictive capabilities when compared to other codes.

6.0 Introduction

This section provides a short summary of each code used in this study, emphasizing the physics implementation relevant to the current project (i.e., thin target applications). These summaries are presented in alphabetical order by code name. Furthermore, if any update/improvement has been made to the code as a result of this study, they are explained in this section.

6.1 FASTRAD

[Contributed by Remi Benacquista, Athina Varotsou, and Alexandre Cappe of TRAD]

FASTRAD® is a simulation software developed by TRAD [ref. 1]. It is dedicated to the simulation of radiation effects for space applications. It consists of a set of tools that perform modeling (e.g., Standard for the Exchange of Product (STEP) import, invalid shapes detection and correction, overlap detection, material and component database, etc.) and calculation of radiation effects and post-processing of the results. The calculation tools include the sector analysis (ray-tracing), the Forward Monte-Carlo (FMC), the Reverse Monte-Carlo (RMC) and the finite element methods. Various quantities can be estimated with these tools including total ionizing dose (TID), displacement damage or total non-ionizing dose (TNID), transmitted fluence and internal charging (i.e., incoming current density, charge deposition, electric field, potential).

Previous studies focused on the comparison between several tools including FASTRAD [refs. 2, 3]. Other comparisons and validations of the Monte-Carlo tools are available on request. Results presented in this report are computed with the v4.2.4 version using the FMC method.

The physics of particle-matter interactions is based on that of Geant4. Like in Geant4, different processes simulated can be treated like a discrete or a continuous process. Particles are tracked step by step in the propagation. The discrete process is simulated at the end of the step and is, most of the time, the process that sets the step length. The continuous process is simulated through the length of the step to make the incident particle lose energy or change its direction.

Electron transport

The electron transport considers several types of interactions: ionization, multiple scattering, Bremsstrahlung, and Annihilation (not discussed). The ionization is managed as a discrete and continuous process. The creation of the secondary electron is processed as a discrete process while the loss of energy is a continuous process. The model used for the ionization process is the Moller-Bhabha model. For the sake of performance, the elastic scattering interactions are modeled as multiple scattering interactions and use the Urban model. The Bremsstrahlung interactions are discrete/continuous processes and use the Selzer Berger model.

Proton transport

The current (v4.2.4) version of FASTRAD considers only the electromagnetic processes. The hadronic processes are expected to have little impact when considering the full environment spectra, especially for thin target applications. However, the hadronic processes are planned to be integrated in a future version to deal with other types of applications (e.g., linear energy transfer (LET) calculation of heavy ions, lunar or Martian environment, etc.). The ionization interaction uses two different models: the Bragg model for energies below 2 MeV, and the Bethe and Bloch model for higher energies. The multiple scattering interactions use the Wentzel model. The Bremsstrahlung interactions are simulated with the Seltzer-Berger model.

This study focused on thin-targets applications where low-energy particles provide a major contribution to dose. In this scope, several corrections and improvements were made in FASTRAD regarding the multiple scattering of electrons. In addition, several corrections were made on the fluctuation model that adds a random contribution of energy loss during an interaction or during the transport. Following these modifications, comparisons to Geant4 show improved agreement for very-low-energy particles (i.e., 5 to 10 keV electrons and 10 to 100 keV protons) while having no or minimal impact on higher energies.

Figures 6.1-1 and 6.1-2 display some comparisons between FASTRAD v4.2.3 (before improvements), FASTRAD v4.2.4 (after improvements) and Geant4 v11.1.2 for low-energy particles (i.e., 5 keV electrons and 10 keV protons) in a Teflon^{TM} target. All calculations, including those for Geant4, were performed by TRAD considering incident particles with a normal direction, while a cosine distribution will be considered for the direct comparisons.

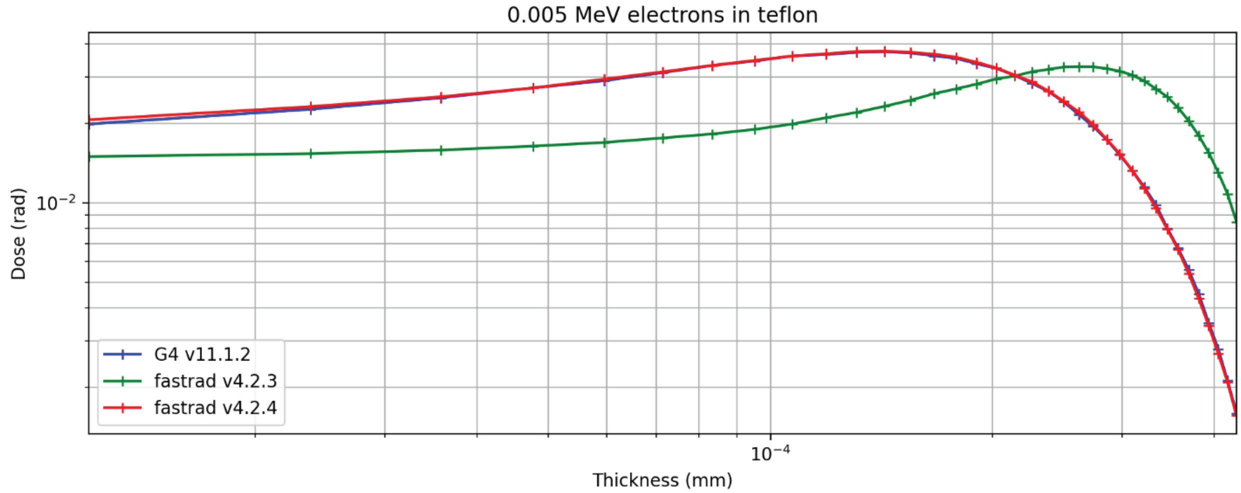

Figure 6.1-1. 5-keV Electron Transport in Teflon
Comparison between Geant4 v11.12, FASTRAD v4.2.3, FASTRAD v4.2.4.

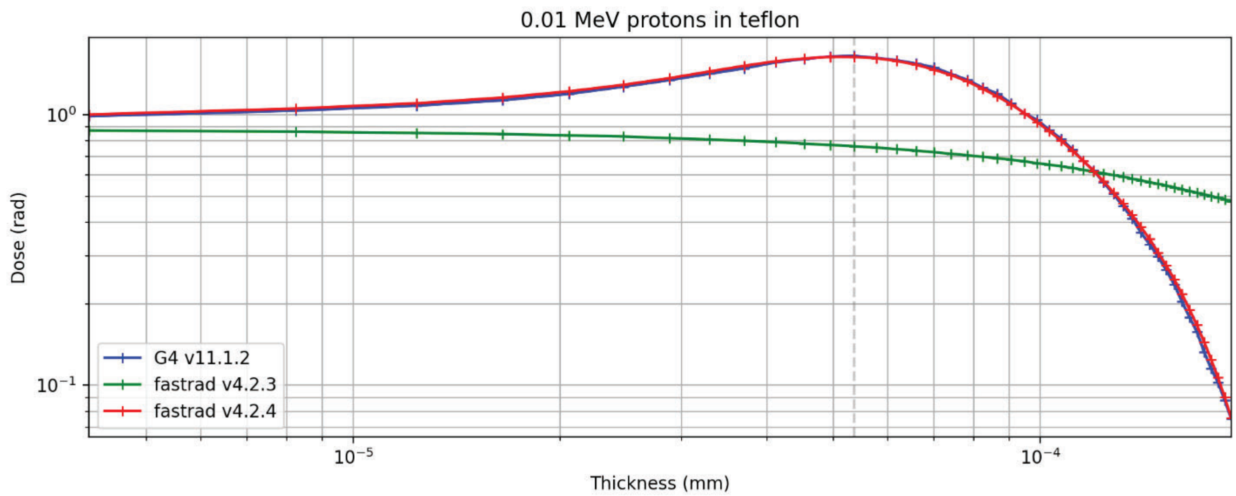

Figure 6.1-2. 10-keV Proton Transport in Teflon
Comparison between Geant4 v11.12, FASTRAD v4.2.3, FASTRAD v4.2.4.

6.2 FLUKA

[Contributed by S. Marin, A. Donadon Servelle, R. García Alía, F. Salvat Pujol, and V. Vlachoudis on behalf of the FLUKA.CERN Collaboration]

Fluktuierende Kaskade (FLUKA) is a general-purpose code for the Monte Carlo simulation of coupled hadronic and electromagnetic radiation showers in complex material geometries [refs. 4, 5, 6]. This code models the transport and interaction of over 60 particle species, including photons, leptons, hadrons, and ions from the keV to PeV scale—neutrons are transported down to 0.01 meV and photons down to 100 eV. A powerful graphical user interface (GUI) [ref. 7] assists users through all FLUKA simulation stages, from the definition, visualization, and debugging of the simulation geometry, to the setting of simulation parameters, run management, processing of the output files, and plotting of scored physical quantities. FLUKAVAL, a validation and benchmarking framework to which all FLUKA releases are subjected to [ref. 8], ensures the stability of FLUKA performances and closely monitors their constant improvement as new physics and technical developments are included. As a result, FLUKA is used in a broad range of applications, including accelerator design, radiation protection, radiation effects in electronics, space research, medical physics, etc.

The relevant aspects of FLUKA's transport and interaction models for the present benchmark concern include:

- *Ionization*: Collisions of charged particles with target e- transferring an energy above the delta-ray production threshold are sampled explicitly; the produced secondary electron is transported (if above transport threshold). The effect of a multitude of collisions with lower-energy transfer is accounted for in an aggregate way over particle steps, relying on a restricted stopping power for the average energy loss onto which energy-loss fluctuations are applied [ref. 9]. The delta-ray production threshold is set to 1 keV in the simulations performed in this work.

- *Coulomb scattering*: As charged particles traverse condensed matter, they undergo intensive elastic scattering on the screened electrostatic potential of target atoms. The cumulative effect of many such collisions along macroscopic particle steps is accounted for in FLUKA by way of a multiple Coulomb scattering algorithm [ref. 10] based on Molière theory, including path-length and lateral-displacement corrections. The single-scattering option is available on demand, as was needed in this benchmark for the thin targets at the lowest proton and electron energies. Nuclear finite-size effects and spin-relativistic corrections are accounted for through form factors. The energy transferred during multiple Coulomb collisions along particle steps is accounted for by means of a nuclear stopping power (relevant for protons below ~10 keV).

- *Bremsstrahlung*: The emission of Bremsstrahlung is especially relevant at the highest electron energies considered here, while in the proton cases it is virtually irrelevant. The FLUKA treatment of Bremsstrahlung emission by e-/e+ is based on the Berger and Seltzer approach [ref. 11].

- *Nuclear reactions*: Nuclear reactions are relevant for the proton irradiation cases considered here. They are treated by FLUKA's general hadron-nucleus inelastic interaction model [refs. 12–15], which at the energies considered here comprise an initial intranuclear cascade, followed by pre-equilibrium emission, an evaporation stage (including a Fermi break-up model for residuals with $A<18$ and a competing fission model for heavy nuclei), leading to a final gamma de-excitation cascade. For the proton energies considered in this benchmark, nuclear reactions lead to the emission of nucleons, light fragments, and photons.

- *Nuclear elastic scattering*: Besides Coulomb scattering, protons undergo nuclear elastic scattering, for which a novel partial-wave-based model was recently included in FLUKA [ref. 16], contributing to the angular spread of the proton flux as a function of depth.

- *Neutron interactions*: In the simulations performed here, neutrons are generated at the higher proton energies through nuclear reactions. Subsequent neutron interactions with nuclei below 20 MeV are treated with a point-wise approach, relying on evaluated neutron data libraries [ref. 17]. Above 20 MeV, neutron reactions are modelled on equal footing with other hadron reactions, while neutron elastic scattering is described based on a model by J. Ranft [ref. 18].

- *Photon interactions*: In the simulations performed here, photons are produced during hadron-nucleus reactions, e-/e+ Bremsstrahlung, and as secondaries in the electromagnetic shower. FLUKA accounts for their subsequent interactions [ref. 19] by explicitly modeling Rayleigh scattering, photoelectric effect, Compton scattering [ref. 20], e-/e+ pair production, and photonuclear reactions [ref. 21]. The relaxation of atomic inner-shell vacancies via fluorescence and Auger electron emission is included. Positrons from pair production events are transported and may annihilate at rest or in flight, contributing further photon pairs.

6.3 GEANT4

[Contributed by Alexander Henderson of MSFC]

Geant4 is a Monte-Carlo-based particle simulation toolkit [refs. 22, 23, 24]. This toolkit provides great flexibility to the end user in terms of geometry, incident particle parameters, detected quantities, and physics used. The modular system of the toolkit allows many different physical processes to be included or excluded as needed: by including only those processes likely to occur in a given scenario, system resource utilization is minimized.

This assessment has separately used the GRAS system, which is built on Geant4 [refs. 25, 26]. The NESC assessment team constructed a simulation independent of GRAS with many similar features. This provides an independent check on Geant4's accuracy. In addition, GRAS is implemented in Geant4 version 10.7.p04, while Geant4 version 11.1.2 was used for the independently constructed program. There are a few other technical variations, though they are not expected to greatly impact results.

For this effort, the NESC assessment team used mono-energetic incident particles in a cosine angular distribution incident on a rectangular slab. The slab's cross section was set to 4 m square to minimize particles exiting out the side. The thickness was set to be at least twice the CSDA range for the energy considered to approach the semi-infinite slab model used by SHIELDOSE-2. Very thin detectors were placed behind each layer of the thicknesses specified in SHIELDOSE-2's tables to replicate the assumptions used in SHIELDOSE-2 to the extent possible.

The "G4EmStandardPhysics_option4" physics package was used, which includes the particles: electron, positron, muons, pions, kaons, protons, anti-protons, deuteron, triton, He3, alphas, and heavy ions. For brevity only the processes used for protons, electrons, and gamma-rays are listed as those are the only particles assumed to be significant in these simulations. The following physical processes are implemented by this package: Every particle has a 'multi-scattering' process implemented. Gamma rays additionally have Compton scattering in separate models for above and below 2 MeV, photoelectric effect, gamma conversion, and Rayleigh scattering. Electrons and protons have Bremsstrahlung processes implemented. For electrons, there are additionally separate normal and high-energy (above 100 MeV) multi-scattering models, Coulomb scattering, and normal and low-energy (below 0.1 MeV) electron ionization. Protons additionally have proton ionization, pair production, and nuclear stopping. Tests conducted using other relevant physics package options have shown minimal variations. Production cuts were set to 1 nm.

6.4 GRAS

[Contributed by Giovanni Santin of ESA]

GRAS is a Geant4-based tool enabling common radiation analysis types (e.g., TID, TNID, fluence, single event effect (SEE), path length, charge deposition, dose equivalent, equivalent dose, instrument detection response, imaging sensor background, etc.) in generic three-dimensional (3D) geometry models. GRAS draws from the strength of Geant4 in particle-matter interaction physics modelling and geometry description and augments it with ease of use in defining typical use cases for radiation analyses, from dosimetry to SEEs and detector response. Traditional FMC (Direct) and RMC (Adjoint) are available options.

Input instructions are provided to GRAS via text files (macros) in Geant4 User-Interface (UI) text format. Generic geometry models are input in geometry description markup language (GDML) or in GMSH[1] format, which can be used as exchange formats for complex computer aided design (CAD) models. Simpler models can be created with macro commands only, with the built-in multi-layered shielding simulation analysis (MULASSIS)[2] or Geant4-based microdosimetry analysis tool (GEMAT)[3] modules. Output (e.g., scalars with associated statistical errors, histograms) is provided to text files in a spreadsheet comma-separated value (CSV) format. Detailed event-by-event analyses for fluence, energy deposition, secondary particle creation, are available via tuples from ROOT output files.

The main GRAS software design requirements are flexibility and modularity of the application. Thanks to flexibility, GRAS can be used for obtaining a variety of simulation output types for generic (e.g., GDML or C++) 3D geometry models, avoiding the creation of a tailored C++ Geant4-based application for every project. Thanks to a modular design, the GRAS analysis type capabilities can be easily extended by advanced users.

The GRAS tool and related documentation are available with the "European Space Agency Public License – v2.4 – Strong Copyleft (Type 1)" license from the European Space Software Repository (ESSR) at https://essr.esa.int/.

The simulations performed for this code comparison study were executed with GRAS v5.2.1. For the geometry description, the built-in MULASSIS multi-layer geometry was used, with slab shape option. The multi-layer model included a fixed number of 100 thin layers of the material under study. The SHIELDOSE-2 'semi-infinite' configuration is mimicked with the addition of a 100-g/cm2-thick back layer of the same material. The simulations were run with the Geant4 reference physics list EM-opt4, with a value of 1 μm for the production cuts. For this multi-layered slab configuration, the source particles are generated from a single central point in front of the entry face of the first geometry layer, with emission directions only into the 2π sector of the layers, with a cosine-low-biased distribution (i.e., enhancing the production in the directions closer to the normal to the layers). The output of the simulations includes TID values as tallied in the single layers with the 'dose' GRAS analysis module.

6.5 ITS

[Contributed by Brian Zhu of JPL]

ITS is a software package developed by Sandia National Laboratories (SNL) that performs Monte Carlo solutions of linear time-independent coupled electron/photon radiation transport problems, with or without the presence of macroscopic electric and magnetic fields of arbitrary spatial dependence. The continuous-energy ITS codes used in this study are based originally on the ETRAN (Electron TRANSport) code [ref. 27], which combines microscopic photon transport with a macroscopic random walk for electron transport. As ETRAN was limited to studies of one

---

[1] http://gmsh.info//

[2] https://www.spenvis.oma.be/help/models/mulassis.html. Multi-Layered Shielding Simulation Analysis

[3] https://www.spenvis.oma.be/help/models/gemat.html. Geant4-based Microdosimetry Analysis Tool

material, the ITS codes were developed to simulate realistic physical problems, allowing for complex geometries consisting of different materials. The original ITS codes were designed for electron transport from 10s of MeV to 1 keV. Updates were made to extend the energy range of the code from 1 keV to 1 GeV for electrons and photons [ref. 28] and updated the physical models, enhanced user friendliness, and added additional user options [ref. 29]. More recently, the integration of particle tracking within CAD geometries and the capability of performing adjoint particle transport within CAD geometries were added [ref. 30].

The processes included in the electron/photon continuous-energy transport include [ref. 29]:

1. Electron/Positron: Energy loss straggling, elastic scattering, production of knock-on electrons, impact ionization followed by production of fluorescence photons and/or Auger electrons, Bremsstrahlung production, and the production of annihilation radiation.
2. Photon: Coherent scattering, pair production, the photoelectric absorption with the production of photoelectrons, auger electrons, and fluorescence photons, and incoherent scattering with the production of scattered electrons.

Running the continuous-energy ITS (version 6.7.112) analysis is a two-step process [ref. 31]. The first step was to create a valid cross-section file using the XGEN program. One of three continuous-energy Monte Carlo codes (i.e., TIGER for one-dimensional (1D), CYLTRAN for two-dimensional (2D), and ACCEPT for 3D geometries) was used for particle transport analysis. For this study, the TIGER 1D simulation code was used without any adjustment in the default physics options for electrons and photons. Mono-energetic electrons were simulated using a cosine angular distribution incident on aluminum, Teflon™, and Z-93 slabs with total thicknesses of 1.25x the CSDA range of the incident electron.

6.6 MCNP

[Contributed by Robert Singleterry of LaRC]

(A) Introduction and Background

The MCNP 6.2 [ref. 32] Monte Carlo code system was used to calculate doses in thin materials of aluminum, Z-93 paint, and Teflon™. A theory or physics manual is no longer publicly available for MCNP 6.2. However, a theory and user manual exists for the latest release of MCNP designated as Version 6.3.0 [ref. 33] and is the source of the information that is not included in the publicly available Version 6.2 user manual. MCNP 6.3.0 was released by RSICC (Radiation Safety Information Computational Center at Oak Ridge National Laboratory (ORNL)) during this project and therefore was not used in the calculations. Any physics models not directly referenced can be found in either of the two identified MCNP user manuals.

MCNP differs from other Monte Carlo codes described in this report because it is fundamentally an engineering tool and not a physics tool. By default, most of the esoteric physics is turned off for increased throughput. Also, most fair game biasing options are turned on by default to increase throughput. Unfair game biasing techniques can be used to increase throughput, but those biasing techniques were not used in these calculations. MCNP is input desk driven and it is not necessary to write, compile, or verify code to use MCNP.

MCNP is mostly used in the nuclear reactor and nuclear criticality community, but is being used increasingly in the space, accelerator, fusion, and radiobiological protection communities. Because of the engineering mode of design and operation for this code, it is the fastest time-tosolution code available for 99% of the engineering use cases that exist. MCNP can be used by novices to the communities that MCNP serves.

(B) Monte Carlo Fundamentals and Variance Reduction

The Monte Carlo technique is a random walk of particles from a source to the edge of the geometry, energy grid, time grid, or some other aspect of the physical problem being simulated called phase space. These random walks are called histories identified by the starting or source particle. Analog Monte Carlo sets the weight of the particle at a value of 1, which does not change during a history. Only 1 particle is followed until it exits the phase space. If that history does not pass through or hit the tally (i.e., the region where a quantity of that particle is to be recorded), then that history was ineffective. While MCNP can use analog Monte Carlo, it is inefficient as many of the histories do not contribute to the tally.

The variance, or the first moment of the mean, goes as 1/N, where N is the number of histories that pass through the tally (i.e., not the number of histories used to get histories that hit the tally). A more familiar term is standard deviation and goes as $1/\sqrt{N}$. To determine if the tally has converged and the mean represents the expected value, MCNP calculates 10 checks to aid the user in determining how accurate the mean is in a statistical sense to the expected value.

MCNP has many variance reduction techniques available. The terms fair and unfair game have been mentioned. A ‘fair’ game means that the variance technique does not push particles in a history towards a tally and away from phase space regions with no tally. The particle’s weight during a history is changed strictly through the physics of the interactions. An ‘unfair’ game does push particles in a history towards a tally and away from phase space regions without a tally. Ultimately, these techniques reduce the variance in a tally without increasing the number of histories that must be generated. Fair game variance reduction can be used by novice users to increase their throughput. Unfair games need to be understood so that spurious results are not obtained and recognized by the user. All MCNP calculations in this report were performed with the default implicit capture variance reduction technique.

The implicit capture, or survival biasing, variance reduction technique allows the particle weight to change as a function of the interaction. When a particle has an interaction, if that particle is absorbed, then in analog transport that particle history is finished and a new particle history is started back at the source. For implicit capture, at the same absorption interaction, the particle’s history continues only with its weight reduced by the 1, the absorption cross section divided by the total cross section. Therefore, the history has a greater chance of hitting the tally and decreasing the variance in that tally with the same number of histories as analog Monte Carlo.

(C) Physics

Many physics models are included in MCNP. Figure 6.6-1 outlines energy regions and particles and what type of models are used.

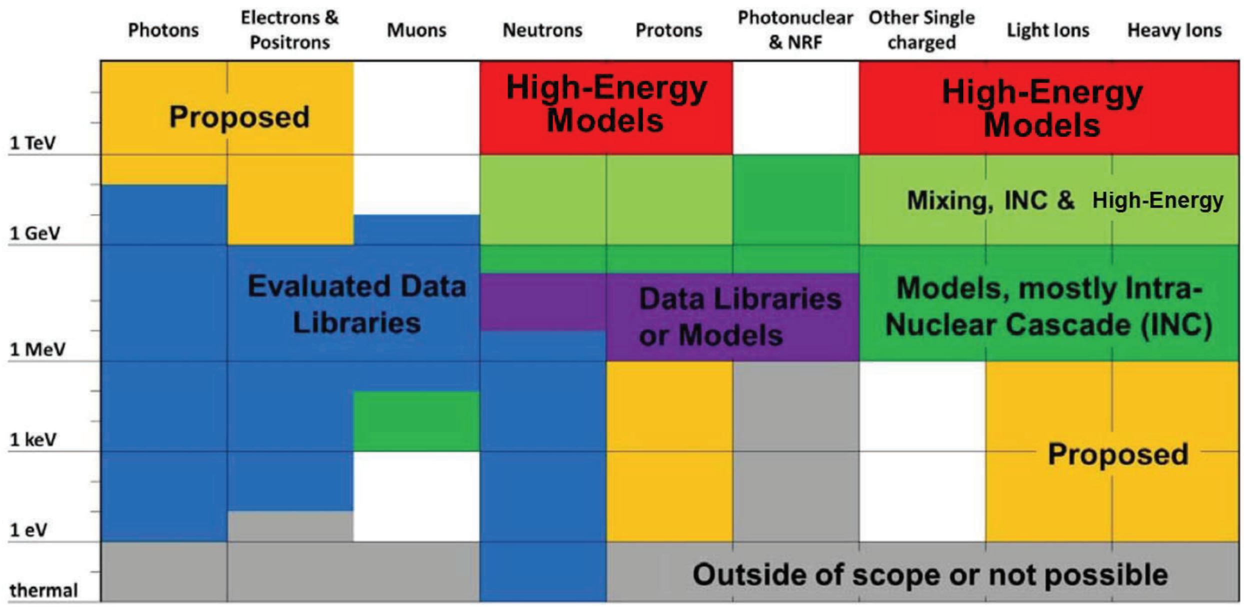

Figure 6.6-1. Model Types Used by MCNP by Energy and Particle

For charged particle stopping powers, MCNP6 uses the continuous slowing down approximation with coefficients computed by the Bethe-Bloch formula with Sternheimer and Peierls density effect corrections. Ionization potentials from International Commission on Radiation Units & Measurements (ICRU) Report 37 are used. A low-energy SPAR model[4] is used below 1.31 MeV/AMU[5]. A linear interpolation between the two models is used between 5.24 and 1.31 MeV/AMU. Muon stopping powers are defined in Reference 34.

For energy straggling, Landau theory is used for electrons, and Vavilov theory is used for heavy charged particles (e.g., hadrons and mesons). A gaussian distribution is used at high energies. Coupled photon/electron physics are controlled by libraries. All relevant physics is included in the libraries and are based on Evaluated Nuclear Data File (ENDF)/B-VI.8. Below 1keV, single event transport is used [ref. 35].

For this effort, the highest energies of the source particles are limited to 100 MeV protons and 10 MeV electrons. Therefore, the high energy models used by MCNP are not relevant and will not be discussed in this paper. Relevant physics that is off by default was turned on. Those physics options are:

1. Light and heavy ion recoil for neutrons using two-body kinematics
2. Light ion recoil for protons using two-body kinematics and the appropriate ionization potential
3. NCIA or neutron capture ion algorithm which creates light ions from neutron capture
4. Photonuclear effects

[4] A computer program to calculate stopping powers and ranges for muons, charged pions, protons, and heavy ions

[5] AMU = atomic mass unit

6.7 NOVICE

[Contributed by Thomas Jordan of EMPC]

(A) Code Overview

NOVICE is a Fortran code for radiation environments, transport, and effects analysis, created and developed by Thomas M. Jordan and licensed by EMPC. NOVICE has the unusual feature of providing all major analyses: Ray Trace, FMC, and Adjoint RMC, in one code. Other uncommon NOVICE characteristics include its ability to analyze all types of space radiation effects, including, but not limited to, TID and SEE, and its use of point versus volume detectors. NOVICE features a 3D Graphical User Interface (GUI) for CAD/CSG (Constructed Solid Geometry) modeling.

NOVICE is widely used in space exploration, defense, and commercial programs. Most significant science and defense programs, including the GPS constellation, Hubble Space Telescope (HST), James Webb Space Telescope (JWST), Solar Dynamics Observatory (SDO), Magnetospheric Multiscale (MMS) program, and numerous commercial/communications programs, rely/relied on NOVICE.

For physics modeling, NOVICE features data libraries from US national laboratories for neutral and charged particles:

1. Multi-group cross sections from ORNL SCALE and SNL Coupled Electron-Photon Cross Section (CEPXS).
2. Point-value cross sections from the National Institute of Standards and Technology (NIST), the Naval Research Laboratory (NRL), and the SNL, Los Alamos, National Laboratory (LANL), and Lawrence Livermore National Laboratory (LLNL).

For physics modeling, NOVICE features data libraries from US national laboratories for neutral and charged particles:

1. Multi-group cross sections from ORNL (SCALE) and SNL (CEPXS).
2. Point-value cross sections from NIST, NRL, SNL, LANL, and LLNL.

The Adjoint and FMC 3D analyses provide particle simulation. Ray-trace approximations use tabulated attenuation tables for dose, damage, charging, x-ray interface dose-enhancement, and integral fluxes with multiple thresholds, integral linear energy transfer (LET) fluxes, upsets for multiple threshold critical charges, pC (pico-Coulombs), all of which are generated internally. Ray-trace parametric gives incremental shielding as stereolithography (STL) files for 3D printing.

In Earth orbit, the dominant radiation environments are trapped electrons and protons from the Van Allen belts and heavy ions from Solar Particle Events (SPE) and Galactic Cosmic Rays (GCR). Trapped and SPE particles dominate total-dose/damage/charging effects. SPE and GCR (i.e., heavy ions with atomic numbers 1 through 92) dominate SEEs. By contrast, Jovian local space has more intense trapped radiation with electrons to 1 GeV. Lunar space regolith albedo secondary environments/transport/effects are documented, power-law spectra suffice.

NOVICE environment modeling includes both particle energy and the space-time character of position-direction-time. The combination is called a 'source' or an 'initial phase space distribution'. Similarly, radiation effects include particle energy and the space-time character of position-direction-time; the combination is called a ‘detector’, the ‘tallied phase space distribution’, or the ‘scored phase space distribution’.

The connection between environments and effects is ‘particle transport’. In the generality of solving particle transport problems, mathematically a double integral over initial and scoring phase space dQ dQ’ where Q = x,u,e,t and dQ = dV dU dE dT, or in linear algebra notation where linear counting of phase space intervals dQi around Qi covering all phase space:

$$A = \text{Answer} = [\text{Source}]\ [\text{MultiCollisions}]\ [\text{Detector}] = \mathbf{S\ M\ D} \tag{1}$$

where

$$\mathbf{M} = M(Q,Q') = \mathbf{N + NCN + NCNCN + \ldots = N + NCM = N + MCN} \tag{2}$$

$$\mathbf{N} = N(Q,Q') \ \text{free-flight, } \exp(-ks),\ k = \text{total cross-section, } s = |\mathbf{x' - x}| \tag{3}$$

$$\mathbf{C} = C(Q',Q) \ \text{collision, } C = d2k(Q',Q)/dUdE, \text{ single-scatter + secondaries (explicits)} \tag{4}$$

$$\mathbf{M}^{-1} = \mathbf{N}^{-1} - \mathbf{C} \ \text{from: } \mathbf{M^{-1}\{N = M - MCN\}N^{-1}} \text{ and } \mathbf{N^{-1}\{N = M - NCM\}M^{-1}} \tag{5}$$

Condensed-history ion transport adds CSDA energy loss to N (e' = e - s<L>) where L is LET, and for C, uses angular and energy-loss straggling with Poisson/plural scattering for any k>0 explicitly being retained.

(B) Physics Implemented in NOVICE Relevant to this Study

Particle type and energy source spectra are generated internally from: Short Orbital Flux Integration Program, SOFIP[6] (for trapped AE8/AP8 models and AL solar flares), GCR (for z = 1-92 CREME96[7] spectra from GCR and SPE), analytic formulae (fission neutron, black-body x-ray, exponential, power-law, Gaussian), a tabulation saved in a library format specific to fragmented data retrievals, or an external file with paired energy-spectrum (differential, interval-group, integral) including an International Radiation Environment Near Earth (IRENE), SPace ENVironment Information System (SPENVIS)[8] AE9/AP9 output, or a requirements document table.

Typical particle type and energy detector responses are: unity for counting particles (integral flux/fluence by thresholds, solid-angle bins, moments), linear-energy-transfer L(e') for energy-deposition/dose in the material at the detector location (or any other target material in the limit of a point detector), biological dose-equivalent (using quality factors), non-ionizing energy loss (NIEL) tabulations (neutron recoils and NRL ion data by target material with secondary electron slowing down spectra weighted by electron NIEL for photon damage), photon dose-enhancement (from secondary electron slowing down spectra for material pairs), lineal-energy-loss thresholds (biological), LET thresholds for upsets, and induced ionization thresholds for upset/latchup on device specific geometry/materials.

SOFIP source spectra are saved in a FluxFile and used to generate 1D tabulated attenuation tables (TATs) using SHIELDOSE-1 or -2 for transport in aluminum with several total dose targets. Alternatively, 1D Adjoint RMC is used for any shield/target material combination with

[6] https://ntrs.nasa.gov/citations/19790015709

[7] https://creme.isde.vanderbilt.edu/

[8] https://www.spenvis.oma.be/

FluxFile data by particle type/energy at every thickness and TATs for rad_cGy/rem_cSv, NIEL-damage, and stopping density. TATs can be defined from requirement tables.

Heavy-ion z=1-92 source spectra are transported using numerical integration, with a saved FluxFile and rad_cGy/rem_cSv dose-thickness TATs. Another numerical procedure converts FluxFiles to log spaced threshold tables of: integral-fluxes, integral LET fluxes, and integral-upset-latchup for different threshold charge pC by device.

Several numerical methods are used in NOVICE transport analysis for space applications. Direct numerical integration and adjoint/FMC particle simulation are used for detailed physics in simple 1D symmetric solid geometries. This 1D analysis serves two purposes: first a basic understanding of how an environment-effect pair is reduced by material between the source and detector, a prime example is SHIELDOSE output tables. The second purpose is the production of tabulated attenuation tables, TATs, for effect reduction with incremental shield thickness, used in ray-trace applications that interpolate the tables on mass thickness, ray by ray.

All source-spectra and detector-response energy distributions, once modeled and used to generate 1D TATs, are retained for subsequent forward/adjoint 3D Monte Carlo particle simulations.

Monte Carlo particle simulation and ray-trace approximations are used in NOVICE for the complex 3D solid/shell geometries that include: space systems, enclosures, devices, astronaut phantoms computerized anatomical female (CAF) and computerized anatomical man/male (CAM), and habitats. Geometry modeling systems include CSG, combinatorial solid geometry, and CAD. CSG dominated space applications in the late 1900s and is still used for heritage subsystems and quick models (e.g., test setup). CAD includes anything from the current modeling systems with interface files in Initial Graphics Exchange Specification (IGES), Standard for the Exchange of Product Data (STEP), Advanced Computerized Implementation of Standards (ACIS), and Virtual Reality Modeling Language (VRML) formats (i.e., legible text files) with bill-of-materials in text or spreadsheet formats. Overlaps and undefined space are allowed and handled consistently, and undefined space can be atmosphere filled.

Particle energy distributions (e.g., spectra, transport, responses) are critical, and are described in logarithmic detail from 1 eV through 1 TeV per AMU for heavy ions with 10, 100, to 1000 intervals per decade. This energy detail is an essential part of SDEF outputs for MCNP and includes uniform importance-weighting to achieve accuracy at all material depths

The NOVICE GUI features numerous proprietary capabilities with emphasis on viewing phase-space particle sources and detectors, SEE parameters, and openGL 3D graphics for CAD geometry models; systems, subsystems, devices, and components, to visualizing the location of detector points used for most ray-trace and adjoint RMC analysis. NOVICE maintains interfaces with MCNP and ITS, input and output, where a TOPAS-GEANT4 interface is anticipated.

(C) EMPC code updates made for this project

Two changes were made in NOVICE to accommodate the project's requirements. Modifications were made to SHIELDOSE-1 and -02 within NOVICE, and the NIST ESTAR and PSTAR libraries[9] were added as options to accompany NOVICE's pre-existing libraries.

---

[9] https://physics.nist.gov/PhysRefData/Star/Text/intro.html

1) Modifications to SHIELDOSE-1 and -2
   a) F to E formats for low-energies and small-thicknesses
   b) Mono-energetic spectra, with work in process
2) NIST ESTAR/PSTAR element libraries for electrons and protons
   a) NOVICE, option to use NIST elemental stopping-power data
   b) Direct compare NIST/EMPC libraries, with work in process
      i) Proton and electron, 1eV to 1TeV with log spacing
      ii) Forward-adjoint reduced-order (FARO) algorithms

D) Calculated results with incident electrons and protons for this project

1) Using *adjoint 1D with narrow spectrum approximation -- 13Al only
2) using *adjoint 3D with narrow spectrum approximation -- 13Al only
3) using *beta 3D FMC, mono-energetic energies -- 13Al, Teflon™, and Z93-paint

7.0 Analysis – Comparison to the SHIELDOSE-2 Look-up Tables

This section summarizes the results from a series of comparisons between SHIELDOSE-2 and other codes where the comparisons were performed on simple and representative problem setups Specifically, because the interest was in understanding the capability/validity of SHIELDOSE-2, the comparisons were performed for the geometry/material relevant to the SHIELDOSE-2 look-up tables at selected energies (see the Phase 1 report for more details on the SHIELDOSE-2 look-up tables). The comparison for the lowest energy of the SHIELDOSE-2 look-up tables were included because the thickness applicability is closely related to the lowest energy of electrons or protons used in building these tables.

7.1 Problem Setup

The problem set up was repeating the material and geometry used in the SHIELDOSE-2 look-up table construction. This consisted of the material and geometry is an aluminum slab, where the slab thickness is defined as 1.25*CSDA range in cases of electrons or 1.0*CSDA range in cases of protons. The energies and the CSDA ranges used in the simulations are shown in Table 7.1-1. As with the original SHIELDOSE-2 tables, the slab is divided into 50 sublayers. Hence, one sublayer thickness is 0.025 of the CSDA range for electron cases and 0.02 of the CSDA range for proton cases. The incident particles were simulated with a cosine-law distribution to emulate the isotropic space environment. The energy deposition at each layer was computed. It was instructed that each code should employ the best and the most accurate computation algorithms available in each code for this thin target application.

Table 7.1-1. Energies of Electrons and Protons used in the Comparisons and the Respective CSDA Ranges in Aluminum

Electron, MeV	Range, g/cm^2	Range, cm	Proton, MeV	Range, g/cm^2	Range, cm
0.005	1.09E-04	4.04E-5	0.01	5.94E-05	2.20E-5
0.01	3.54E-04	1.31E-4	0.1	2.63E-04	9.74E-5
0.1	1.87E-02	6.93E-3	1.0	3.95E-03	1.46E-3
1.0	5.55E-01	2.06E-1	10.0	1.71E-01	6.33E-2
10.0	5.86E+00	2.17	100	1.00E+01	3.70

7.2 Simulation Results and Discussion

Figures 7.2-1 to 7.2-5 show the results for electrons which include the contributions from Bremsstrahlung, and Figures 7.2-6 to 7.2-10 for protons. As noted, because the main objective of these comparison study is to provide a reference database based on the most accurate simulations by each code compared to the SHIELDOSE-2 tables, deep-dive to understand the root cause of discrepancies is avoided. Furthermore, the code developers could use the results presented to check the transport physics implementation in their respective codes.

General observations include:

1. As shown, there are generally larger discrepancies at low energies while the agreements are typically better at higher energies. The lowest energy results (i.e., 0.005 MeV electron and 0.01 MeV proton) show larger scatter among the codes. This indicates the radiation dose calculations at low energies, which corresponds to thin materials are subjected to larger uncertainties.
2. The NOVICE results for the 0.005, 0.01 and 10 MeV electron cases and for the 1-MeV proton case deviate from other codes' results. The discrepancy arises from EMPC's election to use NOVICE's RMC, instead of its ray trace or FMC options (including SHIELDOSE-1 and 2), in this study. RMC tracks particles from a detector point (i.e., NOVICE) or small volume (e.g., RMCs) to the source, the reverse approach of ray trace or FMC. RMC is accepted as the preferred approach for complex geometries and/or where accuracy can be prioritized over processing time, but it makes simulating mono-energetic incident particles inherently difficult. The goal of using NOVICE's RMC in this study was to demonstrate that, despite that inherent difficulty, RMC can return adequate results with the simple/solid geometries and mono-energetic environments of this study, for which RMC is not optimal.
3. The deviation of the MCNP results of the 0.005-MeV electron and for the 0.01-MeV proton from other code is visible.
4. The results from Geant4 and GRAS are comparable, which is expected because GRAS is a toolkit based on Geant4.
5. FASTRAD's results are comparable to Geant4, which is expected as the physics is based on Geant4.
6. The Geant4 low-energy results show a sudden drop at the lowest thickness point.
7. Generally, the electron and the protons results $\geq$ 1 MeV from Geant4, GRAS, FLUKA, ITS, and FASTRAD are clustered with the SHIELDOSE-2 tables.

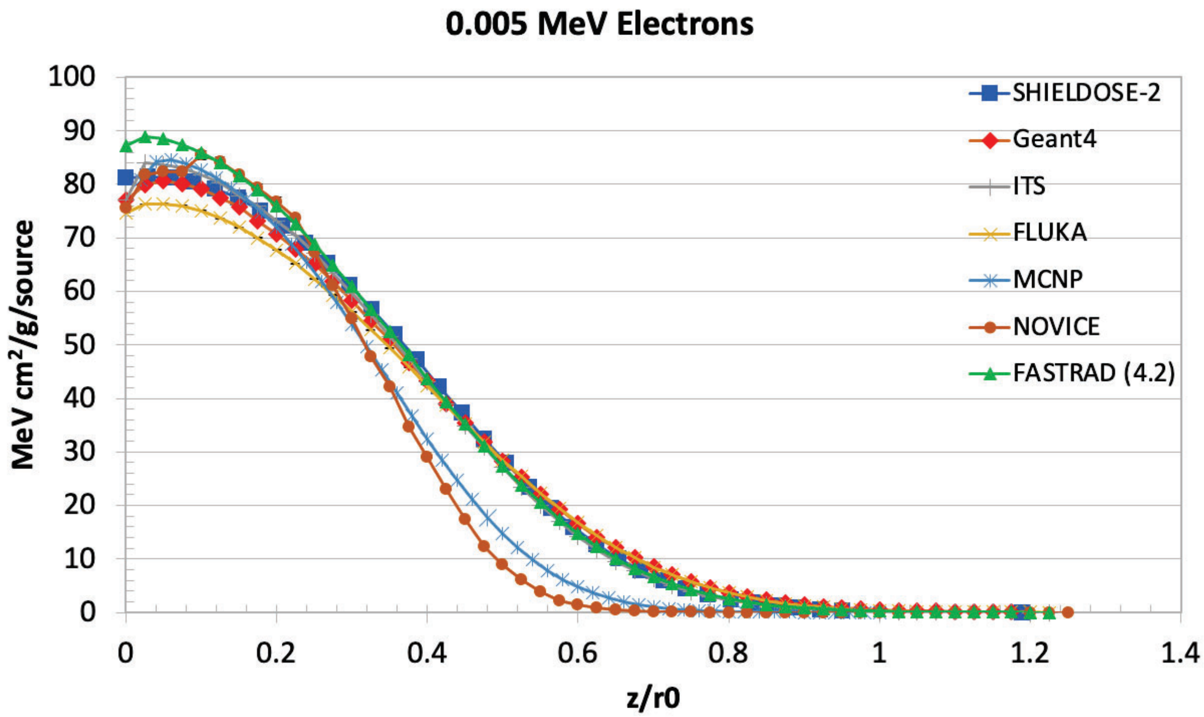

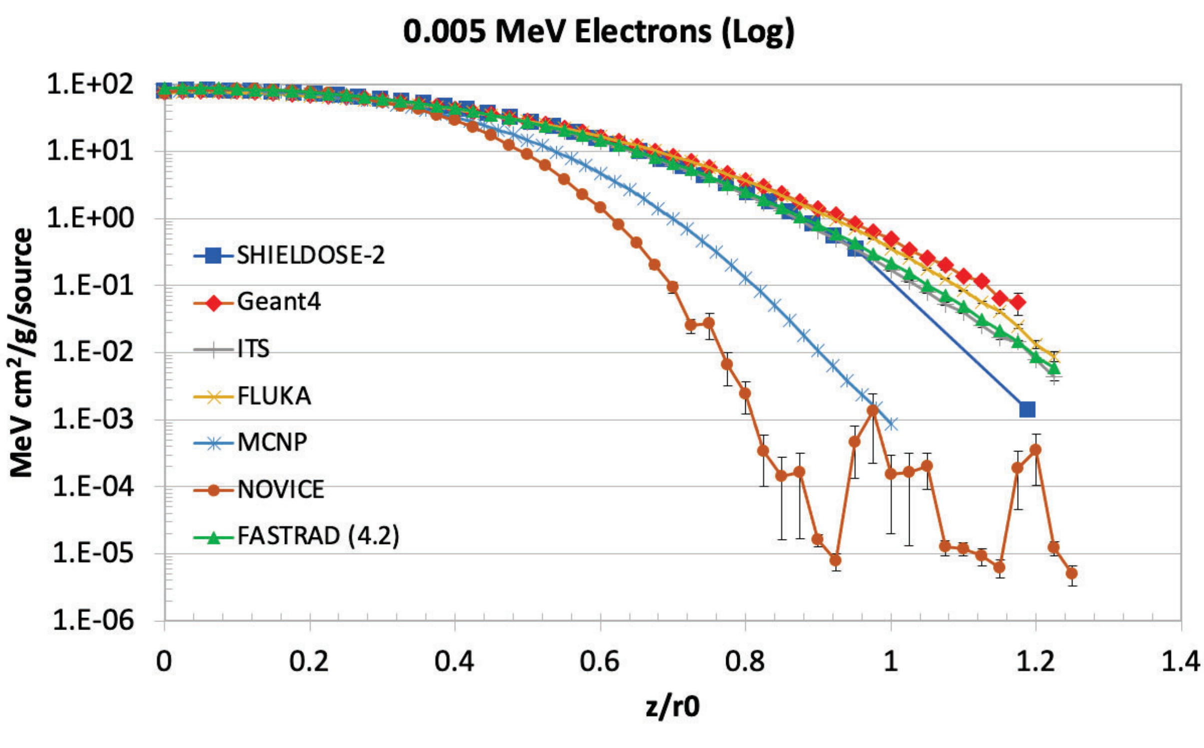

Figure 7.2-1. Comparison for the 0.005-MeV Electron Incident Case (Top: Linear scale, Bottom: Log scale). Note that GRAS is not included in the comparison. The range r_0 of 0.005 MeV electrons in aluminum is 4.04E-5 cm or 0.404 µm.

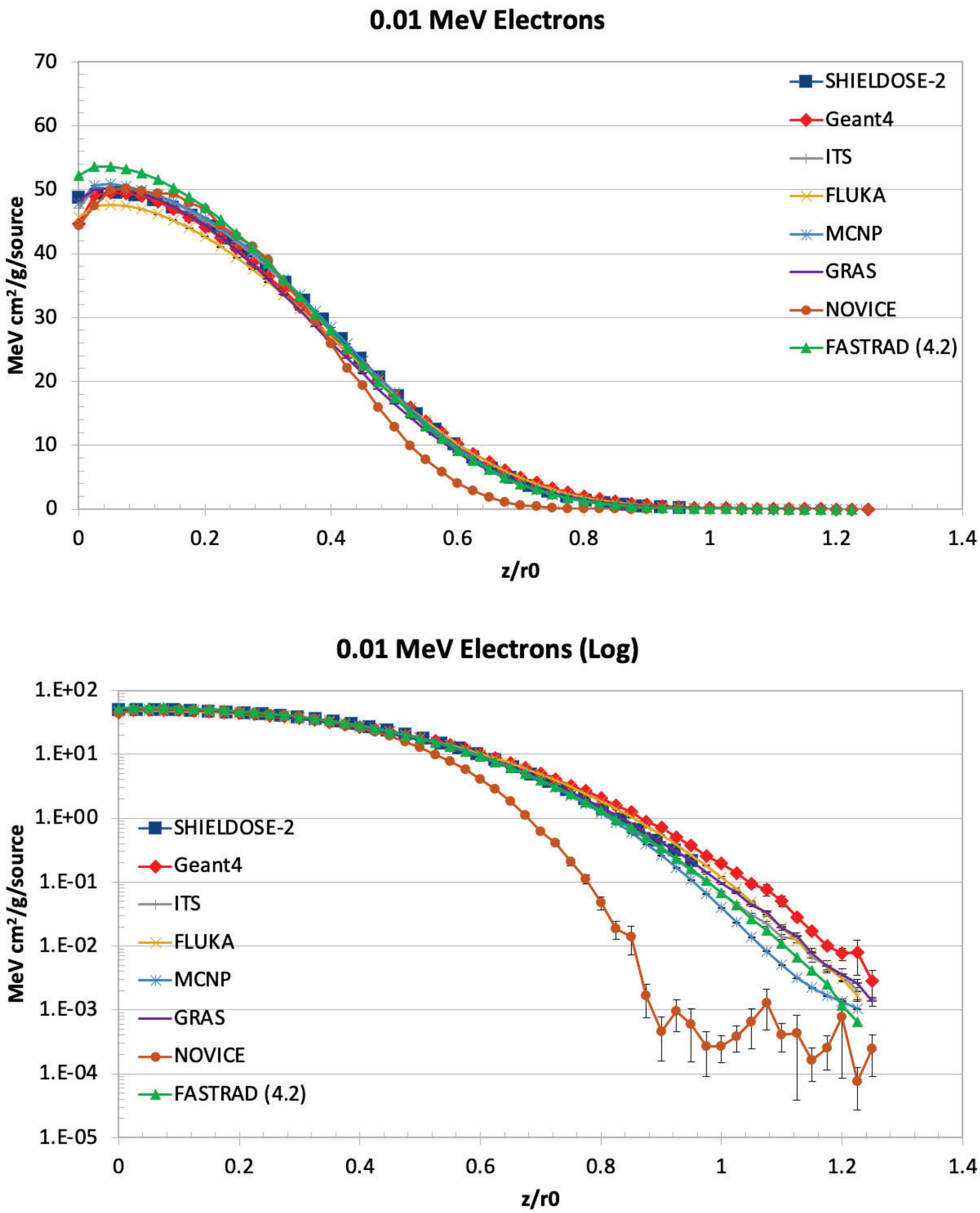

Figure 7.2-2. Comparison for the 0.01-MeV Electron Incident Case (Top: Linear scale, Bottom: Log scale). The range r_0 of 0.01 MeV electrons in aluminum is 1.31E-4 cm or 1.31 µm.

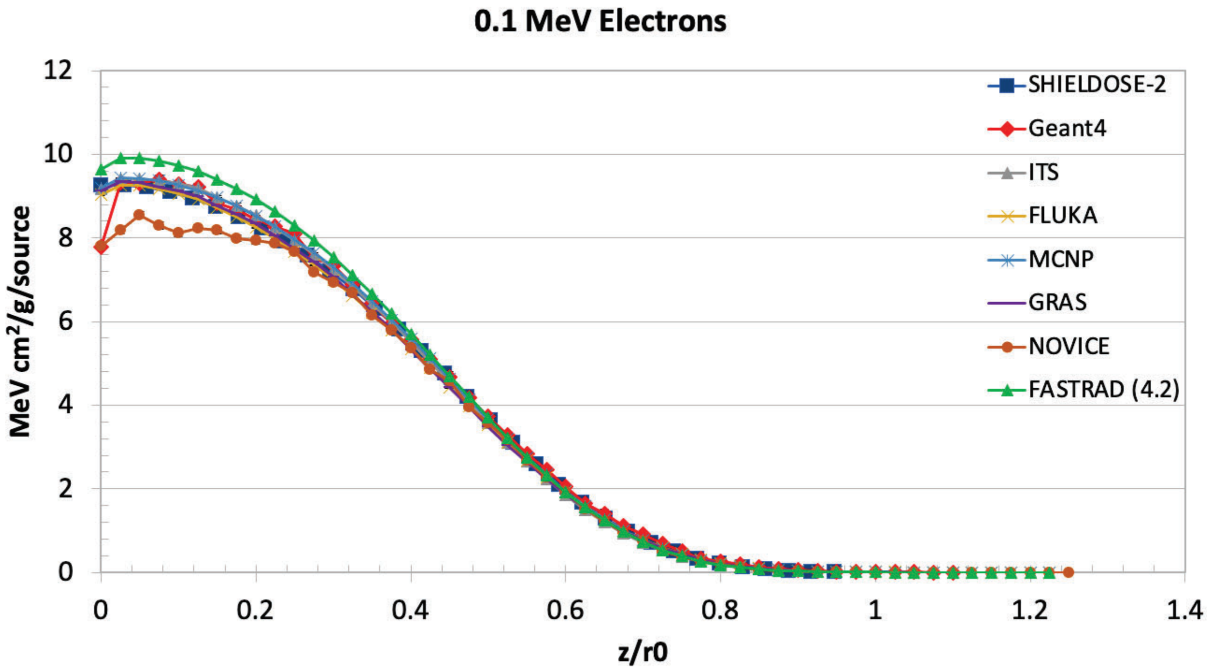

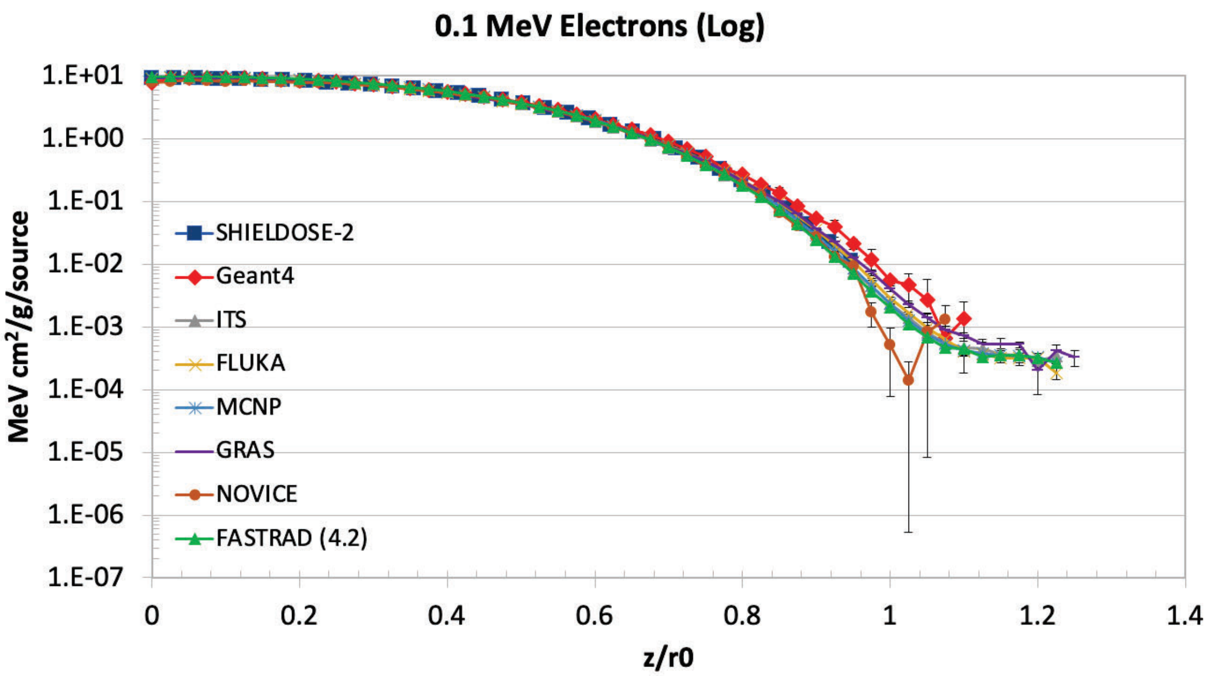

Figure 7.2-3. Comparison for the 0.1-MeV Electron Incident Case (Top: Linear scale, Bottom: Log scale). The range r_0 of 0.1 MeV electrons in aluminum is 6.93E-3 cm or 0.0693 mm.

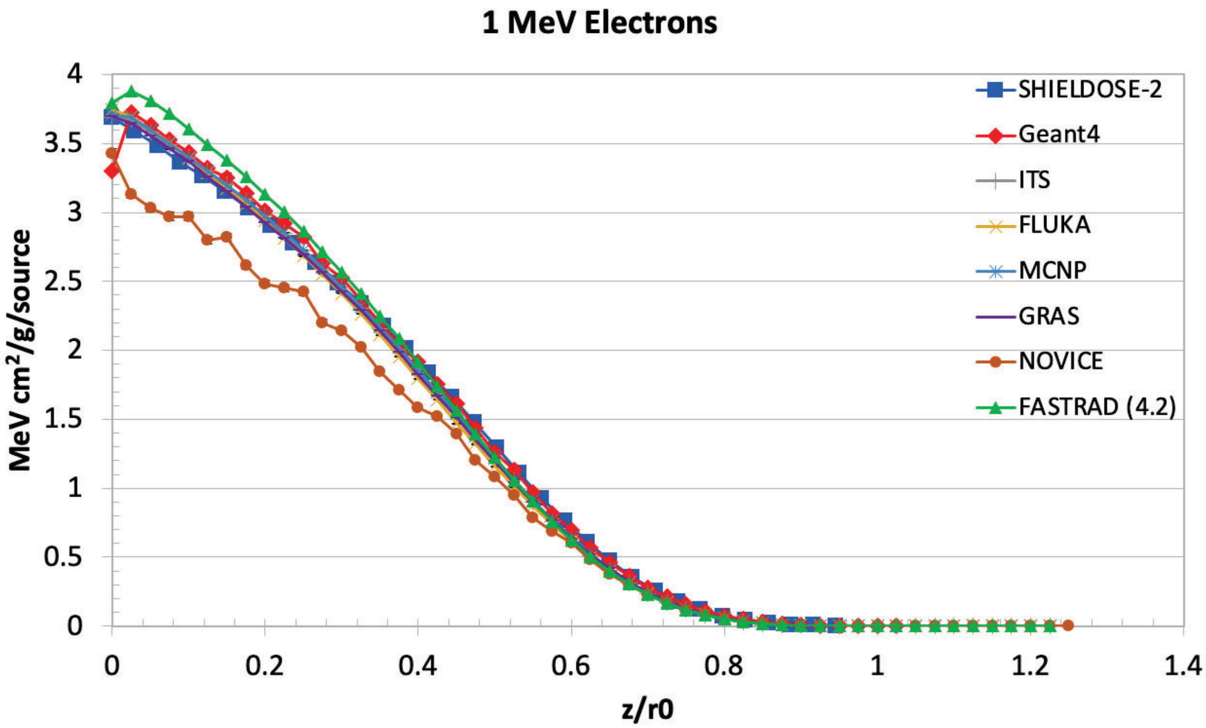

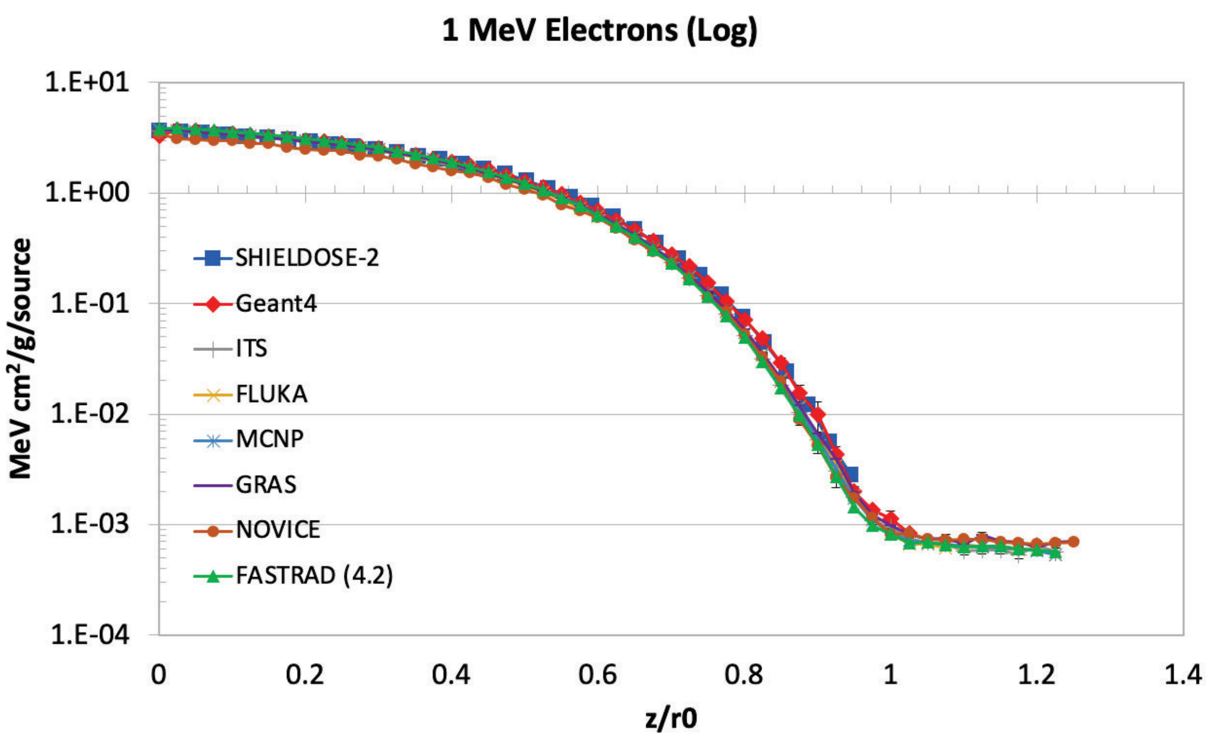

Figure 7.2-4. Comparison for the 1-MeV Electron Incident Case
(Top: Linear scale, Bottom: Log scale). The range r_0 of 1 MeV electrons in aluminum is 0.206 cm.

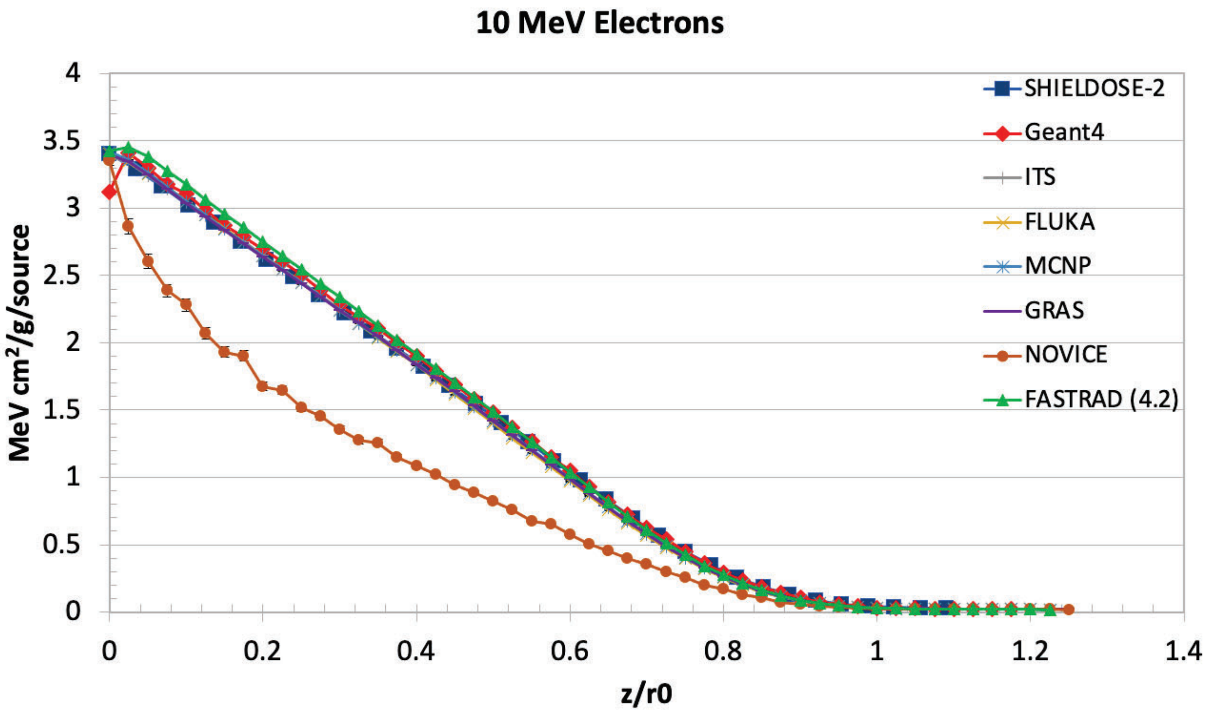

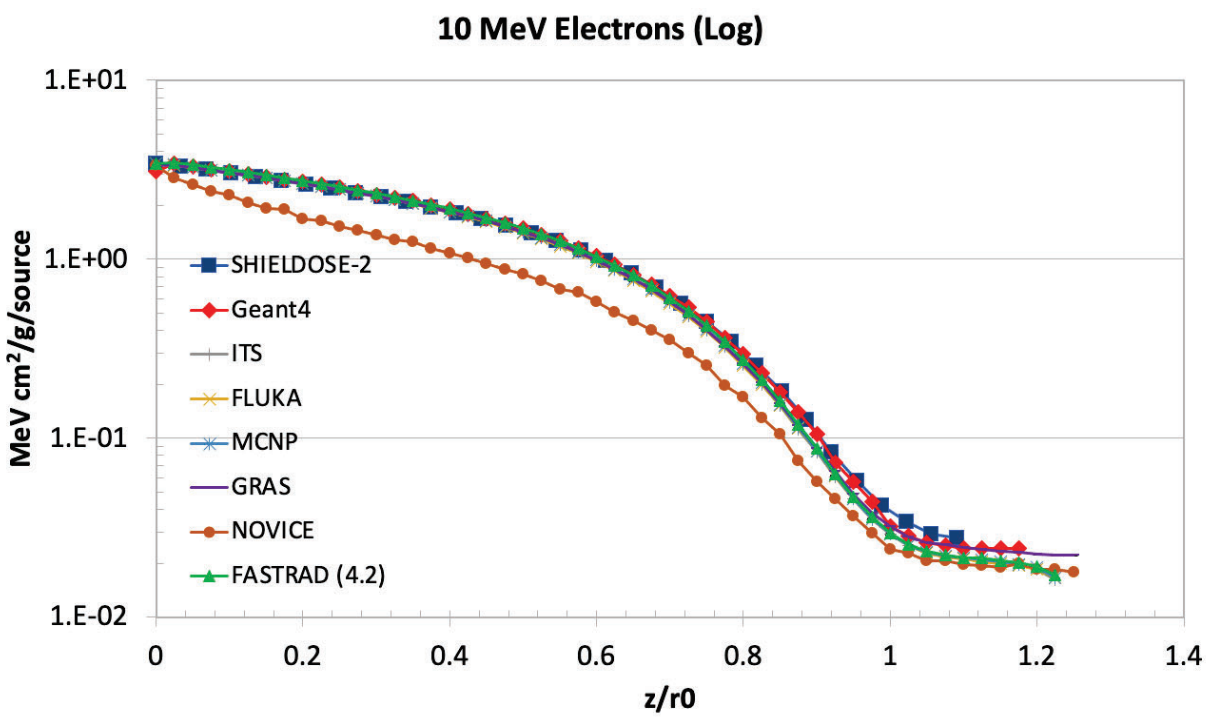

Figure 7.2-5. Comparison for the 10-MeV Electron Incident Case (Top: Linear scale, Bottom: Log scale). The range r_0 of 10 MeV electrons in aluminum is 2.17 cm.

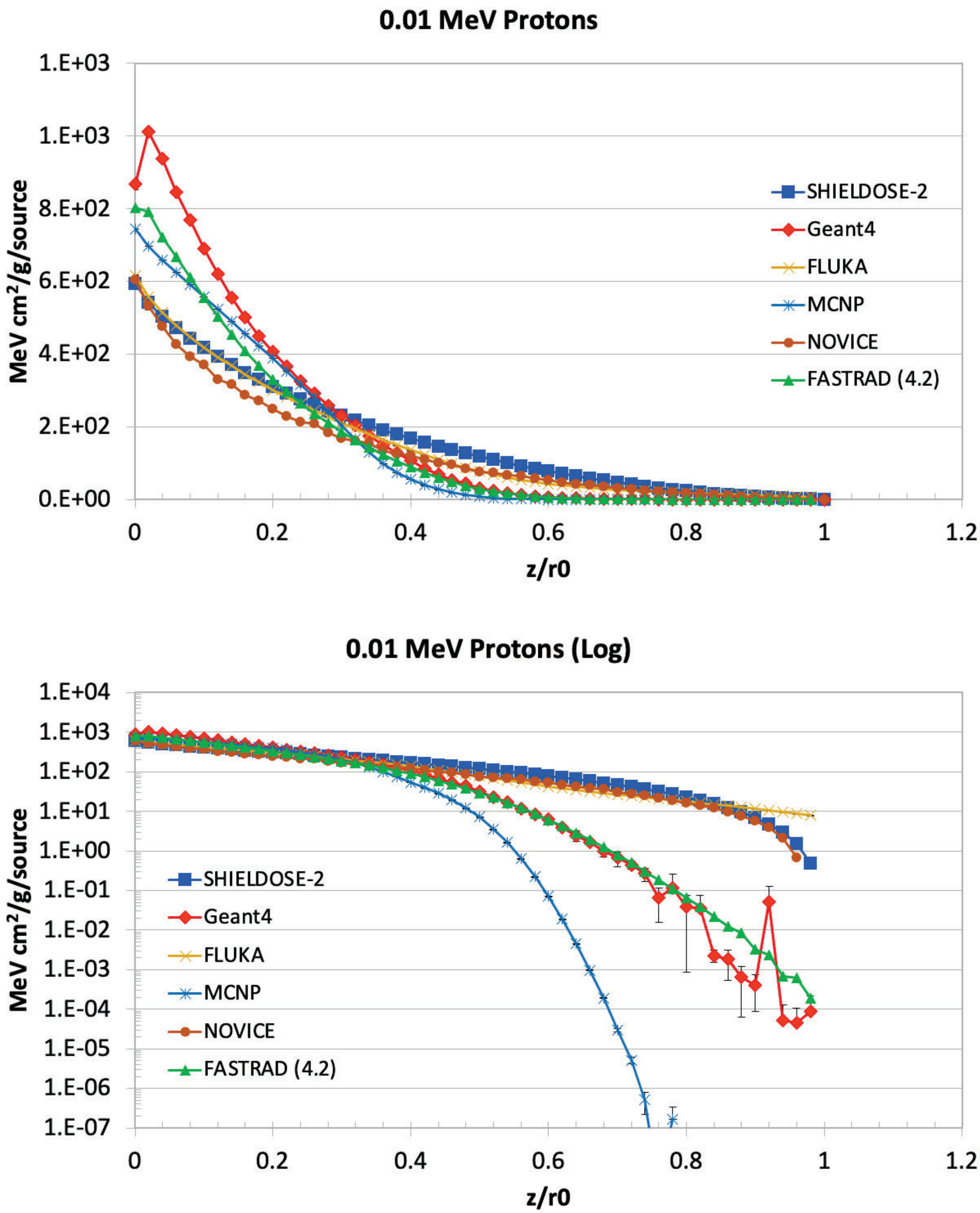

Figure 7.2-6. Comparison for the 0.01-MeV Proton Incident Case (Top: Linear scale, Bottom: Log scale). Note that GRAS is not included in the comparison. The range r_0 of 0.01 MeV protons in aluminum is 2.20E-5 cm or 0.22 µm.

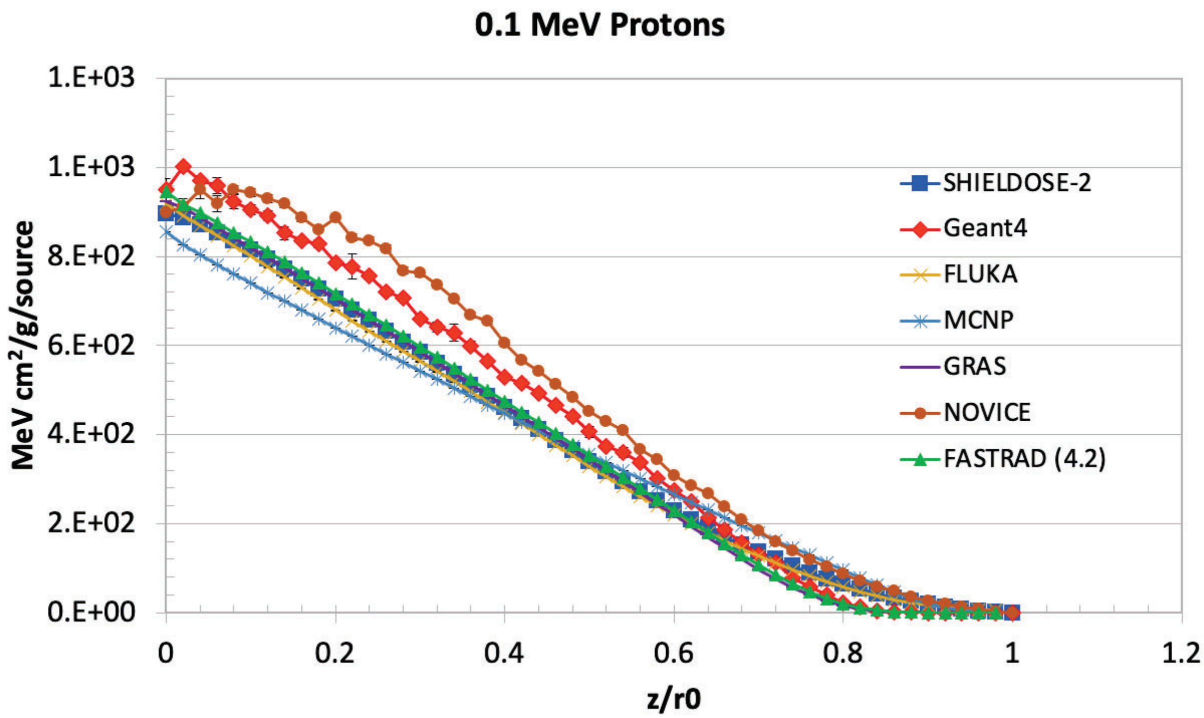

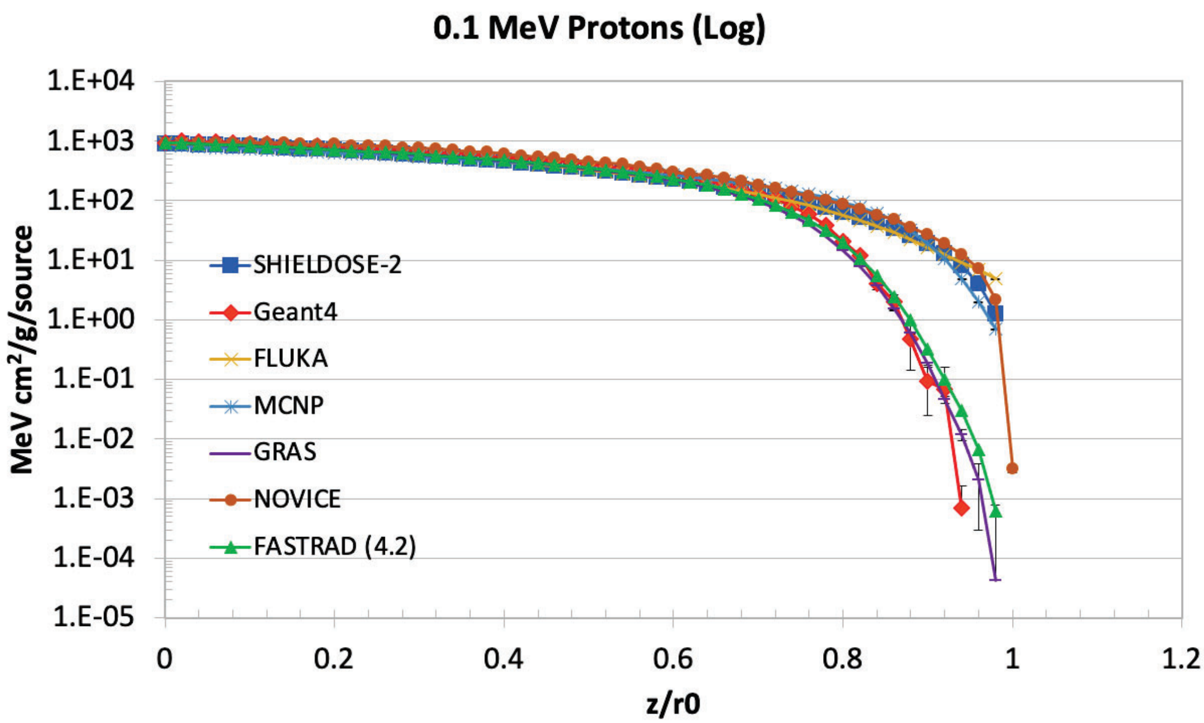

Figure 7.2-7. Comparison for the 0.1-MeV Proton Incident Case (Top: Linear scale, Bottom: Log scale). The range r_0 of 0.1 MeV protons in aluminum is 9.74E-5 cm or 0.974 µm

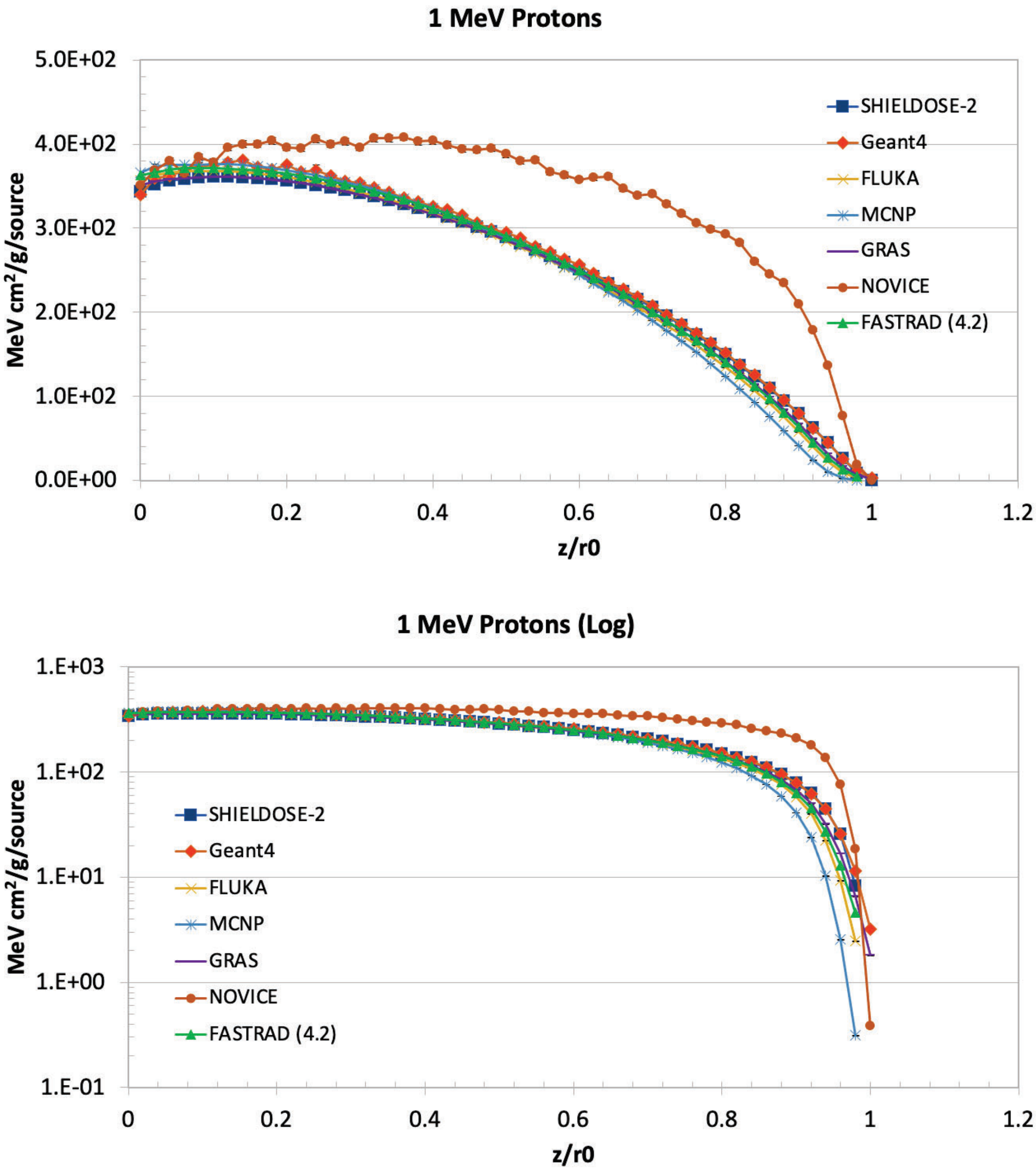

Figure 7.2-8. Comparison for the 1-MeV Proton Incident Case (Top: Linear scale, Bottom: Log scale). The range r_0 of 1 MeV protons in aluminum is 1.46E-5 or 0.0146 mm.

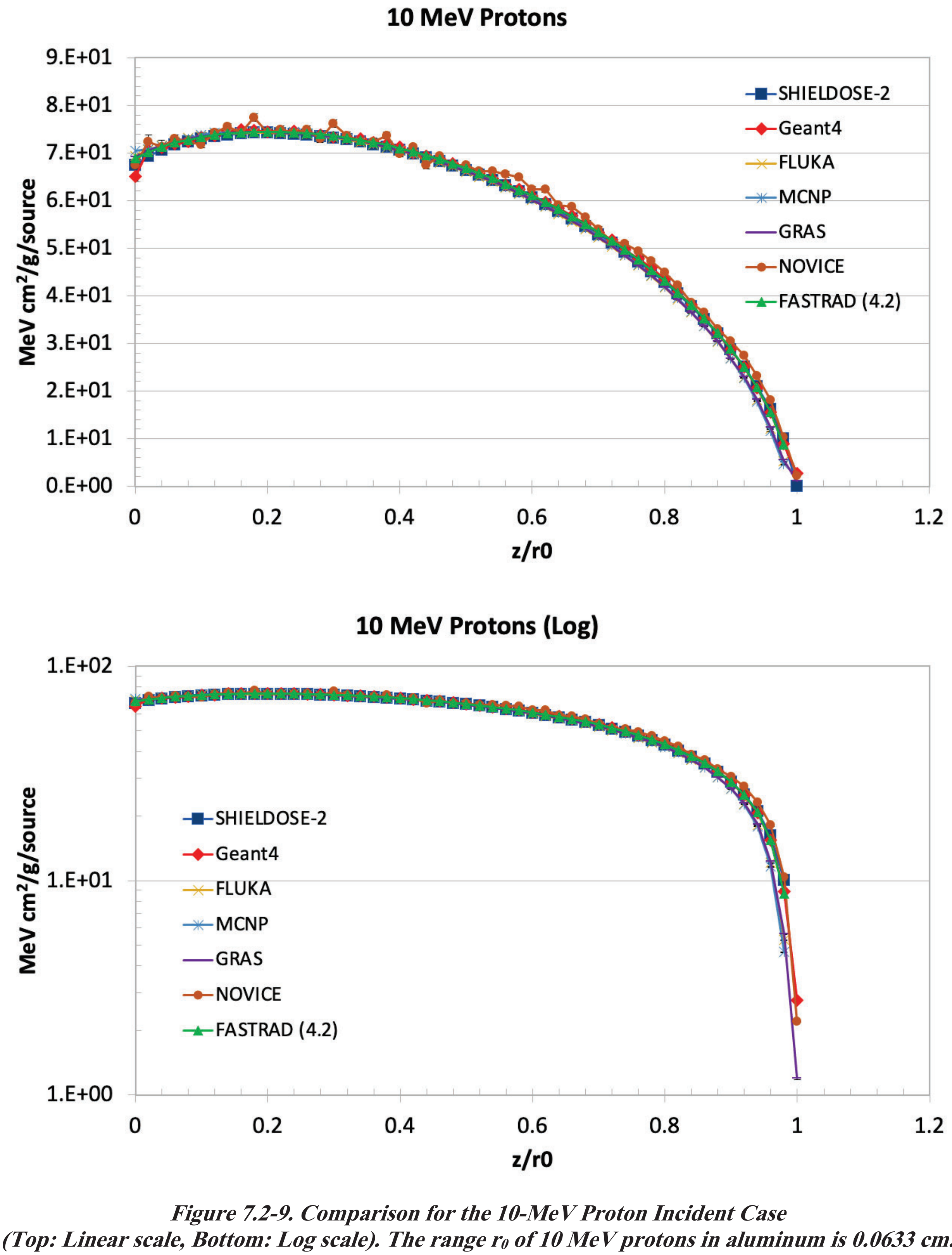

Figure 7.2-9. Comparison for the 10-MeV Proton Incident Case
(Top: Linear scale, Bottom: Log scale). The range r_0 of 10 MeV protons in aluminum is 0.0633 cm.

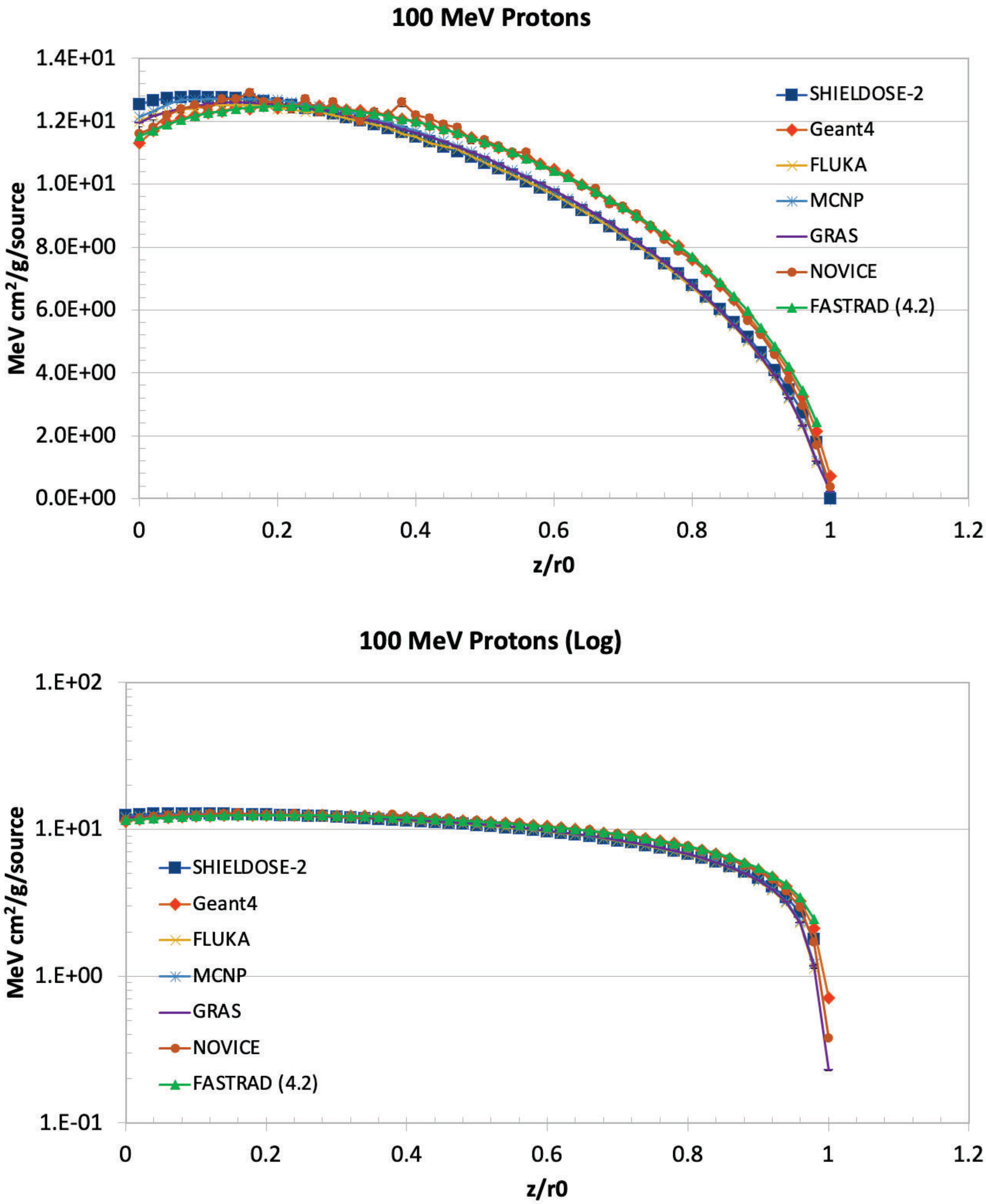

Figure 7.2-10. Comparison for the 100-MeV Proton Incident Case
(Top: Linear scale, Bottom: Log scale). The range r_0 of 10 MeV protons in aluminum is 3.7 cm.

8.0 Analysis – Density Scaling

Another series of simulations was performed to investigate the validity of density scaling for select materials at the request of the Artemis Program. As discussed in the Phase 1 report Section 7.2, aluminum is the only shielding material considered in SHIELDOSE-2. For other detector materials, SHIELDOSE-2 computes the doses using the spectra computed for the aluminum medium (see Equations in Figure 7.1-2 in the Phase 1 report), but with the stopping power for that specific detector material of interest. In the radiation-effect community, when encountered with different shielding media other than aluminum, density scaling is commonly used as an approximation, where material thicknesses are converted to the equivalent aluminum thickness using the density ratio[10]. For example, 1 cm of polytetrafluoroethylene (PTFE) Teflon™ with a bulk density of 2.2 g/cm^3 can be approximated by ~0.81 cm of aluminum with a density of 2.7 g/cm^3, or 0.489 cm of titanium with a density of 4.5 g/cm^3. In this way, the dose-depth distributions computed by SHIELDOSE-2 can be converted to the dose-depth distributions in other shielding materials. Note 'fluence spectra' used in the dose computations are for the aluminum medium. Two materials investigated were Teflon™ and Z93 paint whose material properties are shown in Table 8.0-1.

Table 8.0-1. Density and Elemental Composition of PTFE Teflon™ and Z93 Paint

	Z93 Paint	**PTFE Teflon™**
Density (g/cm^3)	1.95	2.2
Composition (weight fraction)	O: 0.2539 Si: 0.0910 Zn: 0.4017 K: 0.2534	C: 0.2402 F: 0.7598

As for the density scaling, the SHIELDOSE-2 aluminum tables were converted to 'equivalent' Teflon™ or Z93 paint tables for the same electron and proton energies as used in Section 7 using the density scaling. Then, each code was run for Teflon™ or Z93 paint and compare the results to the equivalent Teflon™ or Z93 paint SHIELDOSE-2 tables. The results are presented in the following figures:

(A) Figures 8.0-1 to 8.0-5 for Teflon™ with electron incident
(B) Figures 8.0-6 to 8.0-8.10 for Z93 paint with electron incident
(C) Figures 8.0-11 to 8.0-15 for Teflon™ with proton incident
(D) Figures 8.0-16 to 8.0-20 for Z93 paint with proton incident

Note that the electron figures include the contribution from Bremsstrahlung.

[10] Note there are other methods to convert aluminum thickness to thickness of the material of interest (e.g., References 36, 37, and 38). However, this study focused on the density scaling method.

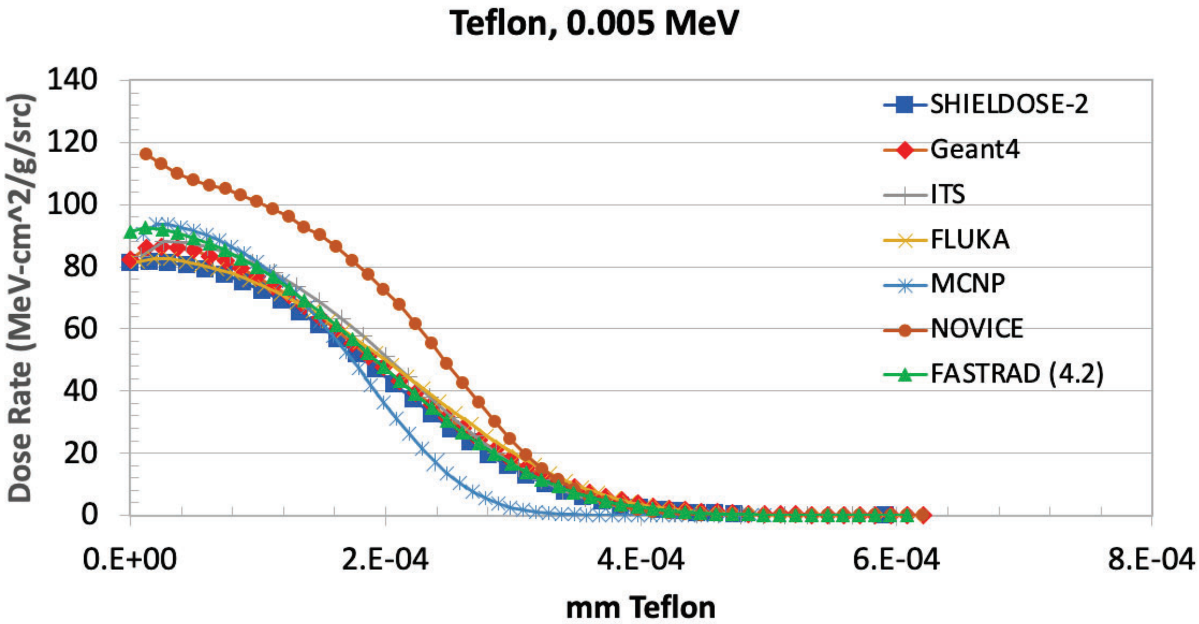

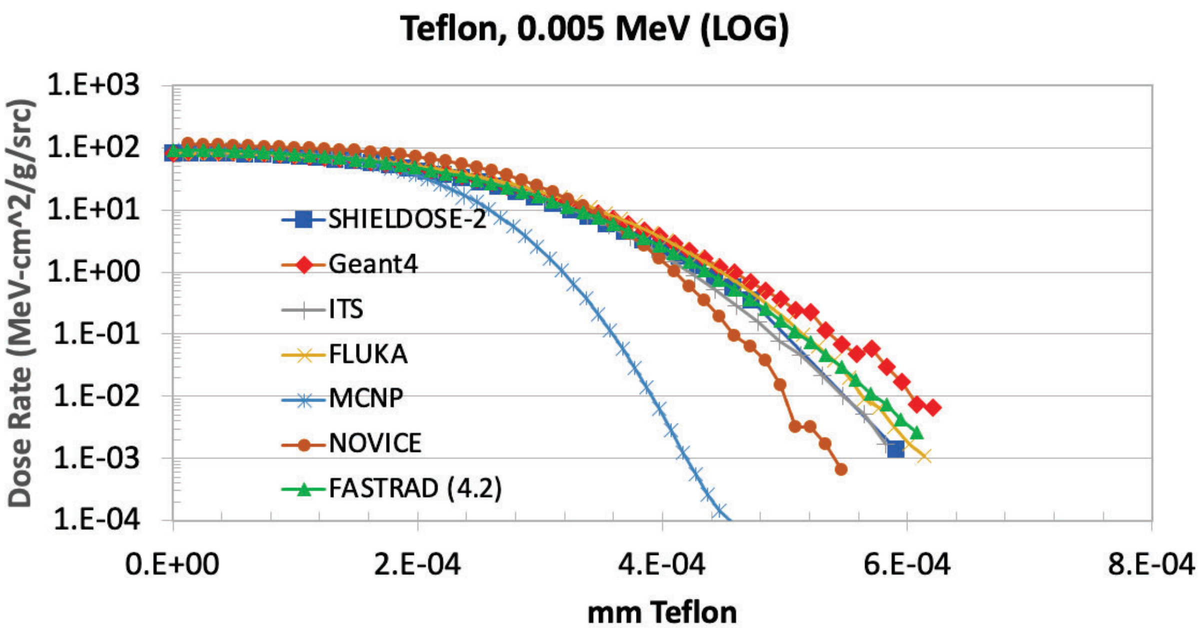

Figure 8.0-1. Density Scaling Comparison for the 0.005-MeV Electron Incident Case for Teflon™ (Top: Linear scale, Bottom: Log scale)

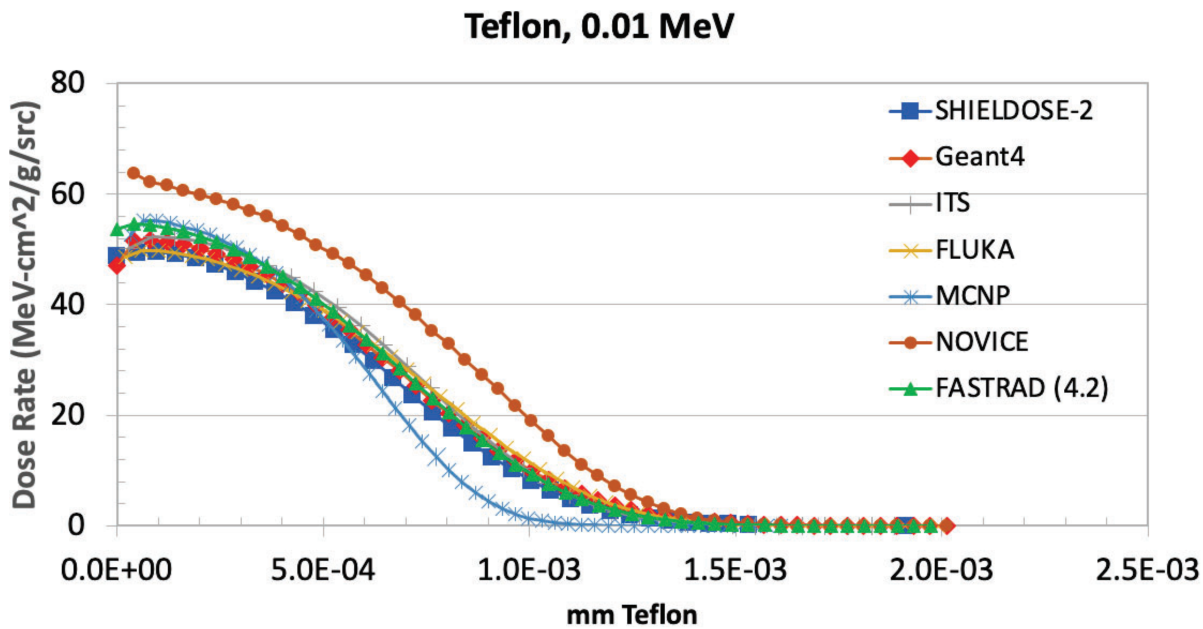

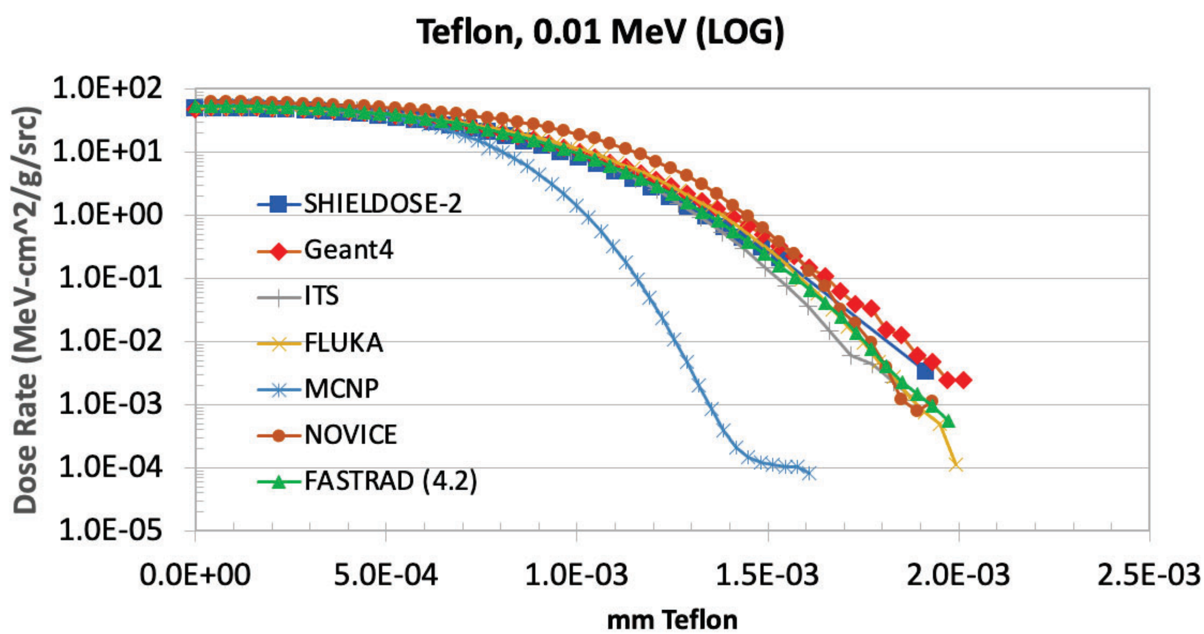

Figure 8.0-2. Density Scaling Comparison for the 0.01-MeV Electron Incident Case for Teflon™ (Top: Linear scale, Bottom: Log scale)

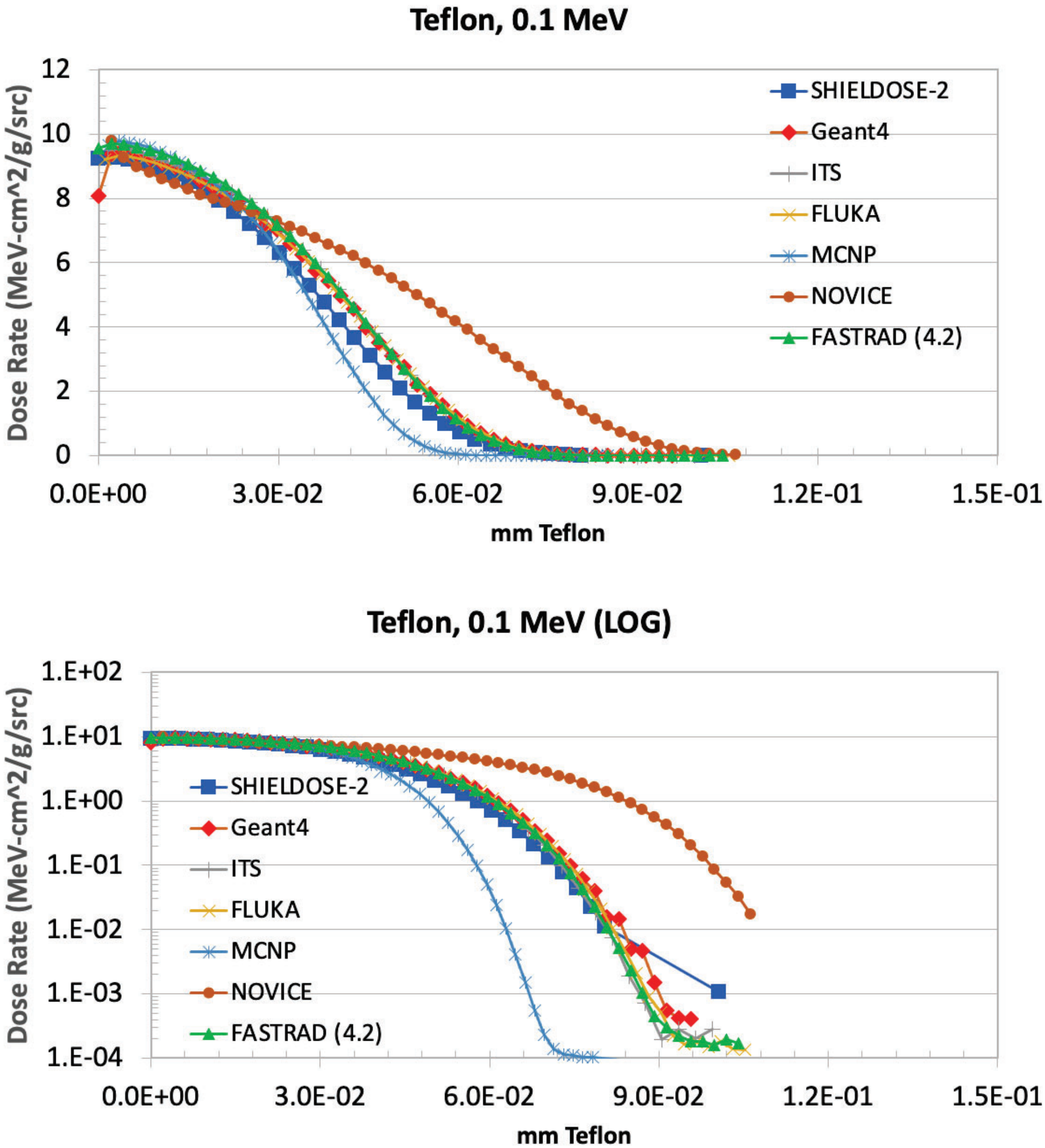

Figure 8.0-3. Density Scaling Comparison for the 0.1-MeV Electron Incident Case for Teflon™ (Top: Linear scale, Bottom: Log scale)

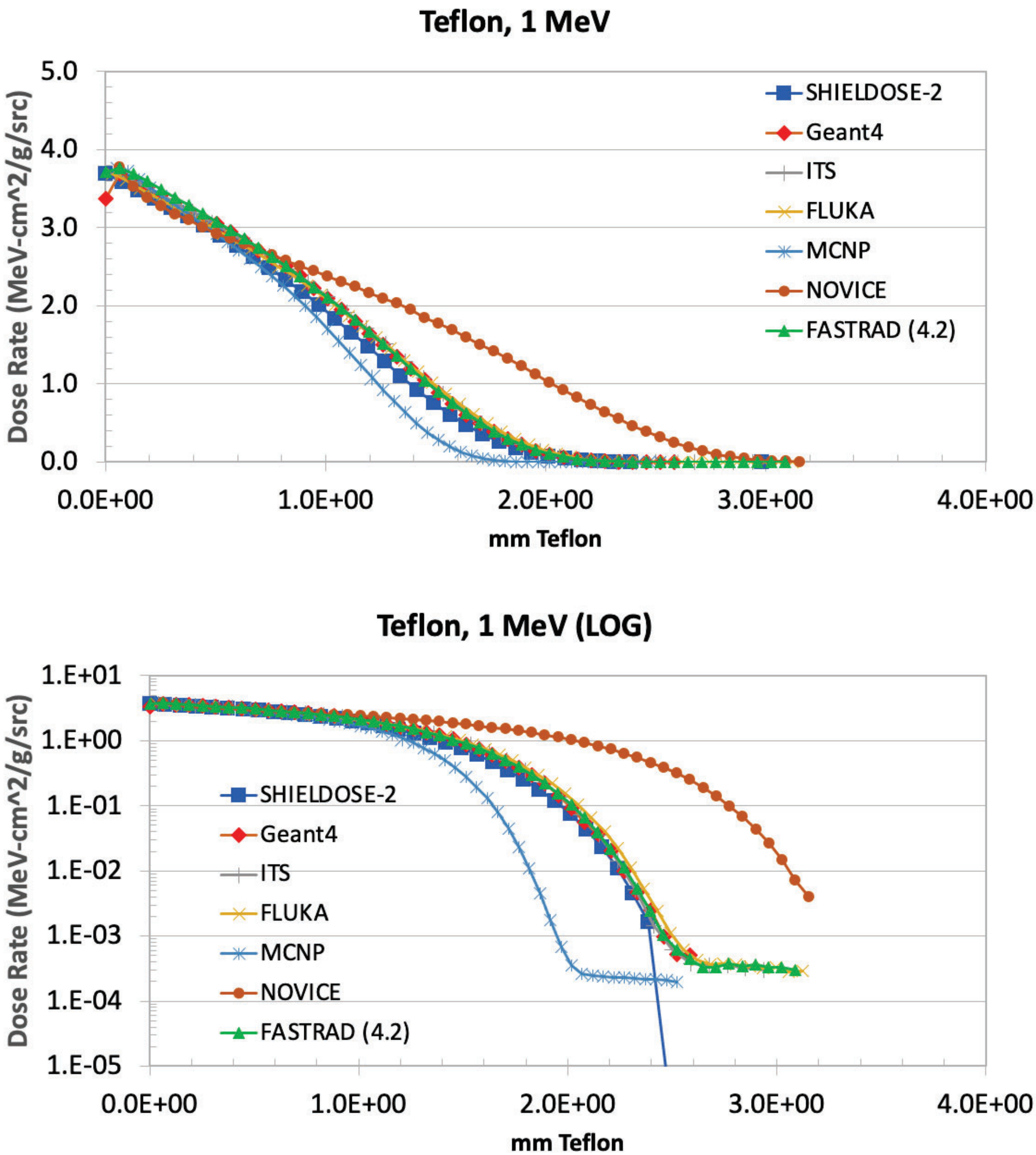

Figure 8.0-4. Density Scaling Comparison for the 1-MeV Electron Incident Case for Teflon™ (Top: Linear scale, Bottom: Log scale)

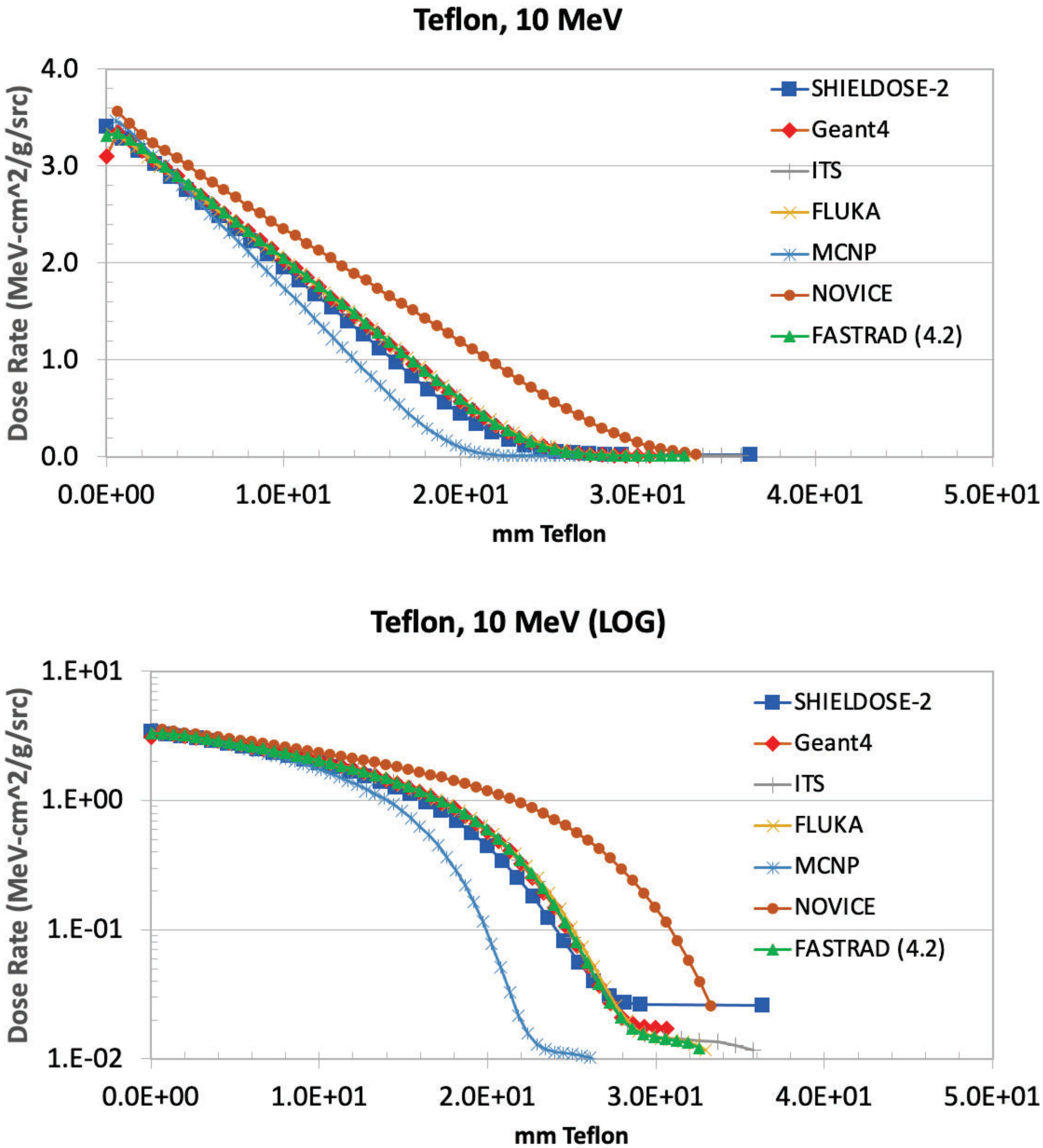

Figure 8.0-5. Density Scaling Comparison for the 10-MeV Electron Incident Case for Teflon™ (Top: Linear scale, Bottom: Log scale)

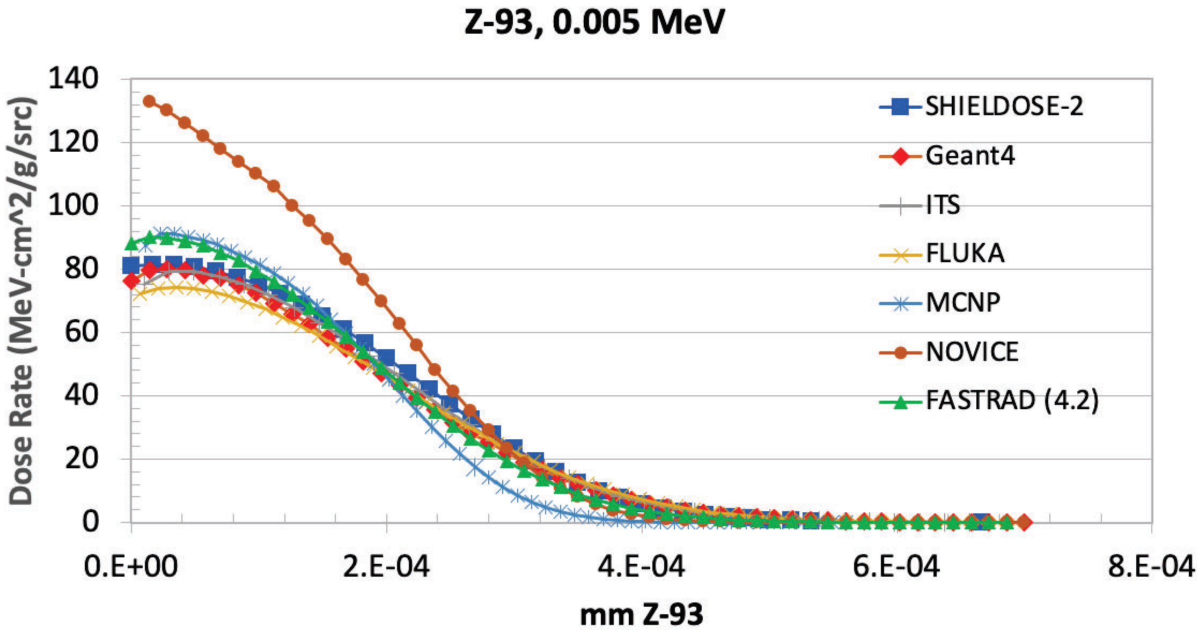

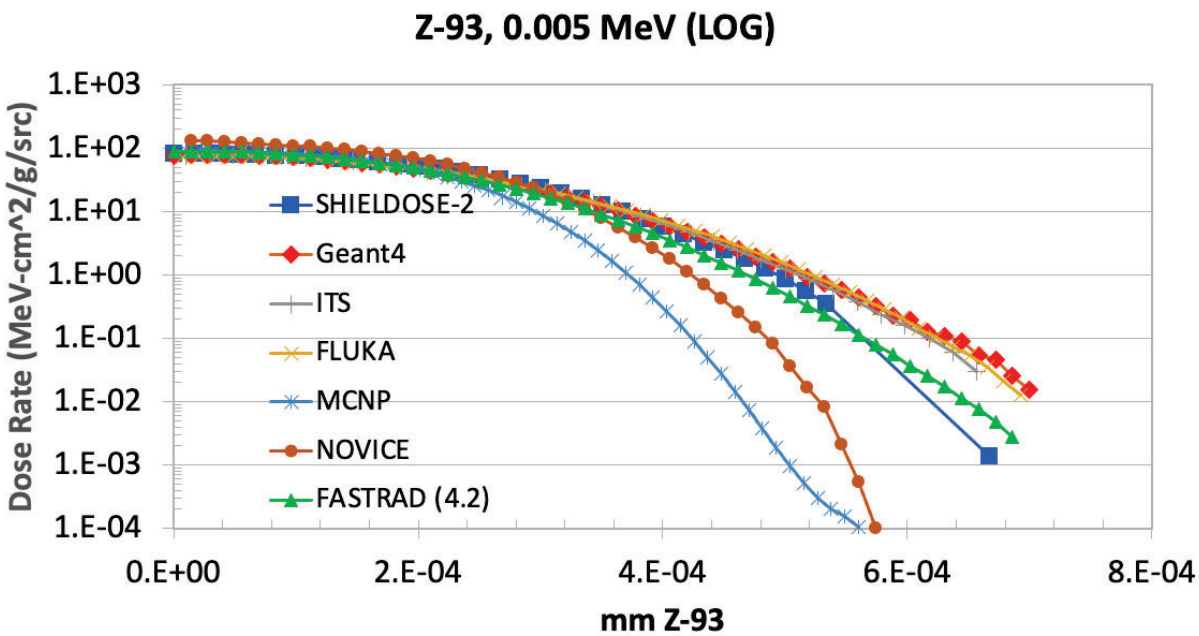

Figure 8.0-6. Density Scaling Comparison for the 0.005-MeV Electron Incident Case for Z93 Paint (Top: Linear scale, Bottom: Log scale)

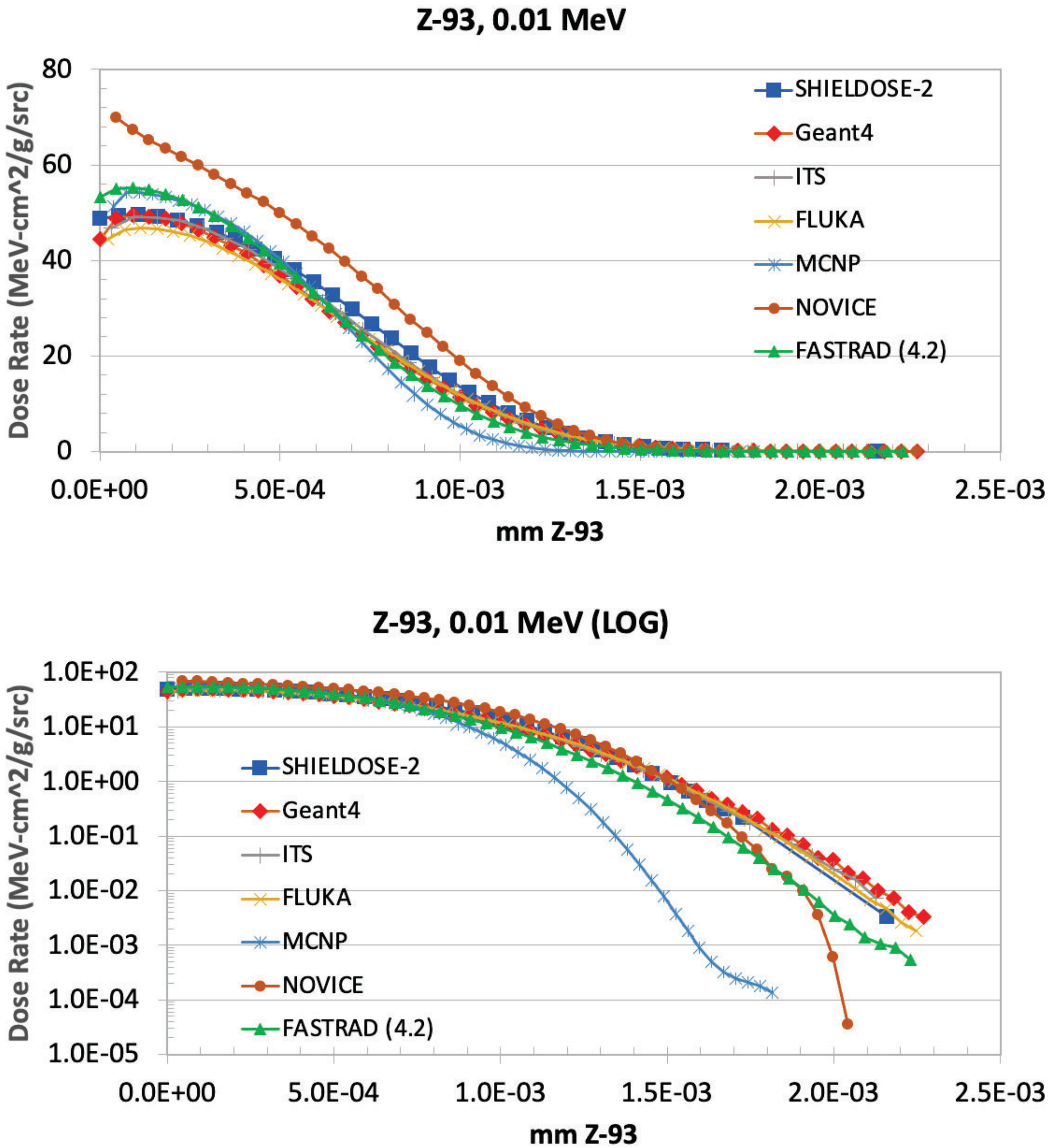

Figure 8.0-7. Density Scaling Comparison for the 0.01-MeV Electron Incident Case for Z93 Paint (Top: Linear scale, Bottom: Log scale)

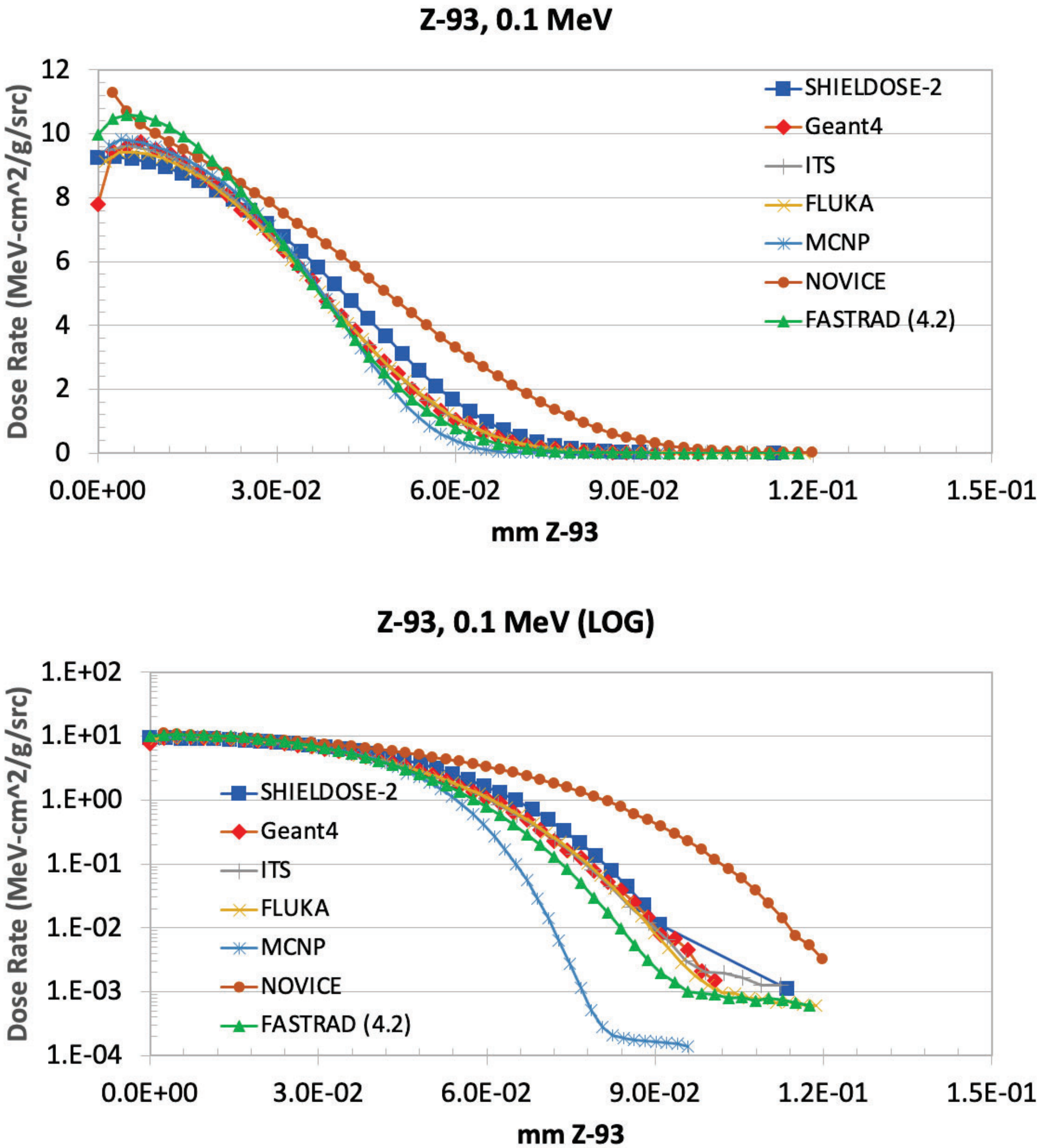

Figure 8.0-8. Density Scaling Comparison for the 0.1-MeV Electron Incident Case for Z93 Paint (Top: Linear scale, Bottom: Log scale)

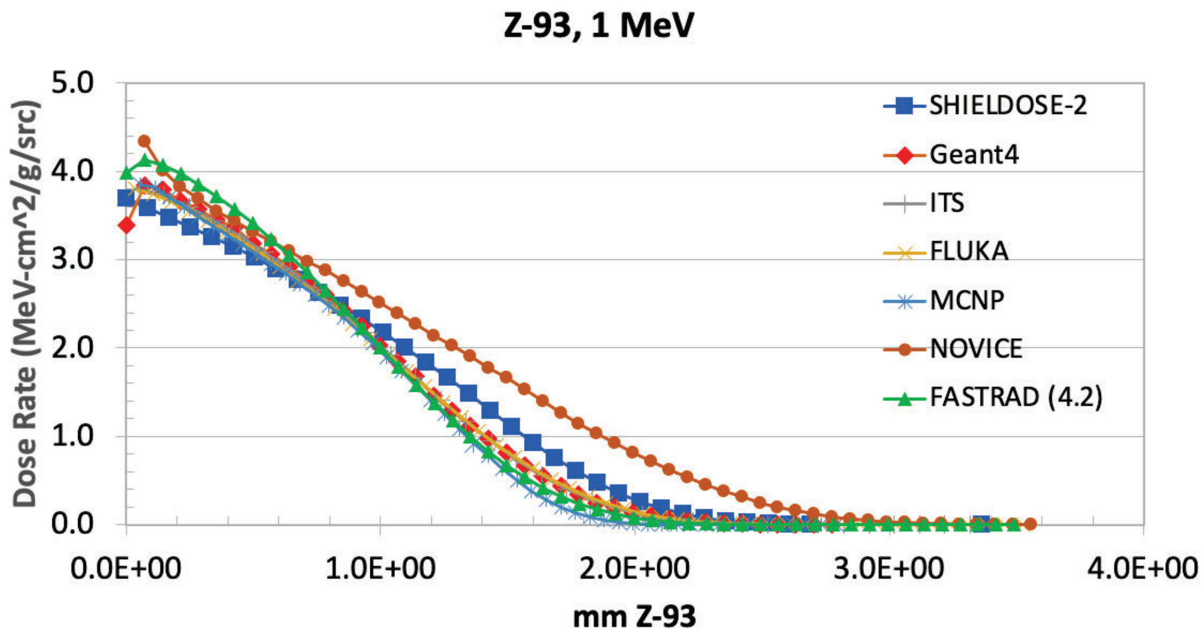

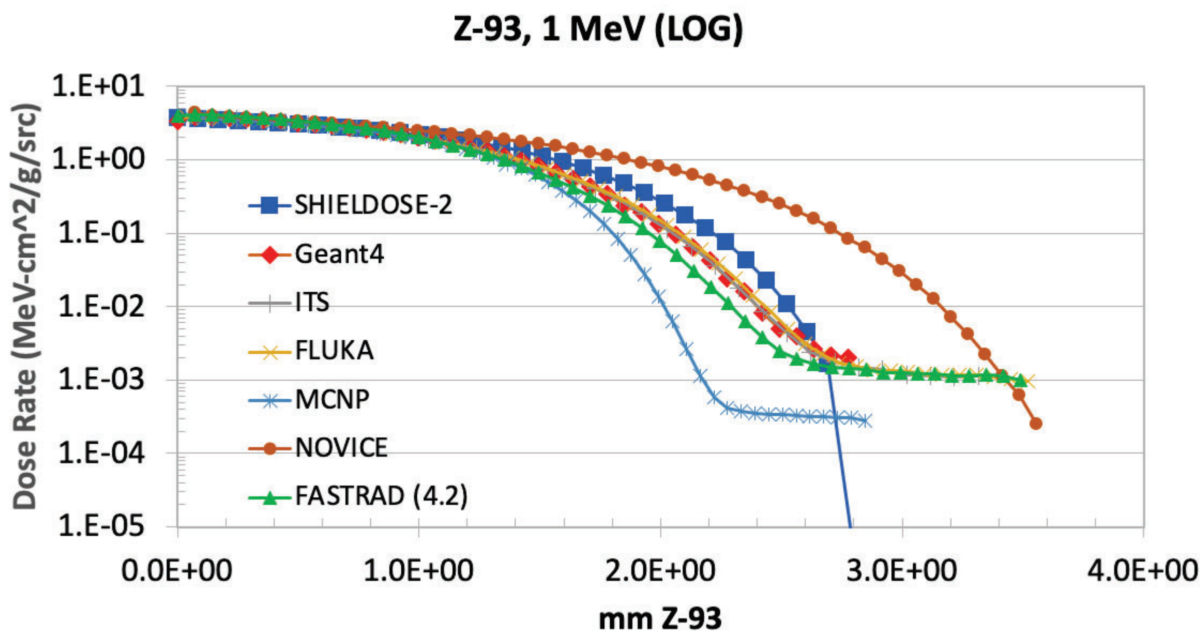

Figure 8.0-9. Density Scaling Comparison for the 1-MeV Electron Incident Case for Z93 Paint (Top: Linear scale, Bottom: Log scale)

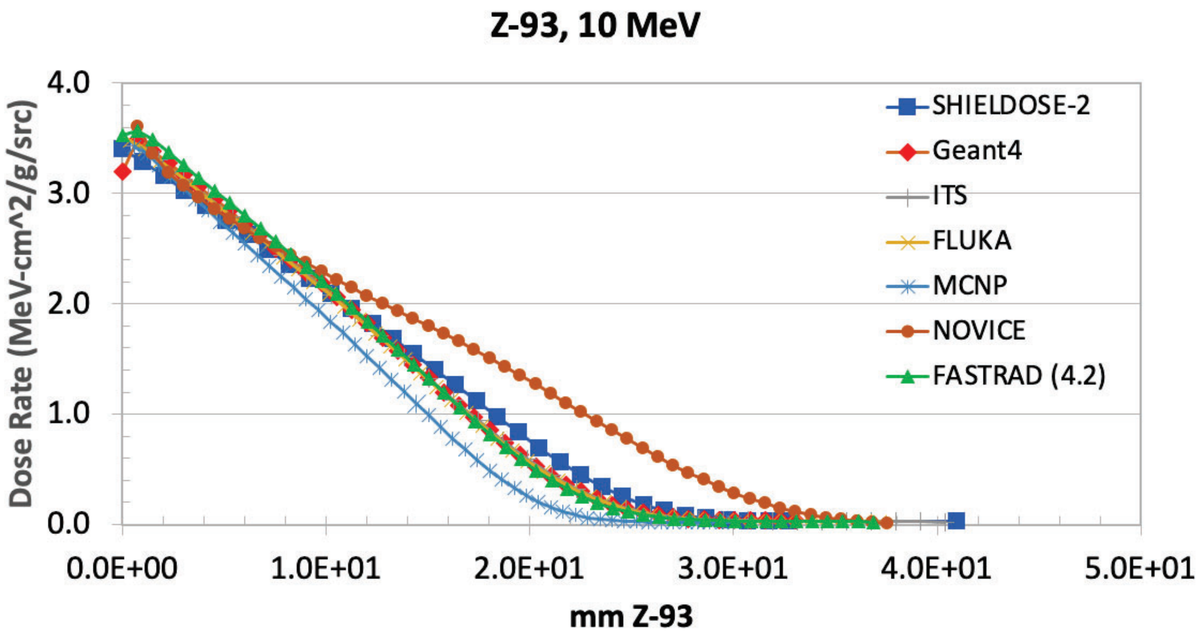

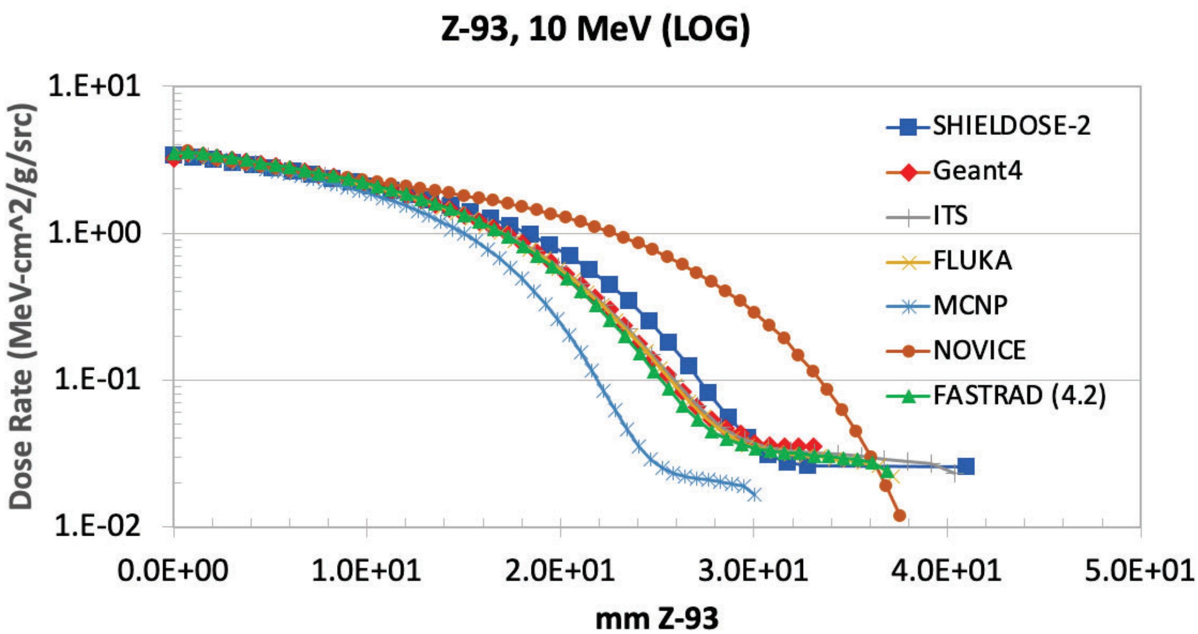

Figure 8.0-10. Density Scaling Comparison for the 10-MeV Electron Incident Case for Z93 Paint (Top: Linear scale, Bottom: Log scale).

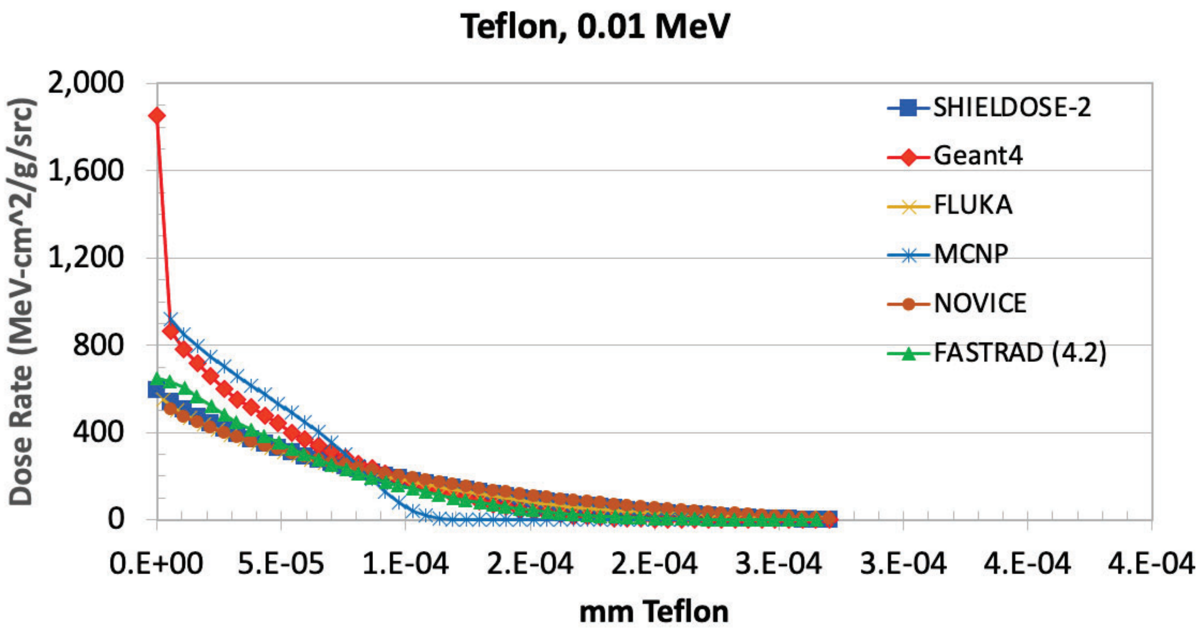

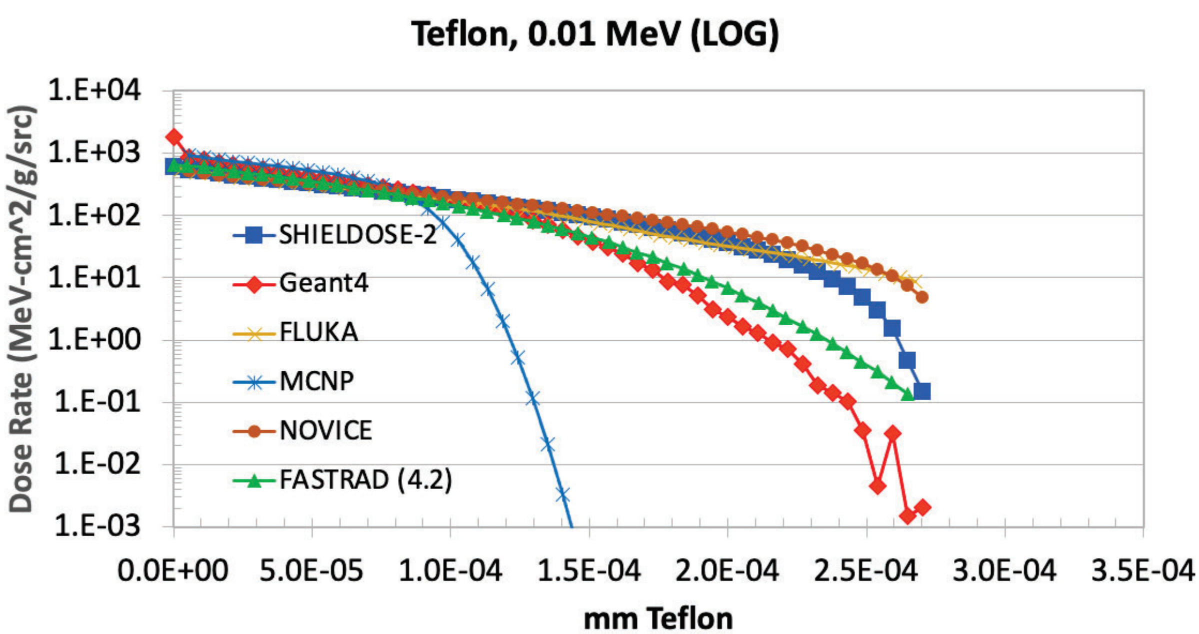

Figure 8.0-11. Density Scaling Comparison for the 0.01-MeV Proton Incident Case for Teflon™ (Top: Linear scale, Bottom: Log scale)

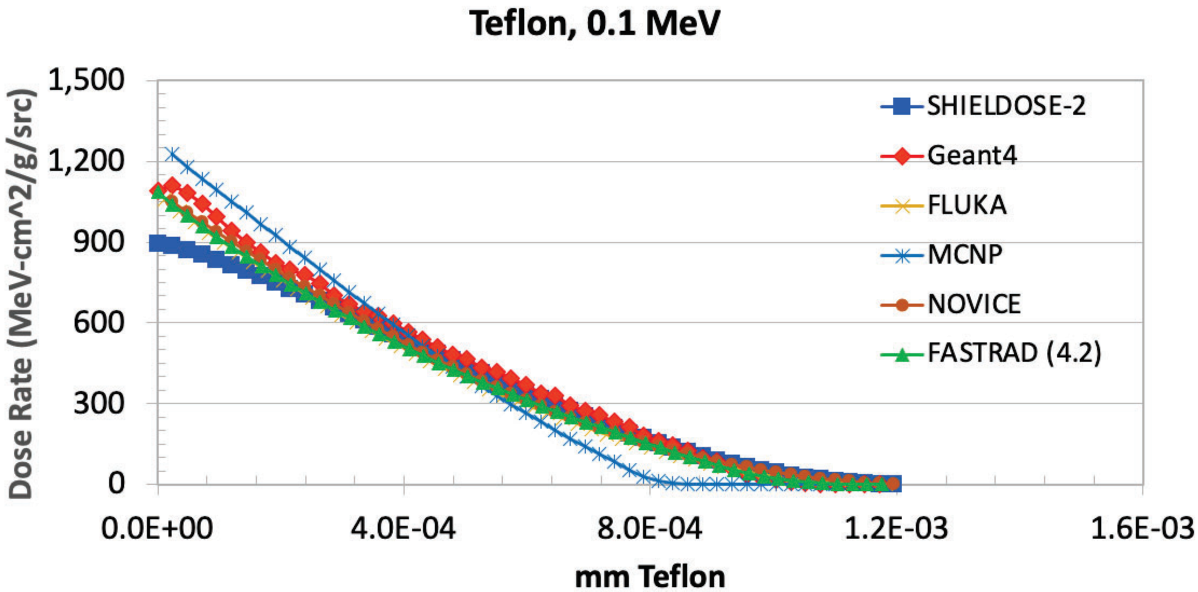

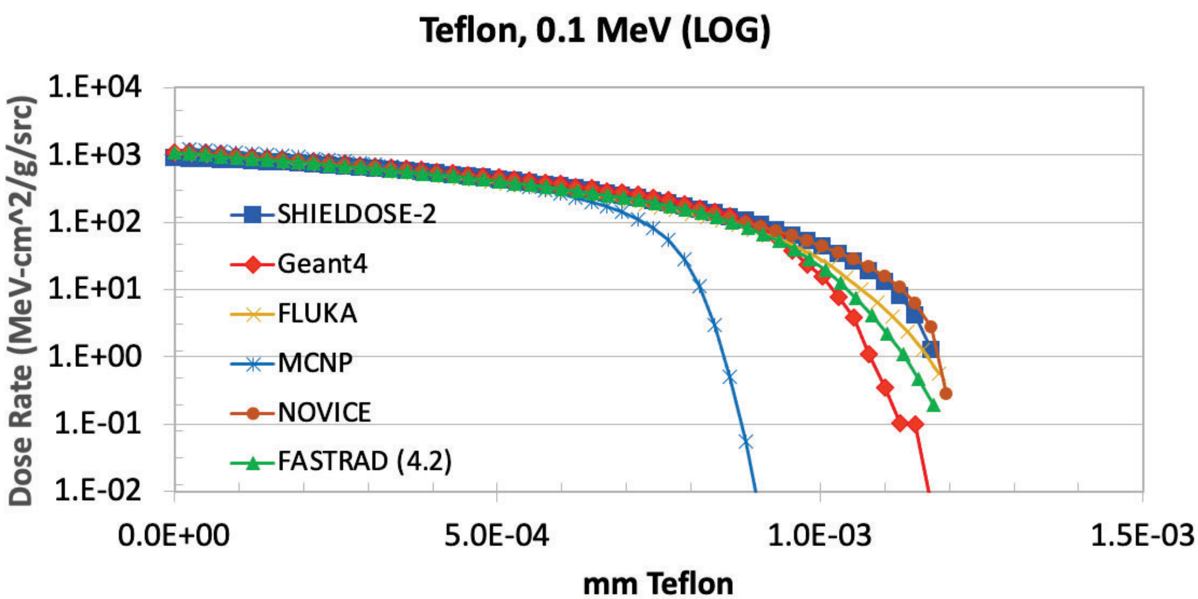

Figure 8.0-12. Density Scaling Comparison for the 0.1-MeV Proton Incident Case for Teflon™ (Top: Linear scale, Bottom: Log scale)

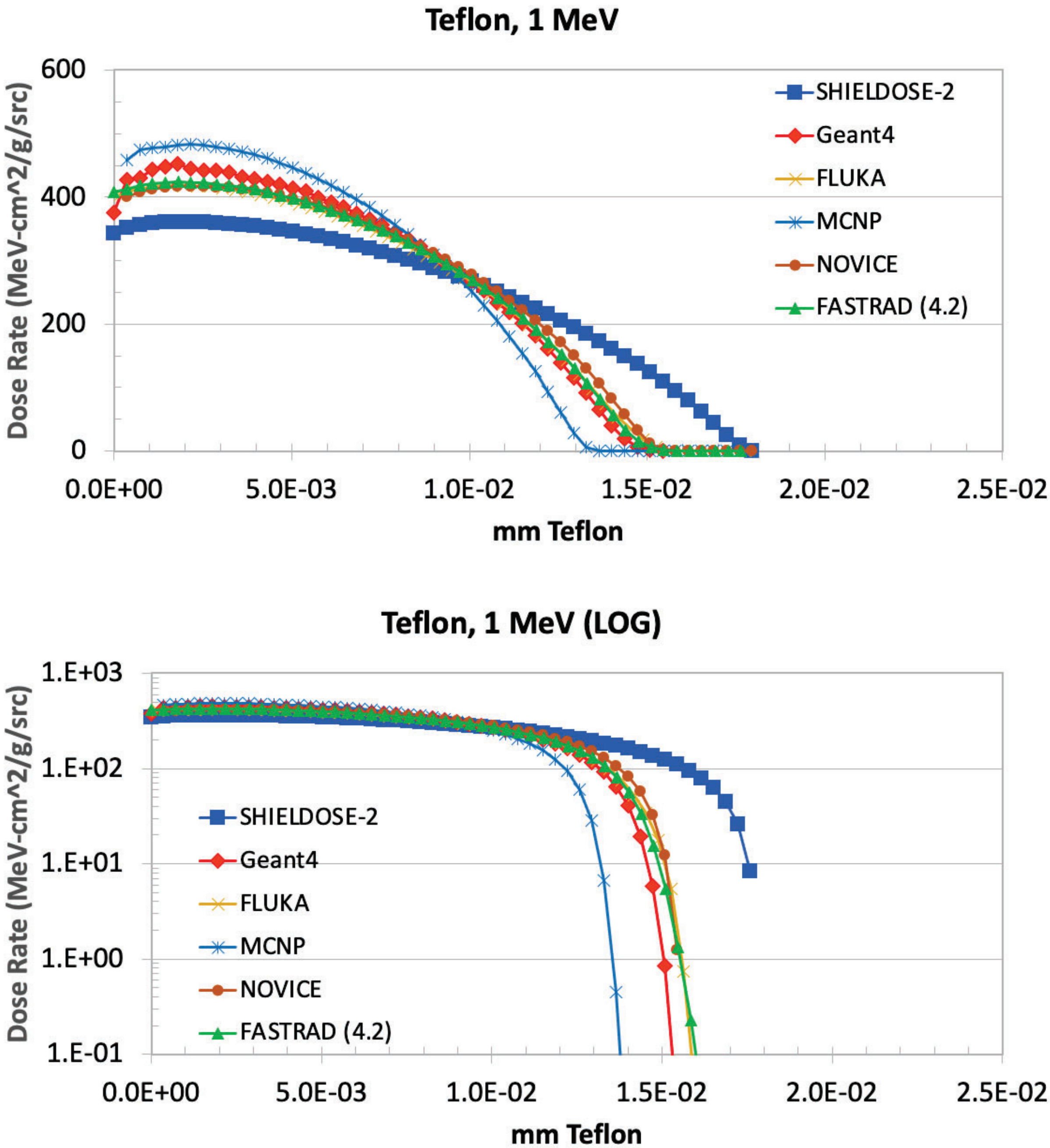

Figure 8.0-13. Density Scaling Comparison for the 1-MeV Proton Incident Case for Teflon™ (Top: Linear scale, Bottom: Log scale)

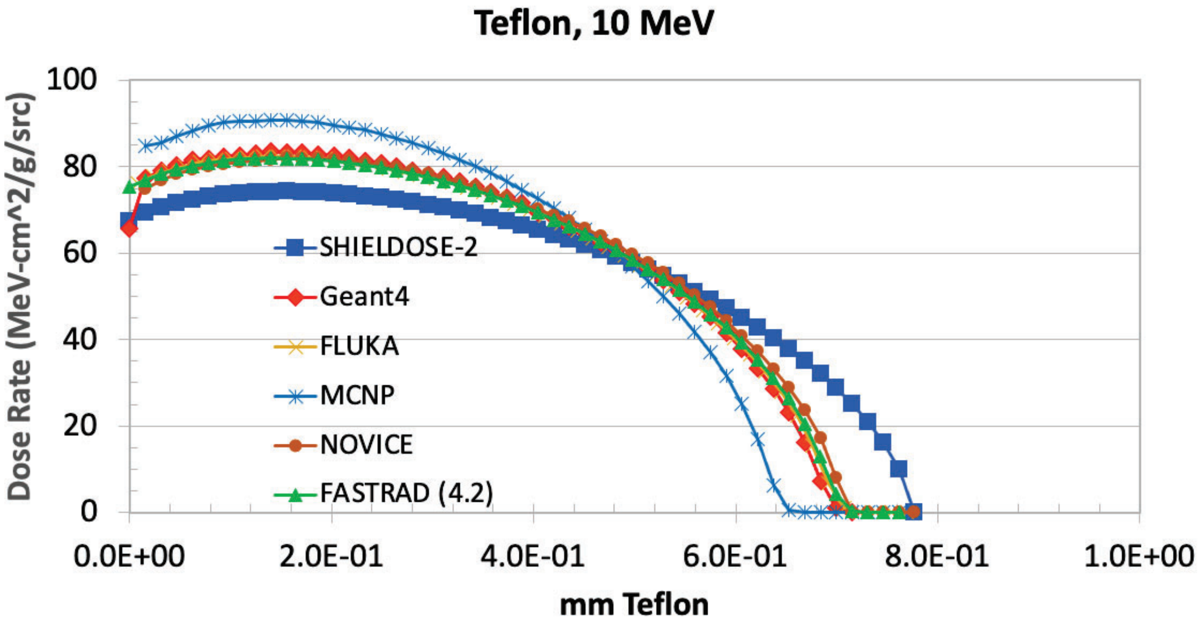

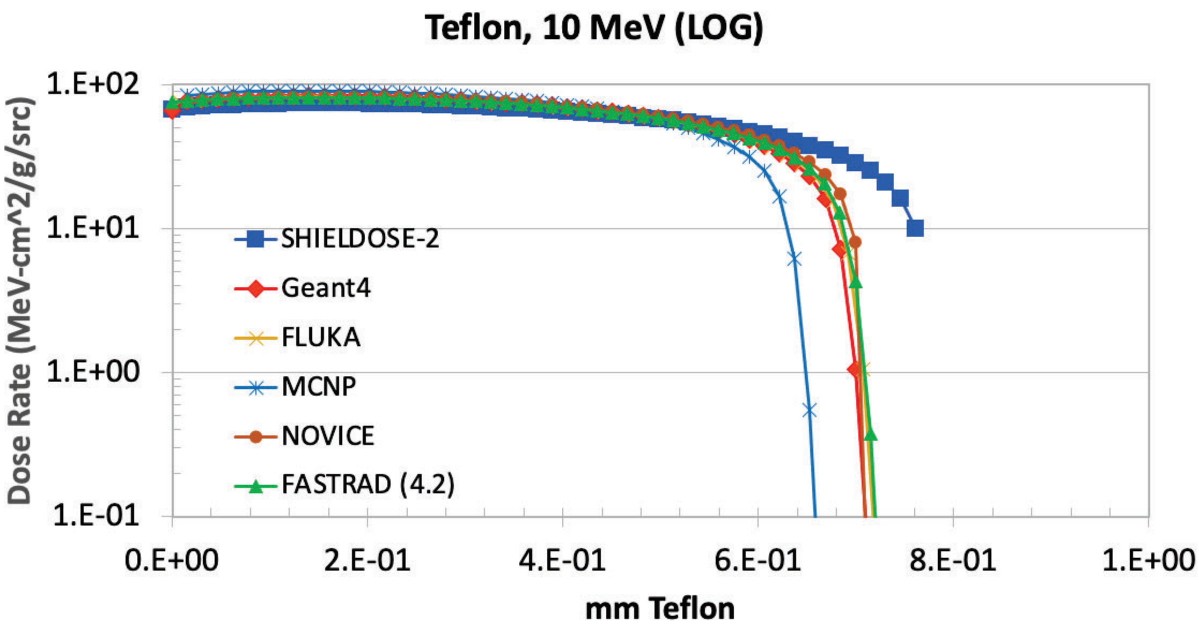

Figure 8.0-14. Density Scaling Comparison for the 10-MeV Proton Incident Case for Teflon™ (Top: Linear scale, Bottom: Log scale)

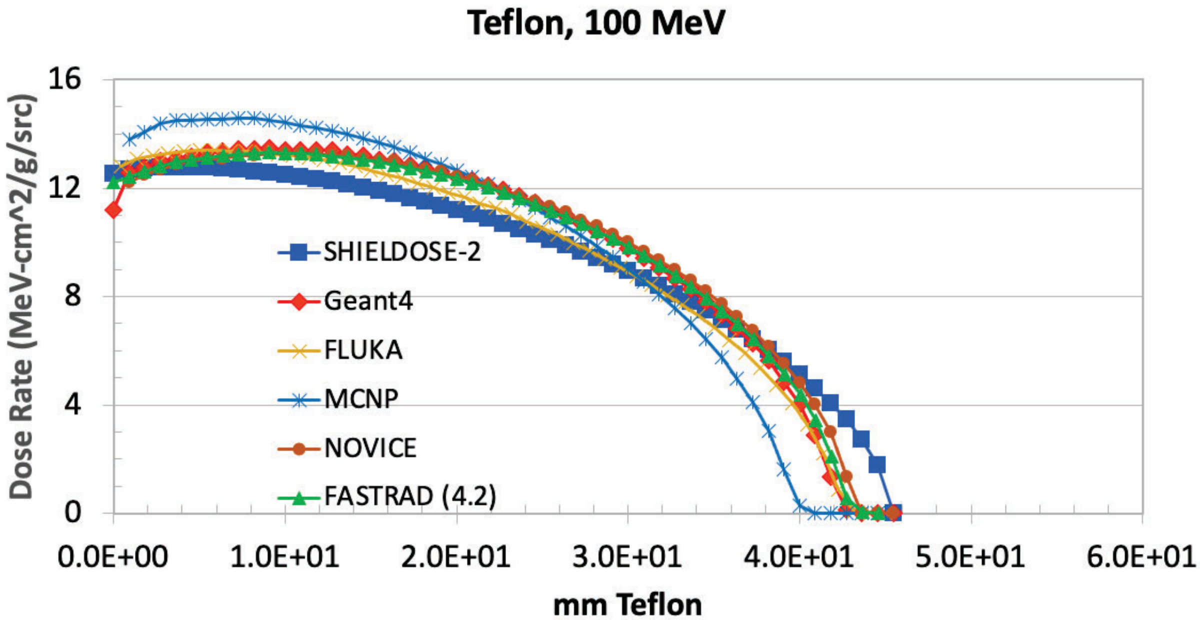

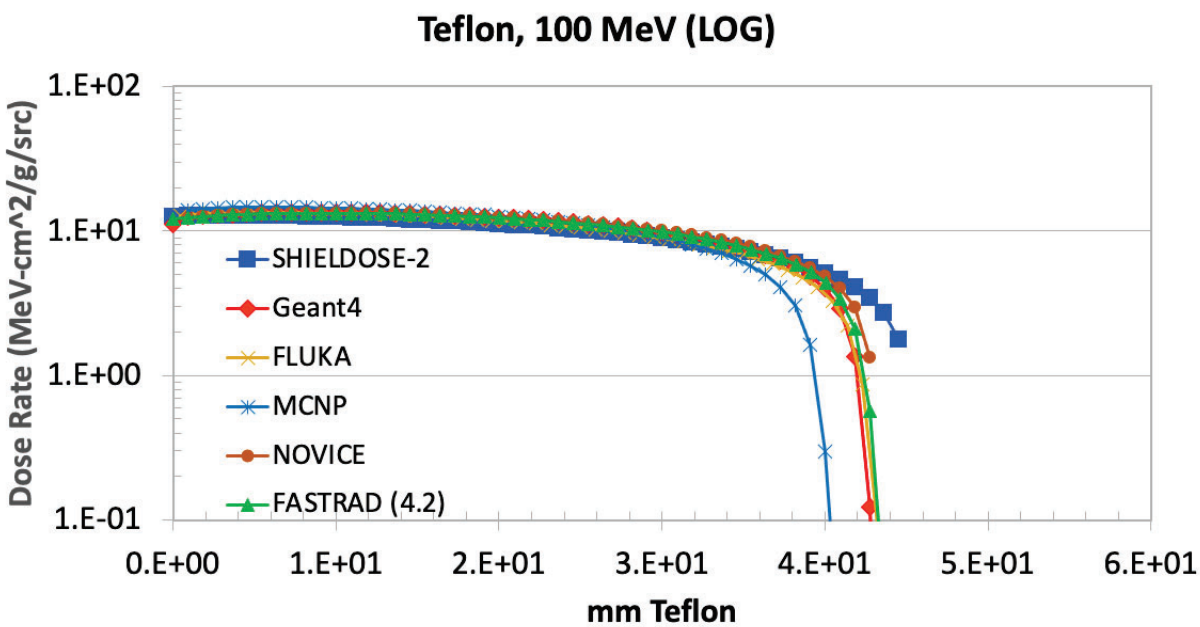

Figure 8.0-15. Density Scaling Comparison for the 100-MeV Proton Incident Case for Teflon™ (Top: Linear scale, Bottom: Log scale)

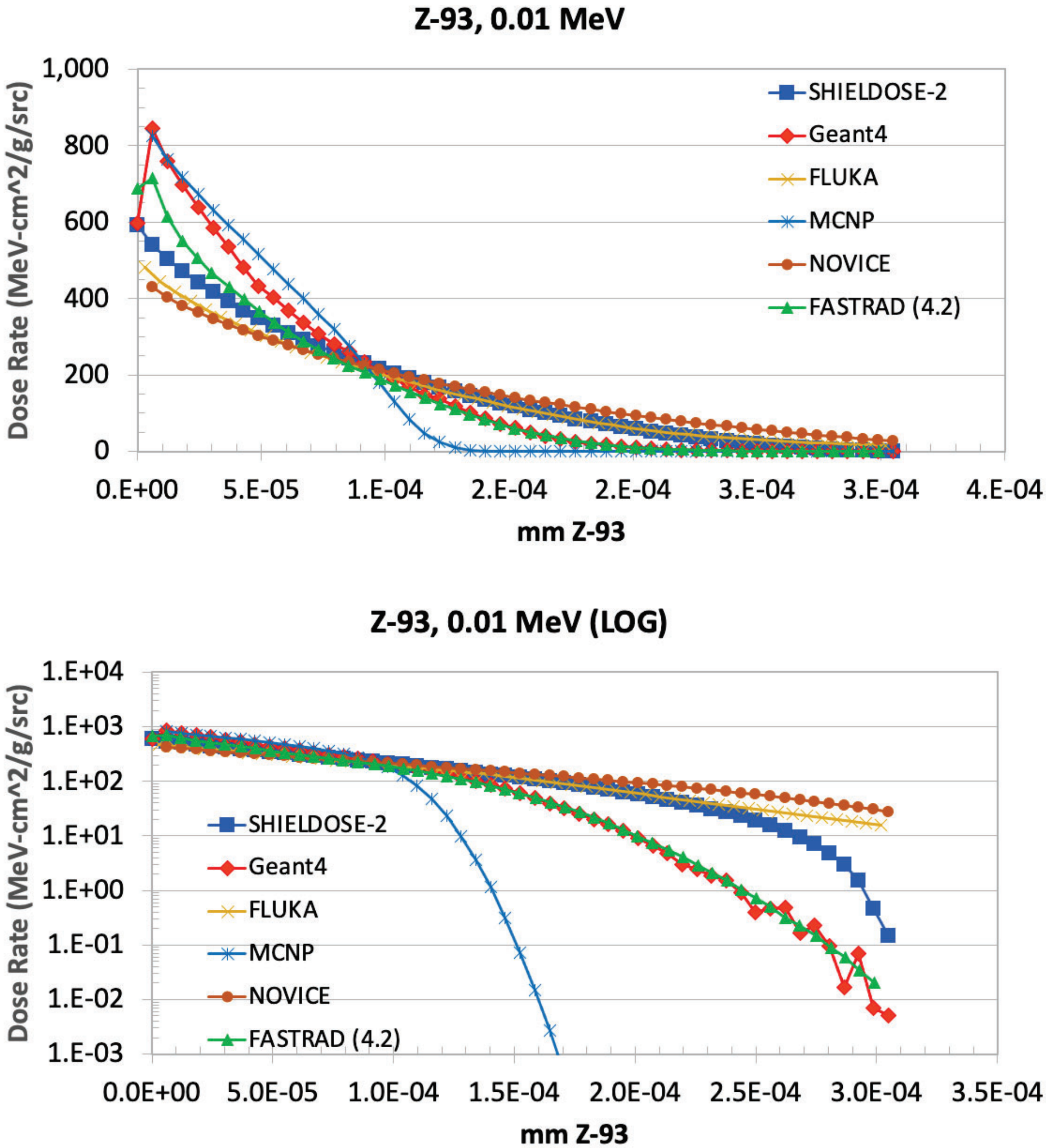

Figure 8.0-16. Density Scaling Comparison for the 0.01-MeV Proton Incident Case for Z93 Paint (Top: Linear scale, Bottom: Log scale)

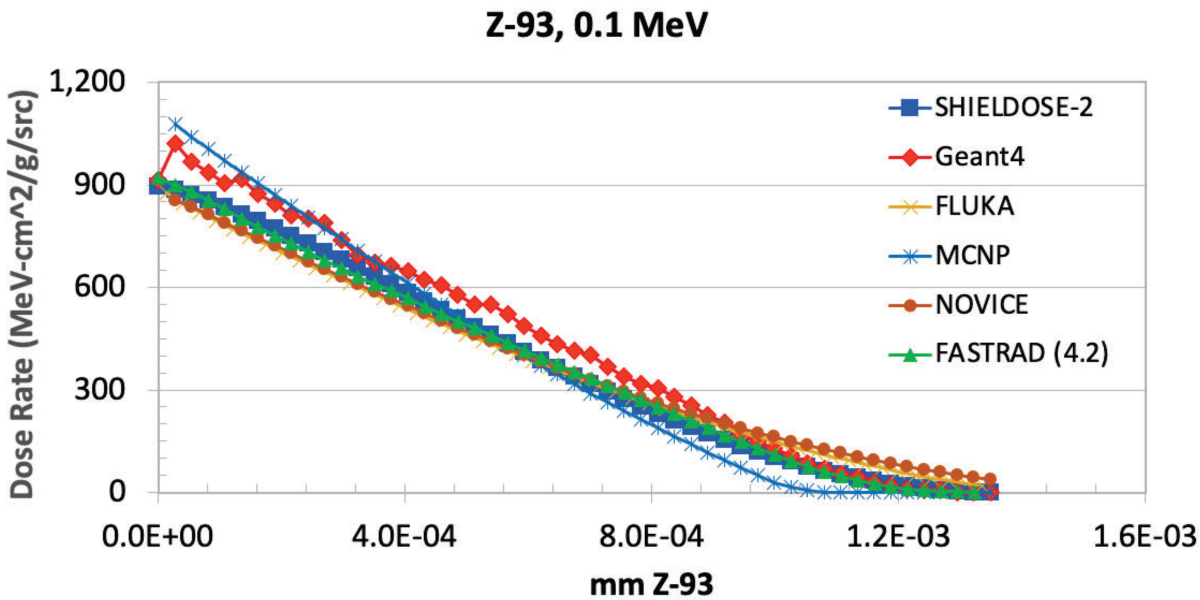

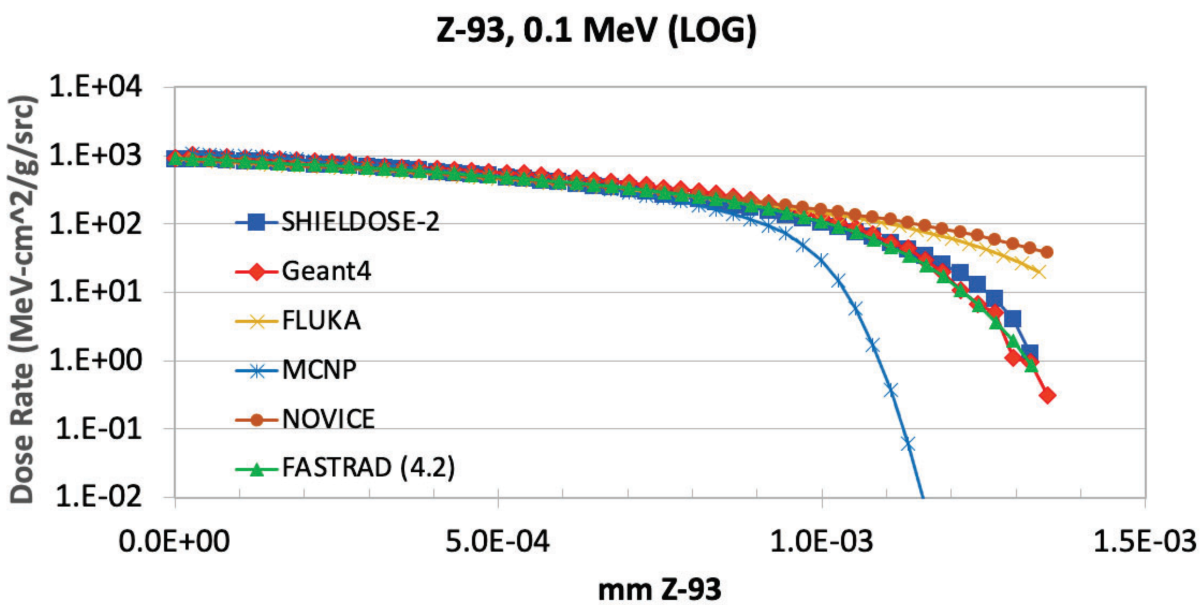

Figure 8.0-17. Density Scaling Comparison for the 0.1-MeV Electron Incident Case for Z93 Paint (Top: Linear scale, Bottom: Log scale).

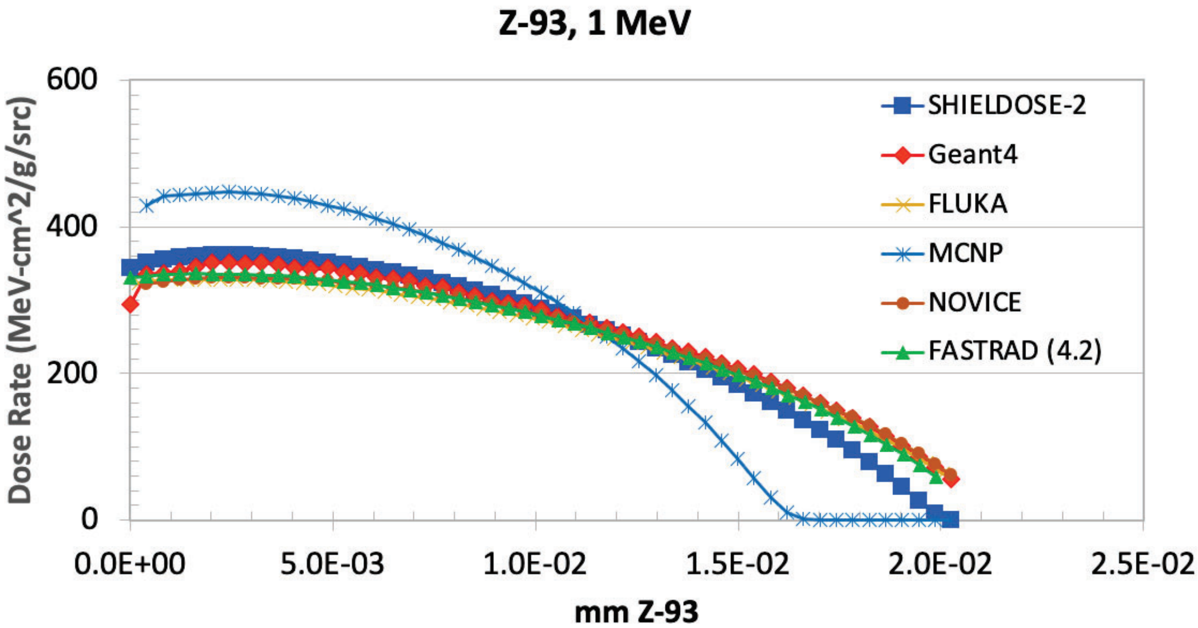

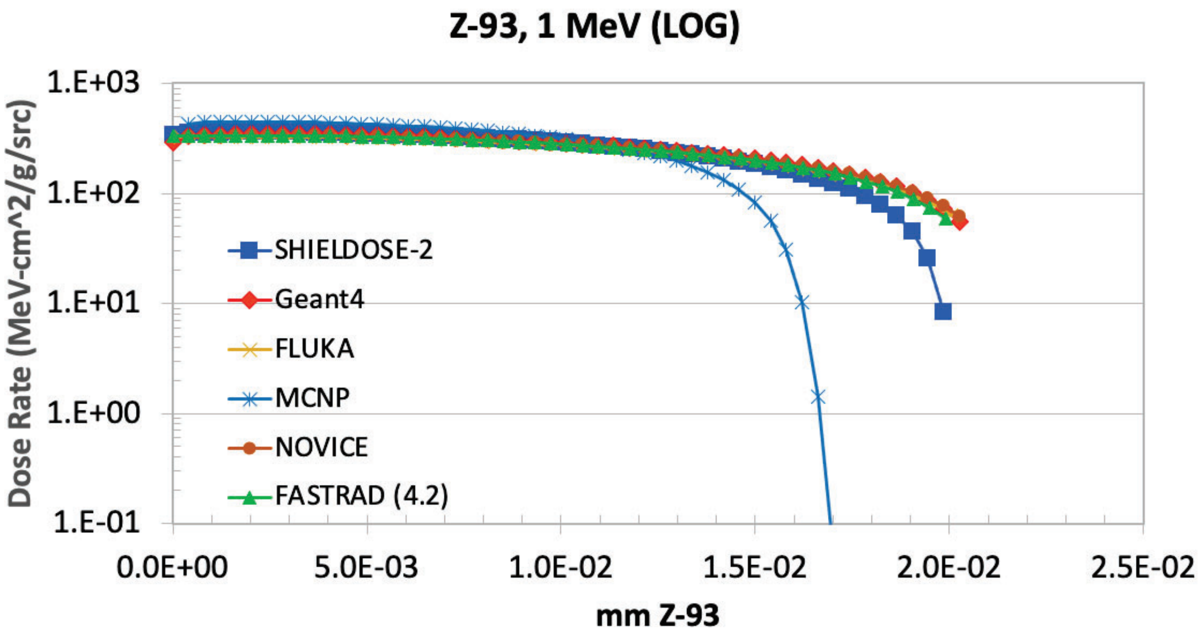

Figure 8.0-18. Density Scaling Comparison for the 1-MeV Electron Incident Case for Z93 Paint (Top: Linear scale, Bottom: Log scale)

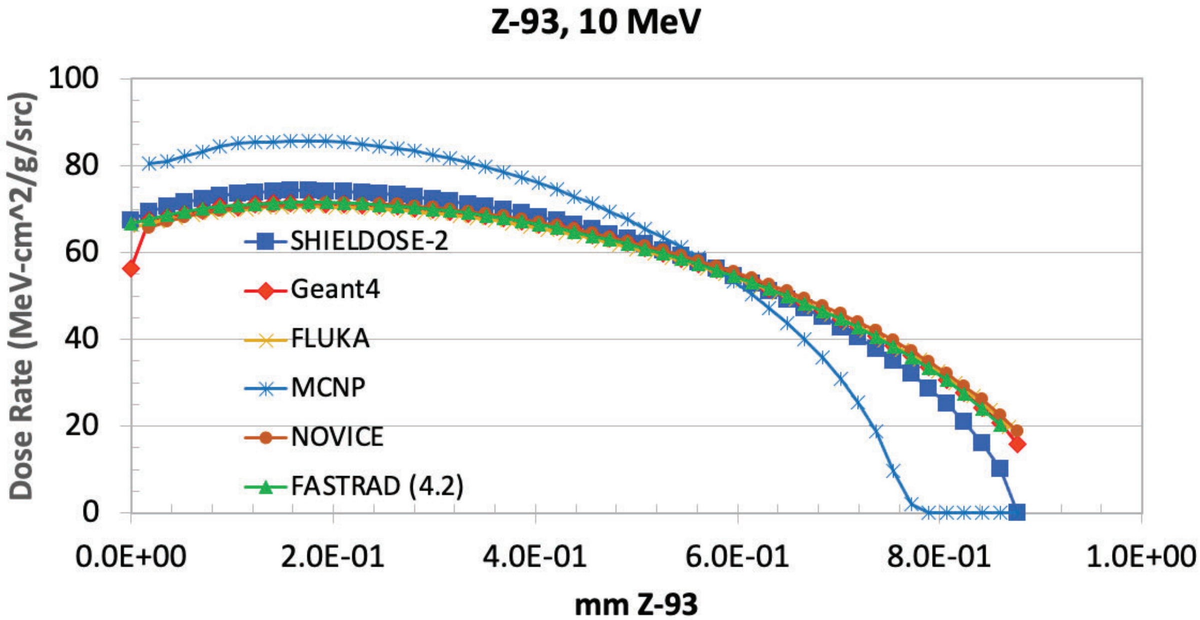

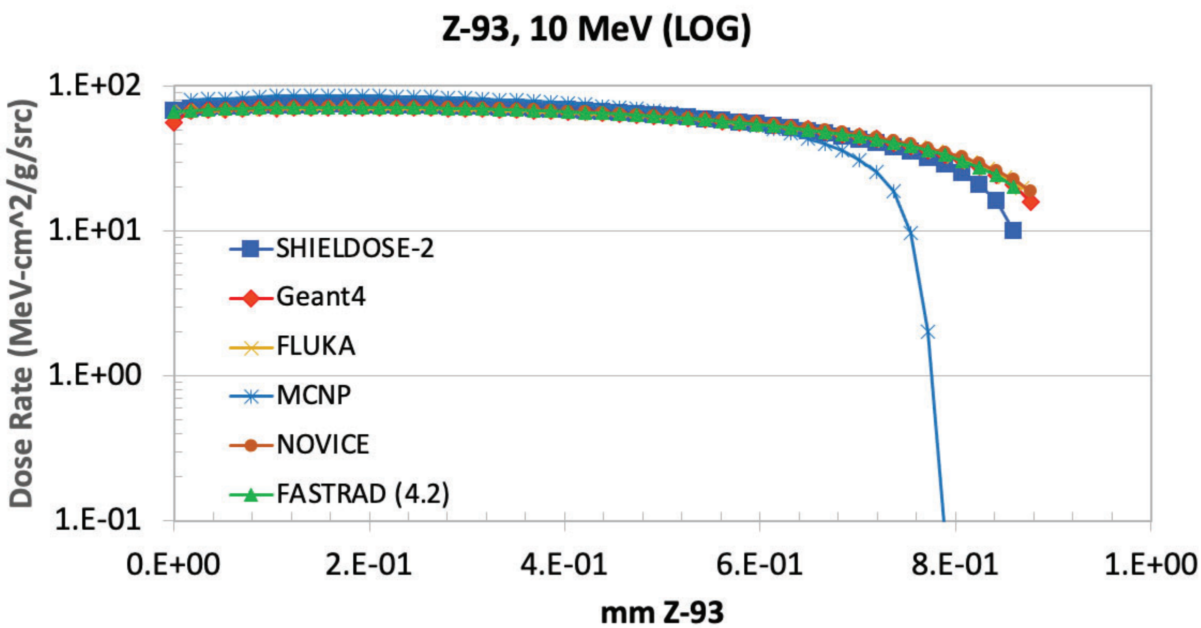

Figure 8.0-19. Density Scaling Comparison for the 10-MeV Electron Incident Case for Z93 Paint (Top: Linear scale, Bottom: Log scale)

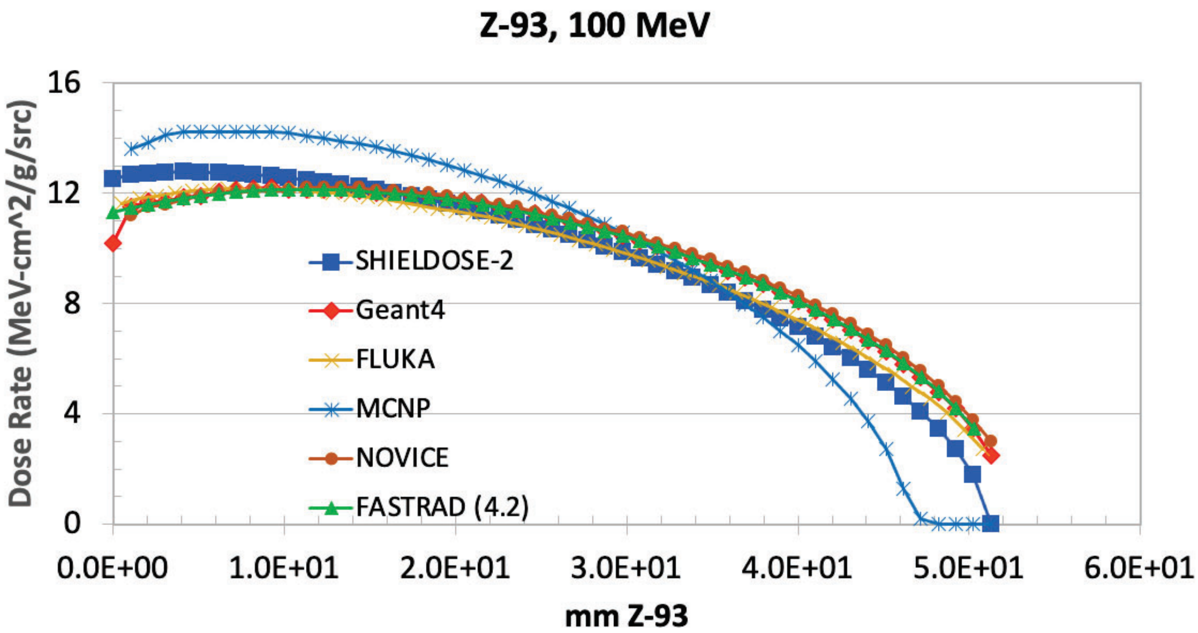

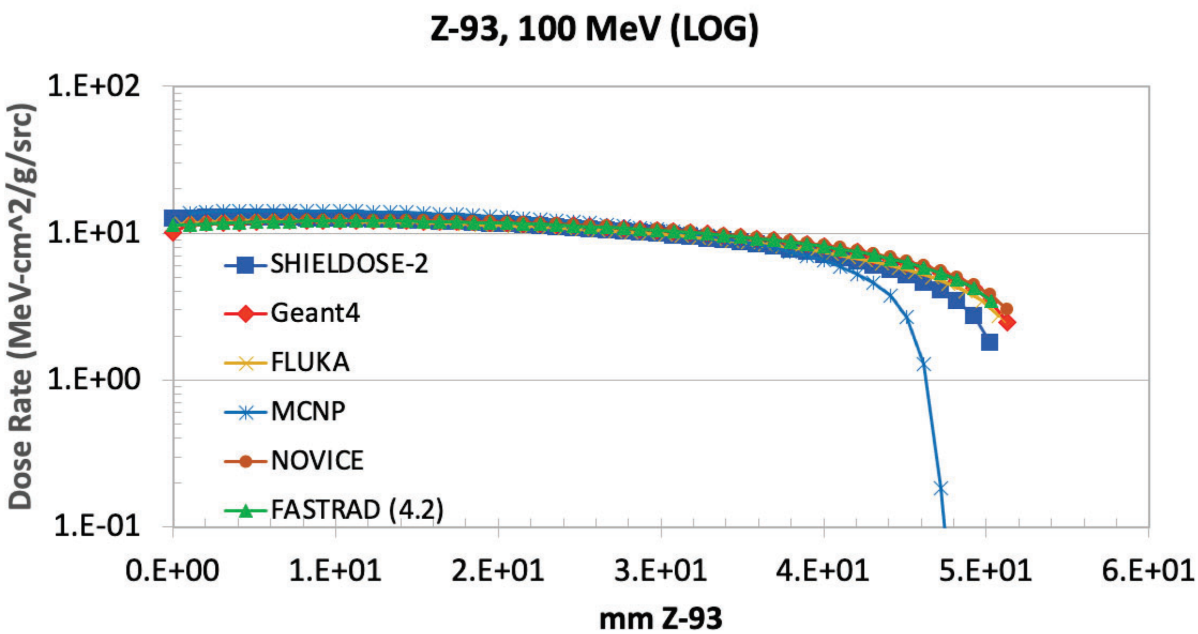

Figure 8.0-20. Density Scaling Comparison for the 100-MeV Electron Incident Case for Z93 Paint (Top: Linear scale, Bottom: Log scale)

No attempt was made to understand the discrepancies between the codes for the density scaling comparisons.

General observations include:

1. For electron cases, MCNP and NOVICE generally deviate from SHIELDOSE-2 and other codes. Except for these two codes, the other codes produced a relatively better agreement to the SHIELDOSE-2 equivalent tables.

2. The proton cases are generally worse than the electron cases as there are large deviations from each other. The deviation of MCNP is most pronounced.
3. For proton cases or electron cases, deviations are generally larger at deeper depths.
4. For proton cases:
   a) For Z93: SHIELDOSE-2 tends to overestimate the deposited dose in the first layers and then underestimated it in the deep layers. This pattern was observed for every energy except for 10 keV.
   b) For Teflon™: the opposite pattern was observed. SHIELDOSE-2 underestimates in the first layers and then overestimates.
   c) There was better agreement between the codes for the Z93 material than Teflon™.
   d) There was better agreement between the codes above 10 MeV, as indicated by the 100 MeV results, where SHIELDOSE-2 is used for evaluating the shielding of electronics, rather than thinner applications focused on in this report.
5. The results of density scaling application to the SHIELDOSE-2 table are not generally reproduced by the codes used in this effort, especially for lower energy electrons and protons. This implies that the density scaling should not be used to the SHIELDOSE-2 results in applications where ≤0.1 MeV electrons or ≤10 MeV protons are important (e.g., material thickness ~0.5 mm).

9.0 Summary

In considering the questions imposed by the Artemis Program, the NESC assessment team summarizes the key conclusions from the study as:

1. Because the thickness applicability is closely related to the lowest energy of electrons and protons used in building the SHIELDOSE-2 table (5 keV for electrons and 10 keV for protons), SHIELDOSE-2 could be used as thin as the ranges corresponding to those energies. The CSDA range of 5 keV electrons is 1.092E-4 g/cm^2 or ~0.40 µm in aluminum and the CSDA range of 10 keV protons is 5.943E-5 g/cm^2 or 0.22 µm in aluminum.
   a. This means that SHIELDOSE-2 could be used as thin as a fraction of µm of material.
   b. However, the accuracy of the results needs validation as the dose profiles in aluminum obtained with other widely used radiation transport tools are not generally in agreement (Figures 7.2-1 to 7.2-10).
2. Application of density scaling to the SHIELDOSE-2 table are not generally reproduced by other codes, especially for low-energy electrons and protons. This implies that the density scaling should not be used to the SHIELDOSE-2 results in applications where ≤0.1 MeV electrons or ≤10 MeV protons are important (material thickness ~0.5 mm). Thicker material results were not the focus of this study.

10.0 Findings and Observations

10.1 Findings

F-1. SHIELDOSE-2 could be used for computing dose in thin materials (i.e., 1 µm or less). (Section 7.0)

F-2. The accuracy of the SHIELDOSE-2 results for thin materials (i.e., 1 μm or less) is not validated as the dose profiles in aluminum obtained with other widely used radiation transport tools are not generally in agreement (Figures 7.2-1 to 7.2-10). (Section 7.0)

F-3. The density scaling should not be used to the SHIELDOSE-2 results in material thicknesses ~ 0.5 mm or less. (Section 8.0)

10.2 Observations

O-1. There are generally larger discrepancies at low energies while the agreements are typically better at higher energies.

- The lowest energy results (0.005 MeV electron and 0.01 MeV proton) show large scatter among the codes indicating the radiation dose calculations at low energies (e.g., thin materials) are subjected to larger uncertainties. (Section 7.2)

O-2. The NOVICE results for the 0.005-, 0.01- and 10-MeV electron cases and for the 1-MeV proton case deviate from other codes' results. (Section 7.2)

O-3. The deviation of the MCNP results of the 0.005-MeV electron and for the 0.01-MeV proton from other code is clearly visible. (Section 7.2)

O-4. The results from Geant4 and GRAS are comparable, which is expected because GRAS is a toolkit based on Geant4. (Section 7.2)

O-5. The GEANT4 low-energy results show a sudden drop at the lowest thickness point, which is suspected to be an artifact of the 'differential' mass of silicon. (Section 7.2)

O-6. Generally, the electron results from Geant4, GRAS, FLUKA, ITS, and FASTRAD are clustered with the SHIELDOSE-2 tables. (Section 7.2)

O-7. FASTRAD's results are comparable to Geant4, which is expected as the physics is based on that of Geant4, (Section 7.2)

O-8. For electron cases in the density scaling comparison, MCNP and NOVICE generally deviate from SHIELDOSE-2 and other codes. Except for these two codes, the other codes produced a relatively better agreement to the SHIELDOSE-2 equivalent tables. (Section 8)

O-9. In the density scaling comparison, the proton cases are generally worse than the electron cases as there are large deviations between them. The deviation of MCNP is most pronounced. (Section 8)

O-10. In the density scaling comparison, for proton or electron cases, deviations are generally larger at deeper depths. (Section 8)

O-11. The results of density scaling application to the SHIELDOSE-2 table are not generally reproduced by other codes, especially for lower energy electrons and protons. This implies that the density scaling should not be used to the SHIELDOSE-2 results in applications where ≤0.1 MeV electrons or ≤10 MeV protons are important (material thickness ~0.5 mm). (Section 8)

O-12. For proton cases in the density scaling comparison:

- For Z93: SHIELDOSE-2 tends to overestimate the deposited dose in the first layers and then underestimated it in the deep layers. This pattern is observed for every energy except for 10 keV. (Section 8)
- For Teflon: the opposite pattern is observed. SHIELDOSE-2 underestimates in the first layers and then overestimates. (Section 8)
- There is better agreement between the codes for the Z93 material than the Teflon. (Section 8)

11.0 Alternate Technical Opinion

By: Thomas M. Jordan, EMPC.

Note by Technical Lead, Insoo Jun: As this is an unsolicited opinion from a participant, the input provided by EMPC has not been altered in any fashion, other than minor grammatical corrections and formatting, to preserve the original intent of the input.

This study started in part as an independent assessment of SHIELDOSE-2's capability for space-radiation dose predictions to materials. Additionally, NASA programs and prime contractors have requested information regarding alternate tools for use when SHIELDOSE is identified as not applicable. See Section 1.0 Notification and Authorization and Section 4.0 Executive Summary, which references the Artemis Program and NESC for initiating the two-phased study.

Opinion:

<u>Scope of Study.</u>

Given the variety and complexity of current, planned, and proposed NASA missions, the greatest benefit of this study is the description and documentation of the various participating software codes.

SHIELDOSE-2, a very capable and well-executed code, is used today in a relatively narrow range of circumstances. A request to examine the several other codes primarily for their merits as stand-ins for SHIELDOSE-2 in that narrow range of circumstances unnecessarily limits the study's contributions. The study can, and should, provide a fuller documentation of the various codes' capabilities and limitations, rather than one focused on standing in for SHIELDOSE-2.

This study includes an examination of codes' capabilities for mono-energetic proton and electron transport in the simplest geometries. However, it is extremely likely that the readers of this study in the coming years will have turned to it because they are tackling complex environments and geometries, not mono-energetic environments and simple solids. The analyses required for current space applications and the concomitant physics and geometry modeling used for actual space systems make a study of only mono-energetics a study of very limited utility, utility which will further decrease quickly over time.

Moreover, a study this fundamental in particle transport, mono-energetic energy deposition, should, at minimum, include the stopping density of the particles being transported, even if just as an appendix, given the importance of both surface and deep dielectric charging.

<u>SHIELDOSE Capabilities Warranting Further Discussion in the Study:</u>

SHIELDOSE-2 has the capability of providing mono-energetic data of the form required for the comparative calculations performed in this study. This study should document that capability much as it documents capabilities for the other codes. In fact, SHIELDOSE requires environment spectra and returns dose-thickness tables for those spectra, probably a better comparison basis than mono-energetics relative to the usual NASA application cases.

SHIELDOSE-2 should be documented along with the other codes in this document for other reasons as well. Over its 30-year history, SHIELDOSE has incorporated several improvements, both protons and electrons, substantial enough to be brought out directly in this study. Specifically, the improvements as to projected range for protons and low-energy improvements in PENELOPE[11] and MCNP for electrons and photons. Over time, it appeared that some SHIELDOSE capabilities were on-then-off for better agreement; that should not have happened, and the best should be shown.

Both SHIELDOSE-1 and -2 have an algorithm that log spaces energy points from minimum to maximum for each of the three spectra: solar proton, trapped proton, and trapped electron. In that algorithm, the energy points are an e-Vector. An associated g-Vector is recalculated at each shield thickness to see if the individual "e" can penetrate that thickness. Using these "g" data, partial sums of the g-Vector provide the break points for the 0-, 25-, 50-, 75-, and 100-percent contribution energies.

These contribution fractions are very informative when examining the relative importance of both low and high energies to a thin layer for actual environments. With this capability, the user controls layer "thinness" and even angstrom layers are not problematic (avoid "large" sudden jumps in the running thickness list). The fractions bring varying, and often substantial, understanding relative to actual layer mechanics/chemistry/biology based on the particle type, energy range, and relative contribution to the total layer energy absorption. Secondary kinematics could also be added for protons and Bremsstrahlung photons.

Proposed Updates to Study

This Alternate Technical Opinion proposes that this study be updated, and its scope expanded, consistent with the below:

1) The expanded discussion of SHIELDOSE-2 described above.
2) The opportunity for each code's representatives to prepare and provide a multimedia presentation discussing any and all aspects of their code relevant to NASA and its contractors. The presentations should be recorded, hosted on the NASA/JPL website, and referenced in this report including stating the host url so that readers can view the presentations.
3) The study should require that the codes run more realistic example problems, including multiple environments and complex space system geometry modeling. This step would enable readers to evaluate numerous features and capabilities of the codes important in performing such analyses, including, for examples, CAD capabilities, multi-core processing to enable faster analysis of complex geometries, and CAF/CAM/ Digital Imaging and Communications in Medicine (DICOM)[12] phantoms for crewed missions.

[11] Penetration and ENErgy LOss of Positrons and Electrons

[12] Digital Imaging and Communications in Medicine

4) The study should require that the codes run typical systems engineering problems. The problems would cause the codes to demonstrate their ability to factor in the effects of radiation transport as to a variety of different materials in a variety of environments.
    a) Specifically, using multi-core/cpu parallel runs, with different random numbers for better statistics, or parametrics on environments or on structural materials, or fractional mixed/layered material compositions, or simply splitting up large detector lists for ray trace and RMC through-put.
5) The study should provide opportunities for the codes to demonstrate key competencies that are important today, and increasingly so, but which are not brought out by the study's current mono-energetic, simple solid geometry exercise. These developments include, but are not limited to:
    a) Using point-value cross sections (PVX) data sources, evaluated libraries. ENDF/B
        i) atomic physics, photons & ions, and nuclear physics, neutrons & ions
    b) FMC point-value photon/electron/heavies
        i) stopping, charging, electric Potential
        ii) bremsstrahlung secondary electron atmospheric dipole, high-altitude electromagnetic pulse (HEMP) driver,
    c) Anomalously Large SPE, direct connect to atmosphere and power grid
    d) Using multi-group cross sections (MGX) data sources, libraries
    e) FMC multi-group neutron/gamma-ray, ORNL Scale libraries
        i) Nuclear Regulatory Commission (NRC)/nuclear power industry, Demonstration Rocket for Agile Cislunar Operations (DRACO) applications, radioisotope thermoelectric generator (RTG)
    f) FMC/RMC multi-group photon/electron SNLCEPXS library
        i) ITS RMC, general utility, possible extension to heavy-ions
    g) Validation of ray-trace methods, spelled out in the Requirements Documentation
    h) Ray trace approximations for electron/Bremsstrahlung/heavies/neutrals
        i) solid-slant-path, shell-minimum-path, solid-shell-weighted
    i) Mesh, grid, CSG, CAD geometry modeling
        i) with bill-of-materials densities and composition links
        ii) with openGL dynamic viewing of objects individually or collectively
        iii) with ray-trace pictures, perspective, and multi-slice parallel cross sections
        iv) pre-sorted object location on large CAD models for ray-trace speed
    j) Buildup and removal for photon and neutron ray-trace approximations
    k) Dose enhancement at material interfaces from primary-photons / secondary-electrons
    l) Numerical integration z=1 through 92 CREME heavy-ions transport
    m) FluxFile repositories, transport analysis; Monte Carlo, finite-element, numerical integration
        i) energy and energy-angle details of particle flux
    n) LET spectra from FluxFiles from z=1 through 92 transport analysis

        i) any shield material, any target material
    o) Small feature analysis using FluxFile detailed particle flux
        i) pulse-heights using analytic chord-length distributions on sensitive volumes
    p) Astronaut Phantoms: old-space camera CAF and CAM in CSG geometry
        i) new-space DICOM images
    q) Critical Organ Dose: skin, blood-forming-organs, lens-of-eye
        i) in the camera phantom system, DICOM equivalent
    r) Graphical User Interfaces
        i) data base management
            (a) PVX and MGX cross section libraries
            (b) materials, elements, isotopes, compounds, mixtures, user-specific
            (c) tabulated environment tables
            (d) trapped radiation belts, solar particle events, galactic cosmic rays,
                1. on-board nuclear, threats, testing, irradiation, medical, ...
            (e) tabulated attenuation tables
                1. 1D slab / sphere geometries, first-look, 3D ray-trace inputs
            (f) phase-space-parameters, sources and detectors, for 3D analyses
                1. position x, direction u, and time t components of Q=x,u,e,t
                2. point, line, area, volume; isotropic, angular, fixed direction
        ii) reconcile CAD model details between old and modifications
        iii) run-stream setup, review, submit, output management
        iv) end-to-end total dose analysis, an example
            (a) environment
                1. trapped and solar spectra
                2. 1d attenuation tables, SHIELDOSE, adjoint 1D
            (b) CAD geometry and bill-of-materials from interface file(s)
                1. openGL visual verification, detector(s) identification
                2. ray-trace views on specific detectors
            (c) ray-trace analysis
            (d) RMC verification
            (e) output management

12.0 Other Deliverables

No unique hardware, software, or data packages, other than those contained in this report, were disseminated to other parties outside this assessment.

13.0 Recommendations for the NASA Lessons Learned Database

No recommendations for NASA lessons learned were identified as a result of this assessment.

14.0 Recommendations for NASA Standards, Specifications, Handbooks, and Procedures

No recommendations for NASA standards, specifications, or procedures were identified as a result of this assessment.

15.0 Definition of Terms

Finding	A relevant factual conclusion and/or issue that is within the assessment scope and that the team has rigorously based on data from their independent analyses, tests, inspections, and/or reviews of technical documentation.
Observation	A noteworthy fact, issue, and/or risk, which is not directly within the assessment scope, but could generate a separate issue or concern if not addressed. Alternatively, an observation can be a positive acknowledgment of a Center/Program/Project/Organization's operational structure, tools, and/or support.
Recommendation	A proposed measurable stakeholder action directly supported by specific Finding(s) and/or Observation(s) that will correct or mitigate an identified issue or risk.

16.0 Acronyms and Nomenclature List

1D	One-Dimensional
2D	Two-Dimensional
3D	Three-Dimensional
ACIS	Advanced Computerized Implementation of Standards
AMU	Atomic Mass Unit
CAD	Computer Aided Design
CAF	Computerized Anatomical Female
CAM	Computerized Anatomical Man/male
CEPXS	Coupled Electron-Photon Cross Section
CREME96	Cosmic Ray Effects on Micro-Electronics (revision 1996)
CSDA	Continuous Slowing-Down Approximation
CSG	Constructed Solid Geometry
CSV	Comma-separated Value
DICOM	Digital Imaging and Communications in Medicine
DRACO	Demonstration Rocket for Agile Cislunar Operations
EM	Electromagnetic
EMPC	Experimental & Mathematical Physics Consultant
ENDF	Evaluated Nuclear Data File
ESA	European Space Agency
ESSR	European Space Software Repository
ETRAN	Electron TRANsport
FARO	Forward-adjoint reduced-order
FLUKA	Fluktuierende Kaskade
FMC	Forward Monte Carlo

GCR	Galactic-Cosmic Radiation
GDML	Geometry Description Markup Language
Geant4	Geometry and Tracking version 4
GEMAT	Geant4-based Microdosimetry Analysis Tool
GeV	Giga-electron-Volt
GPS	Global Positioning System
GRAS	Geant4 Radiation for Space
GSFC	Goddard Space Flight Center
GUI	Graphical User Interface
HEMP	High-altitude Electromagnetic Pulse
HST	Hubble Space Telescope
ICRU	International Commission on Radiation Units & Measurements
IGES	Initial Graphics Exchange Specification
IRENE	International Radiation Environment Near Earth
ITS	Integrated Tiger Series
JSWT	James Webb Space Telescope
keV	Kilo-electron-Volt
LaRC	Langley Research Center
LET	Linear Energy Transfer
MCNP	Monte Carlo for N-Particles
MeV	Mega-electron-Volt
MGX	Multi-Group cross sections
MMS	Magnetospheric Multiscale
MSFC	Marshall Space Flight Center
MULASSIS	Multi-Layered Shielding Simulation Analysis
NCIA	Neutron Capture Ion Algorithm
NESC	NASA Engineering and Safety Center
NIEL	Non-Ionizing Energy Loss
NIST	National Institute of Standards and Technology
NRC	Nuclear Regulatory Commission
NRL	Naval Research Laboratory
ORNL	Oak Ridge National Laboratory
pC	pico-Coulombs
PENELOPE	Penetration and ENErgy LOss of Positrons and Electrons
PTFE	Polytetrafluoroethylene
PVX	Point Value Cross Section
RMC	Reverse Monte Carlo
RSICC	Radiation Safety Information Computational Center
RTG	Radioisotope Thermoelectric Generator
SDO	Solar Dynamics Observatory
SEE	Single Event Effects
SNL	Sandia National Laboratories
SOFIP	Short Orbital Flux Integration Program
SPE	Solar Particle Events
SPENVIS	SPace ENVironment Information System
STEP	Standard for the Exchange of Product

STL	Stereolithography
TAT	Tabulated Attenuation Tables
TeV	Tera-electron-Volt
TID	Total Ionizing Dose
TNID	Total Non-Ionizing Dose
UI	User Interface
μm	Micrometer
VRML	Virtual Reality Modeling Language

17.0 References

1. The 3D CAD Tool For Radiation Shielding Analysis. https://www.fastrad.net/
2. Pourrouquet, P.; et al.: "Comparative study between Monte-Carlo tools for space applications," *2016 16th European Conference on Radiation and Its Effects on Components and Systems (RADECS)*, Bremen, Germany, 2016, pp. 1-7, doi: 10.1109/RADECS.2016.8093121.
3. Jun, B.; Zhu, B. X.; Martinez-Sierra, L. M.; and Jun, I.: "Intercomparison of Ionizing Doses from Space Shielding Analyses Using MCNP, Geant4, FASTRAD, and NOVICE," in *IEEE Transactions on Nuclear Science*, vol. 67, no. 7, pp. 1629-1636, July 2020, doi: 10.1109/TNS.2020.2979657.
4. FLUKA. https://FLUKA.cern
5. Ahdida, C.; Bozzato, D.; Calzolari, D.; Cerutti, F.; et al.: "New Capabilities of the FLUKA Multi-Purpose Code," *Frontiers in Physics* **9**, 788253 (2022).
6. Battistoni, G.; Boehlen, T.; Cerutti, F.; Chin, P. W.; et al.: "Overview of the FLUKA code," *Annals of Nuclear Energy* **82**, 10-18 (2015).
7. Vlachoudis, V.: "FLAIR: A Powerful But User Friendly Graphical Interface For FLUKA," Proc. Int. Conf. on Mathematics, Computational Methods & Reactor Physics (M&C 2009), Saratoga Springs, New York, (2009).
8. Widorski, M.; Bozzato, D.; Froeschl1, R.; and Kouskoura, V.: "FLUKAVAL − A validation framework for the FLUKA radiation transport Monte Carlo code," *EPJ Web of Conferences* **284**, 16006 (2023).
9. Fassò, A.; Ferrari, A.; Ranft, J.; and Sala, P. R.: "New developments in FLUKA modelling hadronic and EM interactions," *Proc. 3rd Workshop on Simulating Accelerator Radiation Environments*, KEK, Tsukuba, Japan (1997).
10. Ferrari, A.; Sala, P. R.; Guaraldi, R.; and Padoani, F.: "An improved multiple scattering model for charged particle transport," Nucl. Instrum. Meth. Phys. Res. B **71,** 412-426 (1992).
11. Seltzer, S. M.; and Berger, M. J.: "Bremsstrahlung spectra from electrons with kinetic energy 1 keV-10 GeV incident on screened nuclei and orbital electrons of neutral atoms with Z = 1-100," *At. Data Nucl. Data Tab*. **35**, 345-418 (1986).
12. Ferrari, A.; and Sala, P. R.: "The physics of high energy reactions," *Proc Workshop on Nuclear Reaction Data and Nuclear Reactor Physics, Design, and Safety*, p 424, World Scientific (1998).

13. Ferrari, A.; Ranft, J.; Roesler, S.; and Sala, P. R.: “Cascade particles, nuclear evaporation, and residual nuclei in high energy hadron-nucleus interactions,” *Z. Phys*. C **70,** 413-426 (1996).
14. Fontana, A.: “Nuclear interaction model developments in FLUKA,” *Proc. 14th International Conference on Nuclear Reaction Mechanisms*, p. 283, CERN (2015)
15. Boehlen, T. T.; Cerutti, F.; Chin, M. P. W.; Fassò, A.; et al.: “The FLUKA Code: Developments and Challenges for High Energy and Medical Applications,” *Nucl. Data Sheets* **120**, 211-214 (2014).
16. Serban, A. G.; Coronetti, A.; García Alía, R.; and Salvat Pujol, F.: “Nuclear elastic scattering of protons below 250 MeV in FLUKA v4-4.0 and its role in single-event-upset production in electronics,” https://doi.org/10.48550/arXiv.2312.12300 (2024).
17. Vlachoudis, V.; Devienne, A.; Froeschl, R.; Harbron, R. W.; et al.: (FLUKA.CERN collaboration), “Recent developments in the point wise neutron treatment for FLUKA v4,” *EPJ Web of Conf.* **284**, (2023)
18. Ranft, J.: “Estimation of radiation problems around high energy accelerators using calculations of the hadronic cascade in matter,” *Particle Accelerators* **3,** 129-161 (1972)
19. Cullen, D. E.; Hubbell, J. H.; and Kissel, L.: “EPDL97: The Evaluated Photon Data Library ‘97 Version, ” UCRL 50400 6 Rev.5 (1997).
20. Boehlen, T. T.; Ferrari, A.; Patera, V.; and Sala, P. R.: “Describing Compton scattering and two-quanta positron annihilation based on Compton profiles: two models suited for the Monte Carlo method,” JINST **7** P07018 (2012).
21. Fasso, A.; Ferrari, A.; Sala, P. R.: “Designing electron accelerator shielding with FLUKA,” *Proceedings of ICRS 8*, AIP, pp. 643–649 (1994).
22. Agostinelli, Allison, J.; Amako, K.; et al.: *Nuclear Instruments and Methods in Physics Research Section A: Accelerators, Spectrometers, Detectors and Associated Equipment*, 2003, Volume 506, Issue 3, Pages 250-303.
23. Allison, J.; Amako, K.; Apostolakis, J.; et al.: *Nuclear Instruments and Methods in Physics Research Section A: Accelerators, Spectrometers, Detectors and Associated Equipment*, 2016, Volume 835, Pages 186-225.
24. Allison, J.; Amako, K.; Apostolakis, J.; et al.: *IEEE Transactions on Nuclear Science*, Feb. 2006vol. 53, no. 1, pp. 270-278.
25. Santin, G.; Ivanchenko, V.; Evans, H.; Nieminen, P.; and Daly, E.: *IEEE Transactions on Nuclear Science*, Dec. 2005, vol. 52, no. 6, pp. 2294-2299.
26. Desorgher, L.; Lei, F.; and Santin, G.: *Nuclear Instruments and Methods in Physics Research Section A: Accelerators, Spectrometers, Detectors and Associated Equipment*. 1–21 September 2010, Volume 621, Issues 1–3, Pages 247-257
27. Berger, M. J.; and Seltzer, S. M.: “ETRAN Monte Carlo code system for electron and photon transport through extended media,” CCC-107, Radiation Shielding Information Center, Computer Code Collection, Oak Ridge National Laboratory, 1968.
28. Mehlhorn, T. A.; and Halbleib, J. A.: “Monte Carlo benchmark calculations of energy deposition by Electron/Photon showers up to 1 GeV,” in *Proceedings of a Topical Meeting on Advances in Reactor Computations*, page 608, 1983, ISBN 0-89448-111-8.

29. Halbleib, J. A.; et. al.: "ITS: The Integrated TIGER Series of Electron/Photon Transport Codes – Version 3.0," *IEEE Transactions on Nuclear Science*, vol 39, no. 4, 1992
30. Franke, B. C.; et al.: *ITS version 5.0: The integrated TIGER series codes*, Technical report, Sandia National Laboratories, 2002, unpublished draft.
31. Franke, B.; et al.: *ITS Version 6.7: The Integrated TIGER Series of Coupled Electron/Photon Monte Carlo Transport Codes User's Manual*: Technical report, SAND2023-12825, Feb 2023.
32. Werner, C. J.; Armstrong, J. C.; Brown, F. B.; et al.: *MCNP User's Manual Code Version 6.2. Los Alamos National Laboratory*, Tech. Rep. LA-UR-17-29981. Los Alamos, NM, USA. October 2017.
33. Kulesza, J. A.; Adams, T. R.; Armstrong, J. C.; et al.: *MCNP® Code Version 6.3.0 Theory & User Manual. Los Alamos National Laboratory*, Tech. Rep. LA-UR-22-30006, Rev. 1. Los Alamos, NM, USA. September 2022.
34. Beringer, J.; et al.: (Particle Data Group), *Phys. Rev*. D 86, 010001 (2012).
35. Hughes, H. G: *An Electron/Photon/Relaxation Data Library for MCNP6*, LA-UR-13-27377 (2013).
36. SSP 30512, Revision C, Space Station Ionizing Radiation Design Environment, 3 June 1994.
37. Badavi et al.: *Validity of the Aluminum Equivalent Approximation in Space Radiation Shielding*, NASA TP-2009-215779, July 2009. https://ntrs.nasa.gov/api/citations/20090026532/downloads/20090026532.pdf
38. Walker et al.: "Investigating Material Approximations in Spacecraft Radiation Analysis," *Acta Astronautica*, Vol. 679, pp. 6-17, 2011. https://doi.org/10.1016/j.actaastro.2011.02.013

REPORT DOCUMENTATION PAGE	*Form Approved OMB No. 0704-0188*

1. REPORT DATE *(DD-MM-YYYY)*	**2. REPORT TYPE**	**3. DATES COVERED** *(From - To)*
10/03/2024	Technical Memorandum	

4. TITLE AND SUBTITLE
Space-Shielding Radiation Dosage Code Evaluation
Phase 2: SHIELDOSE-2 Radiation-Assessment Code

5a. CONTRACT NUMBER

5b. GRANT NUMBER

5c. PROGRAM ELEMENT NUMBER

6. AUTHOR(S)
Jun, Insoo; Alía, Rubén García; Benacquista, Remi; Cappe, Alexandre; Fodness, Bryan; Henderson, Alexander; Jordan, Thomas M.; Marin, Stefano; Milic, Larisa; Pujol, Francesc Salvat; Santin, Giovanni; Servelle, André Donadon; Singleterry. Robert C.; Varotsou, Athina; Vlachoudis, Vasilis; Zhu, Brian X.; Gentz, Steven J.

5d. PROJECT NUMBER

5e. TASK NUMBER

5f. WORK UNIT NUMBER
869021.01.23.01.01

7. PERFORMING ORGANIZATION NAME(S) AND ADDRESS(ES)
NASA Langley Research Center
Hampton, VA 23681-2199

8. PERFORMING ORGANIZATION REPORT NUMBER
NESC-RP-21-01718

9. SPONSORING/MONITORING AGENCY NAME(S) AND ADDRESS(ES)
National Aeronautics and Space Administration
Washington, DC 20546-0001

10. SPONSOR/MONITOR'S ACRONYM(S)
NASA

11. SPONSOR/MONITOR'S REPORT NUMBER(S)
NASA/TM-20240012725

12. DISTRIBUTION/AVAILABILITY STATEMENT
Unclassified - Unlimited
Subject Category Space Radiation
Availability: NASA STI Program (757) 864-9658

13. SUPPLEMENTARY NOTES

14. ABSTRACT
Radiation-transport codes or radiation-analysis tools are used in the spacecraft-design community to define and assess the local radiation levels. Among various radiation-transport/analysis tools available, SHIELDOSE-2 is commonly used in the early spacecraft-design phases because it has been established that it provides reasonably reliable results with relatively rapid computation time. The NASA Engineering and Safety Center initiated a two-phased study: (1) to better understand and document the SHIELDOSE-2 code capabilities and limitations, and (2) to identify alternative tools to use for cases where SHIELDOSE-2 is not applicable. This report provides a summary of the Phase 2 study.

15. SUBJECT TERMS
SHIELDOSE-2; NASA Engineering and Safety Center; Radiation-Analysis Tools; Radiation-Transport Codes

16. SECURITY CLASSIFICATION OF: a. REPORT	b. ABSTRACT	c. THIS PAGE	**17. LIMITATION OF ABSTRACT**	**18. NUMBER OF PAGES**	**19a. NAME OF RESPONSIBLE PERSON**
					STI Help Desk (email: help@sti.nasa.gov)
					19b. TELEPHONE NUMBER *(Include area code)*
U	U	U	UU	69	(443) 757-5802